PROPOSAL

FOR A EUROPEAN

EXTREME LIGHT INFRASTRUCTURE (ELI)

ELI will be the first infrastructure dedicated to the fundamental study of laser-matter interaction in a new and unsurpassed regime of laser intensity: the ultra-relativistic regime (I_L>10^{23} W/cm^2). At its centre will be an exawatt-class laser ~1000 times more powerful than either the Laser Mégajoule in France or the National Ignition Facility (NIF) in the US. In contrast to these projects, ELI will attain its extreme power from the shortness of its pulses (femtosecond and attosecond). The infrastructure will serve to investigate a new generation of compact accelerators delivering energetic particle and radiation beams of femtosecond (10^{-15} s) to attosecond (10^{-18} s) duration. Relativistic compression offers the potential of intensities exceeding I_L>10^{25} W/cm^2, which will challenge the vacuum critical field as well as provide a new avenue to ultrafast attosecond to zeptosecond (10^{-21} s) studies of laser-matter interaction. ELI will afford wide benefits to society ranging from improvement of oncology treatment, medical imaging, fast electronics and our understanding of aging nuclear reactor materials to development of new methods of nuclear waste processing.

Authors list : F. Amiranoff[1], F. Augé[2], H. Backe[3], Ph. Balcou[2], D.-B. Blaschke[4], D. Bernard[5], J.-P. Brasile[6], S. Bulanov[7,8], F. Canova[2], J.-P. Chambaret[2], D. Charalambidis[9], G. Chériaux[2], G. Dollinger[10], F. Druon[11], R. Ferrand[12], N. Forget[13], P. Georges[11], F. Gruener[14], D. Habs[14], F. Hannachi[15], K. Hatsagortsyan[16], D. Hulin[2], S. Karsch[17], K. Kompa[18], F. Krausz[18], K. Kushelnick[19], C. Le Blanc[1], K. Ledingham[20], G. Malka[14], V. Malka[2], J. Meyer-ter-Vehn[18], P. Mora[21], G.-A. Mourou[2], N. Naumova[2], F. Pegoraro[22], G. Petite[23], A. Piskarskas[24], M. Pittman[25], F. Plé[25], A. Pukhov[17], M. Roth[4], R. Sauerbrey[26], A. Rousse[2], D. Schardt[4], J. Schreiber[14,17], S. Sebban[2], F. Sette[27], R. Schuetzhold[28], G. Tsakiris[17], V. Tikhonchuck[29], J. Ullrich[4], H. Videau[5], M. Vrakking[30] , O. Willi[17].

[1]LULI, CNRS-X, CEA, Université Paris XI, 91128 Palaiseau (France)
[2]LOA, CNRS-ENSTA-X, 91761 Palaiseau (France)
[3]Johannes-Gutenberg-Universitat Mainz, D 55099 Mainz (Germany)
[4]GSI, Planckstr.1 64291 Darmstadt (Germany)
[5]LLR, CNRS-IN2P3-X, 91128 Palaiseau (France)
[6]Thalès, STI, 92704 Colombes cedex (France)
[7]Japan Atomic Energy Agency, Kyoto 619-0215 (Japan)
[8]General Physics Institute RAS, Moscow 119991 (Russia)
[9]IESL (Heraklion) 71110, Crete (Greece)
[10]Institut für Angewandte PM, D-85577 Neubiberg (Germany)
[11]IOTA, Bât 503, 91403 ORSAY Cedex (France)
[12]CPO, Bat. 101, 91898 Orsay cedex (France)
[13]FASTLITE Bâtiment 403 Campus de l'X 91128 Palaiseau (France)
[14]LMU, Am Coulombwall 1, D-85748 Garching (Germany)
[15]CENBG, CNRS, IN2P3, Université Bordeaux 1 (France)
[16]Max-Planck-Institut fuer Kernphysik, Heidelberg D-69117 (Germany)
[17]Heinrich-Heine-Universitaet Duesseldorf, D-40225 Duesseldorf
[18]MPQ, Max-Planck-Institut fur Quantenoptik, D-85748 Garching [19]Imperial College, Imperial College London, SW7 2AZ London (U. K.)
[20]Dept. of Physics,Univ of Strathclyde, Glasgow G4 0NG (Scotland)
[21]Centre de Physique Theorique, CNRS-X, 91128 Palaiseau (France)
[22]Dipartimento di Fisica,Universita' di Pisa, 56100 Pisa (Italy)
[23]LSI, CNRS-X, F-91128, Palaiseau (France)
[24]Department of Quantum Electronics, LT-10222 Vilnius (Lithuania)
[25]LIXAM, CNRS-Université Paris XI, Bât 350, 91405 Orsay (France)
[26]Institut für Optik und Quantenelektronik, D07743 Jena (Germany)
[27]ESFR, 6, rue Jules Horowitz,BP 220, Grenoble 38043 (France)
[28]Technische Universität Dresden, ITP, 01062 Dresden (Germany)
[29]CELIA, Universite Bordeaux 1, 33405 Talence cedex (France)
[30]Amolf FOM, Kruislaan 407, 1098 SJ Amsterdam (The Netherlands)

CONTENTS

Part A: ELI PROJECT

A.I Introduction

Since its advent, the laser has been extraordinarily effective in study and technological development at the atomic and molecular level. At the outset, the laser explored the chemical bond in the electron-volt energy range. Technological breakthroughs over the past 20 years (Strickland and Mourou 1985, Mourou 1998) have allowed a rapid six-orders-of-magnitude increase in available intensity (Fig.1). At intensities of 10^{18} W/cm^2, the visible laser-matter interaction is governed by the electron relativistic behaviour creating the domain of relativistic optics. This interaction results in a plethora of novel effects (Mourou 2006): X-ray generation, γ-ray generation, relativistic self-focusing, high-harmonic generation, electron and proton acceleration, neutron and positron production, as well as the manifestation of nonlinear QED effects. The entrance into this relativistic regime is described by the normalized electric field amplitude $a_0^2=I_L\lambda_L^2/(1.37\times10^{18}$ Wμm^2/cm^2), where I_L and λ_L are the laser intensity and wavelength; at $a_0=1$ the electron mass increases by $2^{1/2}$. The above-mentioned relativistic effects arise in the regime $1< a_0 <100$. To date, we have been limited to this parameter space by the physical laser size.

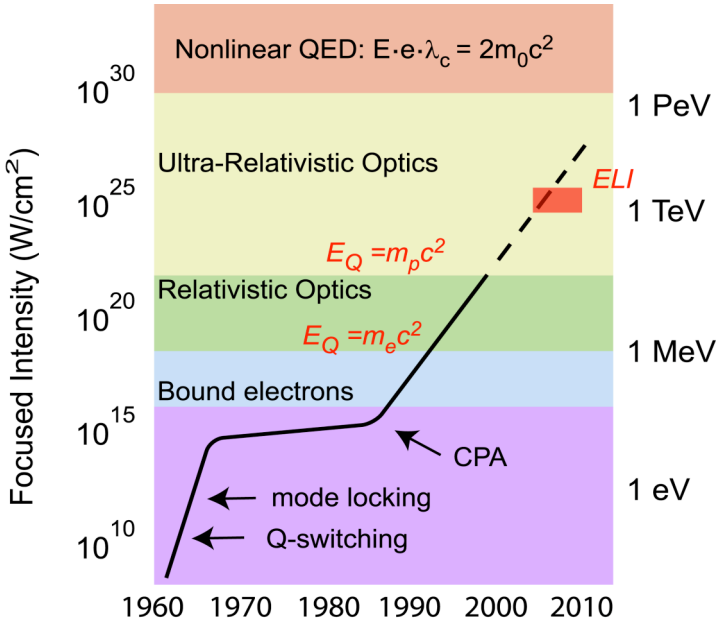

Fig. 1: *History of laser intensity, showing the different laser-matter interaction periods. Over the past twenty years the studies were conducted in the sub-relativistic and relativistic regimes with $1<a_0<100$. ELI will address the ultra-relativistic regime with a_0, $100<a_0<10^4$.*

The limit a_0~100 corresponds to the 100 TW class lasers focused to a diffraction limited spot, and it represents the borderline between a single laboratory unit relying on national funding and an international infrastructure operating on a multinational financial support. The aim of this proposal is to demonstrate that the expected scientific and engineering outcome of the regime defined by a_0 >100 merit the development of an entirely new, European infrastructure capable of exploring these intensities.

Whereas the relativistic regime is defined as $a_0>1$, **ultra-relativistic intensities** ($I_L>10^{23}$ W/cm^2) occur when the proton-normalized vector potential (a_{p0}) approaches unity. In this novel regime, positrons, pions, muons and neutrinos could be produced as well as high-energy photons. Furthermore, this largely unexplored intensity territory will provide access to physical effects with much higher characteristic energies and will regroup many subfields of contemporary physics (viz. atomic physics, plasma physics, particle physics, nuclear physics, gravitational physics, nonlinear field theory, ultrahigh-pressure physics, astrophysics and cosmology).

A.II Motivation: Segueing from Relativistic to Ultra-relativistic Laser-matter Interaction

Refinements in laser technology (short-pulse generation, amplification, spatial, temporal phase and carrier phase control (Baltuska 2003)) combined with super-computer-based plasma simulations have brought the discipline of relativistic laser-matter interaction to a new level of predictability. This was recently demonstrated by the prediction and observation of the 100 MeV quasi-monochromatic beams (Fig. 2) in the "bubble" regime (see Beam Physics). The particle-in-cell (PIC) simulations of several research groups indicate that the ultra-relativistic regime of $I_L=10^{23}$ W/cm^2 which will be accessed in the ELI facility will result in an electron beam of the order of GeV and of duration less than 5 fs. These PIC simulations also indicate that the ultra-relativistic regime will generate multi-GeV proton beams. In turn these protons could generate pion beams that would decay to muon and neutrino beams. These examples illustrate the importance of the ultra-relativistic regime (a_0 ~10^2-10^4) with regard to particle acceleration.

The ultra-relativistic regime opens possibilities of both (i) extreme acceleration of matter such that generation of very energetic particle beams of leptons and hadrons becomes efficient and (ii) efficient production (~10%) of attosecond (Fig. 3) or even zeptosecond pulses by relativistic compression occurring at the rate of $600/a_0$ [as]. These attributes combined with the direct and intriguing effects of the field-vacuum interaction provide the three basic pillars of the ELI programme.

(1) ELI will offer much higher intensity levels either directly with the laser or by relativistic compression. The optical field could then reach the critical field value. In this limit the laser pulse-plasma interaction demonstrates effects of the radiation friction force and quantum electrodynamics effects of nonlinear vacuum polarization and electron-positron pair creation. In this limit, novel mechanisms of ion acceleration occur. Since the energy of the resulting ion bunch can be over 100 GeV per nucleon, this ion acceleration regime would be suitable for quark-gluon plasma studies and could be used in the investigation of neutrino oscillations. An introductory list of applications of ELI laser intensities to strong-field physics is made in the Exotic Physics section. In essence, ultra-relativistic intensities could unify nuclear physics, high-energy physics, astrophysics and cosmology.

(2) Ultra-relativistic interaction will provide beams of photons, leptons and hadrons with unique characteristics, in time structure and energy. By generating user-available 1-100 GeV electron beams, ELI will pave the way for the design of a compact accelerator for high-

energy physics. These particles will be used to generate ultra-brilliant X-ray light sources by laser-assisted synchrotron radiation, linear and non-linear Compton scattering, betatron radiation and free-electron-laser mechanisms. The X-ray output parameters could well be comparable to those of the large-scale XFELs being planned world-wide.

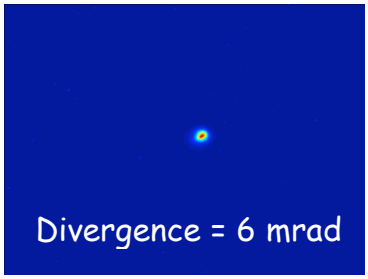

Fig. 2: *Beam divergence of the 170 MeV electron beam*

(3) ELI will provide the opportunity to perform time-resolved science in the attosecond regime in gases, solids and plasmas. It will create the conditions for attosecond XUV-pump/XUV-probe experiments for real-time observation of electronic dynamics in a wide variety of systems. These include intra-atomic processes in complex biomolecules, dynamics in clusters, electron transfer on surfaces, motion in semiconductor nanostructures, and collective dynamics in high-density matter, where it will provide attosecond snapshots of electron transport in plasmas beyond the Alfven limit, a study of particular relevance to fast ignition concept for inertial confinement fusion.

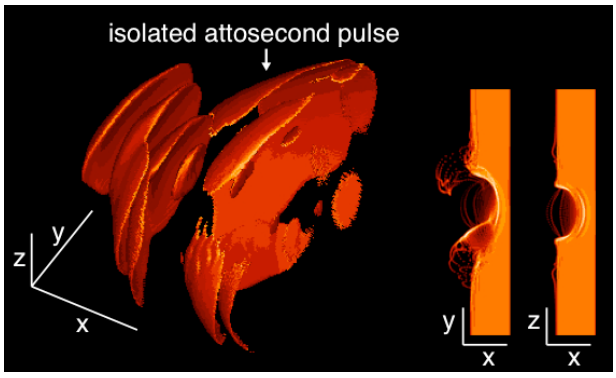

Fig. 3: *Single attosecond pulse produced in the "Lambda-cube" regime (λ^3) when a few femtosecond laser pulse is focused down to a spot of a single wavelength diameter.*

Laser systems of a_0~10 have already reached a size analogous to the funding available in single-nation investment. Investigation in the ultra-relativistic regime (a_0~10^2-10^4) will call for a much larger exawatt power laser system with repetition rate ≥1 shot/min. Such an

infrastructure is possible within the framework of a cooperative European effort and investment.

A.III Short Description

ELI will be a research infrastructure dedicated to European scientists that will extend the field of laser-matter interaction, now limited to the relativistic regime (a_0~10), into the ultra-relativistic regime a_0 ~10^2-10^4. By means of relativistic effects, these extreme intensities will provide access to extremely short pulse durations in the attosecond regime. ELI will comprise three branches: **Ultra-High-Field Science** centred on direct physics of the unprecedented laser field strength, **Attosecond Laser Science**, which will capitalize on new regimes of time resolution, and **High-Energy Beam Facility**, responsible for development and use of ultra-short pulses of high-energy particles and radiation stemming from the ultra-relativistic interaction.

ELI will be modular, starting at the petawatt (kHz) level and subsequently being extended to the sub-exawatt (>1shot/mn). This ultra-high peak power (200 times the peak power of the megajoule project) will be obtained with exceedingly short pulse duration (fs). By relativistic pulse compression, the femtosecond pulses could be further compressed to the attosecond range and the laser power boosted accordingly. ELI will open the possibility of taking snap-shots in the attosecond scale of the electron dynamics in atoms, molecules, plasmas and solids. With the possibility of going into the ultra-relativistic regime, ELI will afford new investigations in particle physics, nuclear physics, gravitational physics, nonlinear field theory, ultrahigh-pressure physics, astrophysics and cosmology. Besides its fundamental physics mission, a paramount objective of ELI will be to provide ultra-short energetic particle (10 GeV) and radiation (up to few MeV) beams produced from compact laser plasma accelerators. ELI will mate its scientific, engineering and medical missions for the benefit of industry and society. For instance, the secondary sources expected in the project will provide X-ray technologies to clarify the complete time history of reactions such as protein activity and protein folding, radiolysis, monitoring of chemical bonds and catalysis processes. This will lead to a better understanding and control of key events during chemical bond formation and destruction. A high impact on society and on new technologies for industry is then expected since these processes will play a major role in creating new drugs or in improving their efficiency.

ELI will aggressively pursue the field of relativistic microelectronic and photonic engineering in partnership with industry for practical and compact MeV-GeV electron acceleration. ELI could represent a major revolution in the field of accelerator electronics. In collaboration with medical doctors, hadron therapy will be developed with this novel source.

In material science ELI will make it possible to clarify of the mechanisms leading to defect creation and aging of materials in nuclear reactors. ELI will be able to produce large quantities of positrons that could be used in positron microscopy and in low dielectric constant studies for fast electronic devices. ELI could also be used to investigate the transmutation of long-lived radioactive elements into short-lived ones for the protection of our environment.

Part B: ELI'S SCIENTIFIC PROGRAMME

Laser-matter interaction in the relativistic regime leads to efficient particle beam generation and efficient pulse compression. ELI will be composed of three branches: **Ultra-High-Field Science** centred on direct physics of the unprecedented laser field strength, **Attosecond Laser Science**, which will capitalize on new regimes of time resolution, and **High-Energy Beam Facility**, responsible for development and use of ultra-short pulses of high-energy particles and radiation stemming from the ultra-relativistic interaction.

ELI will address studies inaccessible by current laser system facilities. ELI will be constructed modularly in three levels: a PW/kHz front end, first stage of 20PW and 1sh/min repetition rate, and third stage extending the power to >100PW. To maximize productivity of ELI it will be made available to users simultaneously with development. The proposed experiments are thus detailed by the corresponding laser power.

B.I Attosecond Science

B.I.1 Attosecond Light Source (ALS)

Attosecond science is a revolution in measurement technology. It provides, for the first time, direct time-domain access to the motion of electrons on atomic scales (Hentschel 2001) and to the oscillations of visible light (Kienberger 2004). With the availability of intense few-cycle light with controlled waveform (Baltuska 2003), single sub-femtosecond XUV pulses can now be routinely generated and measurements with 100-attosecond resolution routinely performed (Kienberger 2004). In spite of these advances attosecond spectroscopic experiments can only be pursued on a limited number of carefully selected systems because of the low photon flux of currently available attosecond sources based on high-harmonic generation in atomic gases.

The front end of ELI (1 J, 5 fs @ 800 nm and 100-1000Hz) will allow exploitation of relativistic light-electron interaction at a solid surface for creating a source of attosecond UV, VUV and SXR light, the **A**ttosecond **L**ight **S**ource (ALS), which surpasses present-day attosecond sources in terms of both peak and time-averaged brightness by 8-10 orders of magnitude and by a couple of orders of magnitude in terms of pulse duration. ALS will provide unique conditions for several entirely new classes of experiments in atomic, molecular and optical physics and is likely to break new ground in AMO sciences. These include pushing the frontiers of nonlinear spectroscopic experiments on dilute samples due to (i) its unsurpassed integrated photon fluse, of nonlinear optics into the soft-X-ray regime due to (ii) its unparalleled peak-power, and of ultrafast science to time resolutions of a few attoseconds owing to (iii) its never-before-achieved pulse durations, and – most importantly – creating the conditions for attosecond XUV-pump/XUV-probe experiments owing to (i)+(ii)+(iii) for real-time observation of electronic dynamics in a wide variety of systems.

These range from intra-atomic processes to motion in complex biomolecules, from dynamics in clusters to electron transfer on surfaces, and from motion in semiconductor nanostructures to collective dynamics in high-density matter.

ALS will ideally complement accelerator-based coherent X-ray free electron lasers such as the XFEL in Hamburg. Whereas XFELs are going to produce highly monochromatic radiation with pulse durations of the order of 100fs, ALS will produce polychromatic light of comparable brightness but by with pulse durations three to four orders of magnitude shorter. Whereas XFELs will be ideally suited to time-resolved studies of structural dynamics of matter, ALS will be the only light source on Earth capable of accessing electronic motion on the atomic scale in real time.

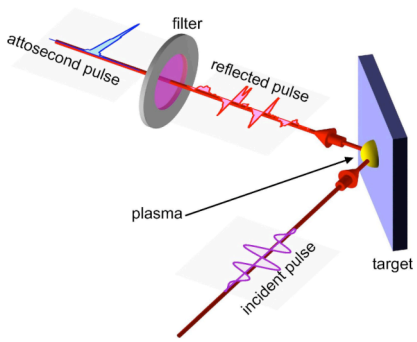

Fig. 1: *Schematic showing the proposed experimental configuration for the generation of attosecond pulses using harmonics from overdense plasmas.*

Relativistic harmonics as a way of producing efficient attosecond pulses

Since the first observation of harmonic generation from solid targets using a tabletop laser system it has become apparent that the interaction of an intense laser pulse with an overdense plasma constitutes an alternative route for producing attosecond pulses via phase-locked harmonics.

Harmonics from relativistic laser-surface interactions offer dramatically increased efficiency of conversion in driving laser radiation into coherent short-wavelength light, resulting from strongly anharmonic relativistic motion of electrons at the solid-vacuum interface. Driving the interaction with 1-joule, 5-fs, 800-nm laser pulses from the front end of ELI to be operated at a repetition rate of (initially) 100 Hz to (ultimately)1 kHz affords promise of creating a coherent a short-wavelength (10 eV – 1000 eV) light source of unprecedented peak brightness and pulse duration, the Attosecond Light Source (ALS).

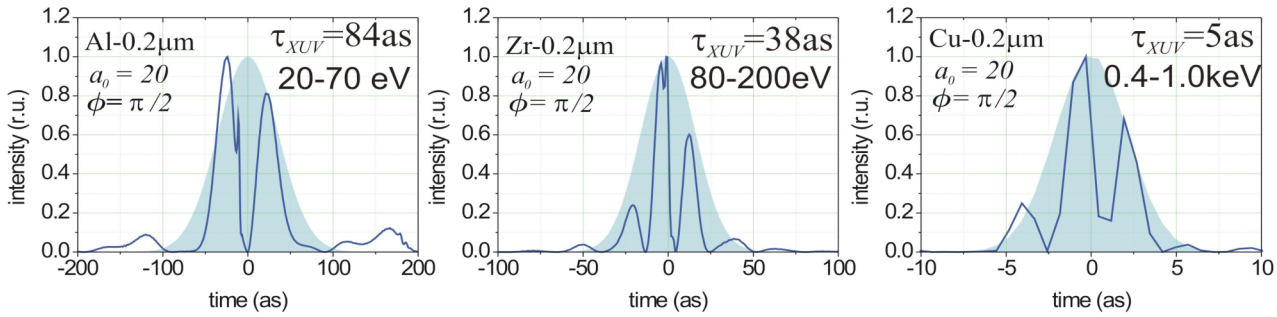

Fig. 2: *The instantaneous intensity of the attosecond pulses produced through the corresponding filter. The shaded area is a Gaussian pulse fit to obtain the duration for each case.*

Here we summarize results of 1D PIC simulations (Tsakiris 2006) estimating the pulse parameters achievable with ALS. The laser pulse (λ_L= 0.8 μm) was modelled as a Gaussian pulse comprising two cycles within the full width at half maximum of its intensity envelope

impinging with p-polarization at an angle of incidence of 45^0 on a planar solid-density plasma (Fig. 1).

The most important parameter pertaining to this interaction is the normalized field amplitude or normalized vector potential, which in terms of the laser intensity I_L and wavelength λ_L is given as $a_0^2=I_L\lambda_L^2/(1.37\times10^{18}$ Wμm^2/cm^2). In the simulations, it was varied between a_0=3 and 100, corresponding to a laser intensity range of I_L= 2×10^{19}–2×10^{22} W /cm^2, thus covering the present-day capabilities in laser technology as well those envisaged for the near future.

The high-repetition-rate front-end of ELI is projected to deliver pulses with an energy of E_L=1 J and a pulse duration of τ_L=5 fs at a carrier wavelength of 800 nm. Being focused to a spot diameter of ~5 μm it will result in peak intensities in excess of 10^{21} W/cm^2, corresponding to $a_0 \approx 20$. Figure 2 shows that under these conditions and by filtering the reflected light in different photon energy ranges with thin (0.2 μm) foils of Al, Zr and Cu results in single attosecond pulses of decreasing duration at increasing photon energies.

The computed efficiencies of converting the energy of the incident laser pulse into the respective reflected attosecond pulses are summarized in Fig. 3. For these experimental conditions, the 1D PIC simulations predict the following ALS pulse parameters of the single attosecond pulse transmitted through one of the above filters:

Spectral range	Number of photons	Pulse duration
20-70 eV (Al filter)	~7 *10^{15}	~80 as
80-200 eV (Zr filter)	~2*10^{14}	~40 as
400-1000 eV (Cu filter)	~2*10^{12}	~5 as

These results were recently corroborated by preliminary 3D PIC simulations (Geissler 2006). The 3D simulations also indicate excellent spatial coherence of the XUV light reflected from the few-cycle-driven relativistic plasma surface. If this spatial coherence materializes, the peak brilliance of ALS will outperform that of any existing or projected light source on Earth in the photon energy range extending from the UV to the SXR range. The unique properties of ALS will open the door to a range of new types of experiments in all forms of matter, including atoms, molecules, clusters, plasmas and solids. Some examples are briefly addressed in the next few pages.

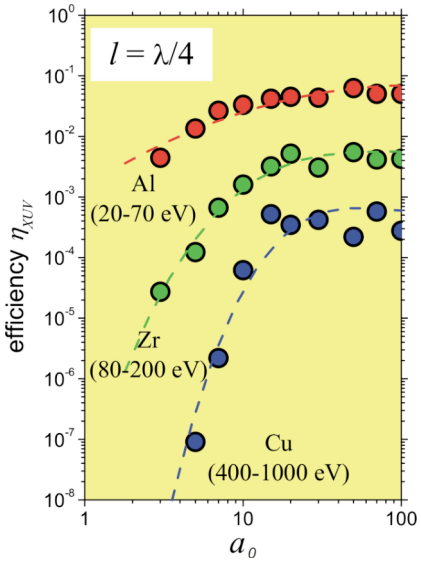

Fig. 3: *Efficiency of the laser into attosecond XUV pulse conversion as a function of the normalized field amplitude.*

B.I.2 Isolated attosecond pulse and electron bunch generation in the λ^3 regime

When a few-cycle laser pulse is focused to the diffraction limit, the laser energy is contained in a near λ^3 volume. This concentration of laser energy provides the highest intensity on target and highest gradients in laser-plasma interaction (Mourou 2002).

Analysis with 2D and 3D PIC simulations of laser and solid-density plasma interaction in the relativistic λ^3 regime reveals formation of *isolated* attosecond electromagnetic pulses and *dense* attosecond electron bunches (Naumova 2004, 2005). The attosecond pattern results from the joint action of incident and generated electromagnetic fields. The bunched electrons, escaping from the target with relativistic velocities, compress the reflected radiation into a train of attosecond pulses (Fig. 4). Ultra-short dense electron bunches scale in energy with dimensionless amplitude, given matching plasma conditions. Synchronous ejection of attosecond electron bunches and of attosecond electromagnetic pulses increases the applicability of both, paving the way to a new kind of optoelectronics – *relativistic optoelectronics*.

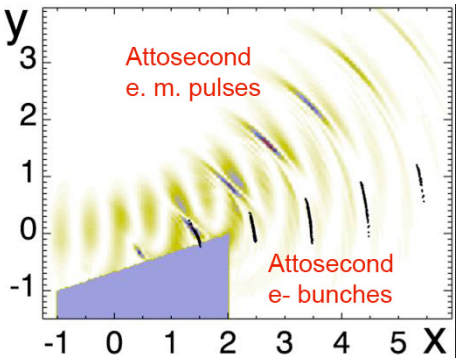

Fig. 4*: Synchronous production of attosecond electromagnetic pulses and electron bunches.*

The analytical model of a relativistically driven charged layer (Naumova 2004) confirms that an oscillating electric field at oblique incidence is sufficient to provide the pulse compression. Depending on the electric field phase, the charged sheet moves from or toward the reflected radiation, forming prominent radiation spikes in time. These features are indeed observed in the reflected radiation in Fig. 4. Consequently, the self-induced relativistic motion of charges in the λ^3 regime directly generates *isolated* attosecond pulses by *reflection, deflection, and compression* (see Fig. 3 of the Introduction). To scale this mechanism of attosecond pulse generation to higher intensities, it is necessary to keep similar slopes in electron density profiles. To do so, the plasma density should be scaled linearly with the driving field strength, maintaining the same balance between charge separation forces and forces arising from the incident fields. With higher field strength, electrons also move faster and the resulting Doppler compression leads to the formation of still shorter pulses.

Using 2D PIC simulations (Nees 2005), it is found that the ratio of a_0/n_0 ~2, where $n_0=n/n_{cr}$, is optimal for the production of isolated attosecond pulses. Boosted-frame 1D PIC simulations are capable of modelling oblique incidence only over a limited range of amplitude, because reflected light is bound to propagate only in the specular direction. Nevertheless, we find that the attosecond pulse duration τ produced follows the dependence

τ=600/a_0 [as] for the ratio a_0/n_0=2 in the range $3<a_0<20$ (Fig. 5). Similar shortening not in λ^3 geometry was obtained with a 1D normal-incidence model (Gordienko 2004, 2005). The advantage of the λ^3 regime is that it provides isolated attosecond pulses with much less input energy for the equivalent a_0.

Using the *scalability* of relativistically produced sub-femtosecond electromagnetic pulses, it is possible to achieve unprecedented intensities within the reflection of the generated compressed pulses from intentionally curved targets or from initially flat targets shaped by the laser pulse itself, as a result of focalization or induced focusing of light, respectively (Naumova 2005).

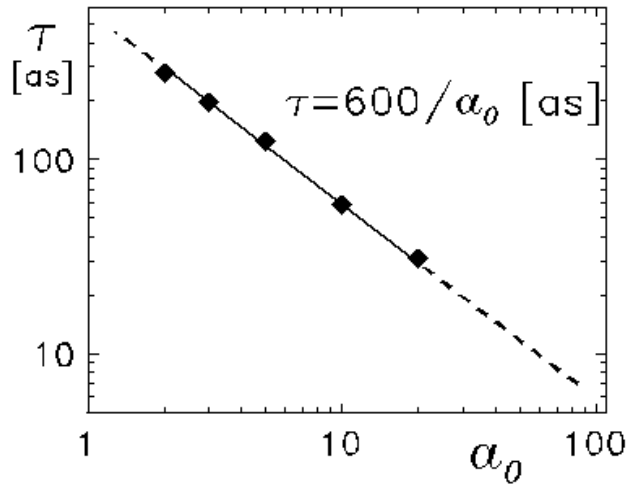

***Fig. 5**: Duration of electromagnetic pulses as a function of the laser amplitude*

B.I.3 Time-domain experiments

B.I. 3.1 Spectroscopy on dilute samples

Highly-charged ions (HCI) as well as cold molecular ions are among the most abundant species in our Universe but are only available in a few earthbound laboratories confined in traps or storage rings. The unsurpassed integrated VUV-SXR photon flux of ALS will permit precision spectroscopy and differential single- and multi-photon ionization measurements for the first time with HCI at all charge states. Quantum-state-resolved photoionization of cold molecular ions will become accessible, this being an indispensable prerequisite for understanding upper-atmosphere chemistry as well as interstellar clouds and reaching out to the questions of how stars are formed and life originated in the Universe.

B.I. 3.2 Inner-shell nonlinear optics and coherent control, relativistic atomic and molecular physics

Nonlinear interactions of optical radiation with bound electrons have so far been restricted to outer shells (valence electrons) due to the unfavourable scaling of multi-photon transition cross-sections with photon energy and the lack of intense short-wavelength sources. ALS will make multi-photon interactions at photon energies in excess of 100 eV discernible for the first time (Fig. 6). New experimental opportunities include the study of multi-photon-induced inner-shell transitions, as well as the selective creation and study of hollow atoms. Furthermore, element-specific microscopy with nanometer resolution may become feasible by detecting multi-photon XUV photoelectrons or Auger electrons with the tightly-focused ALS beam.

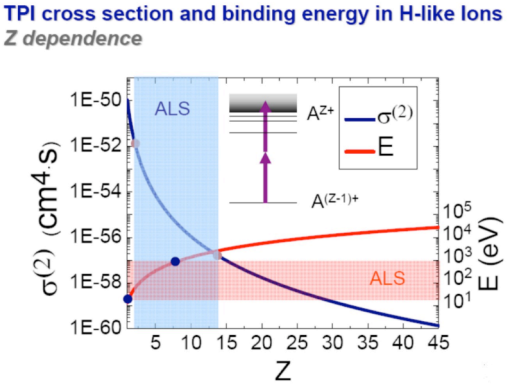

Fig. 6: *K-shell binding energies (E) and generalized Two-Photon-Ionization (TPI) cross-sections. The coloured bands indicate the regions to be accessed by ALS*

Extending optical pulse-shaping techniques into the XUV regime will open the door to inner-shell coherent control experiments.

The ultrahigh peak intensity of ALS will come in combination with a sub-femtosecond rise time. As a consequence, ALS will permit exposure of atoms and molecules to relativistic intensities before their disintegration for the first time, giving rise to light-atom, light-

molecule interactions in which the magnetic field of the radiation starts playing a significant role. Relativistic effects, so far studied only in laser-plasma interactions, will become observable in atomic and molecular systems, constituting an entirely new class of light-matter interactions.

B.I.3.3 Real-time observation of intra-atomic electron dynamics

The fact that two-photon transitions become detectable with ALS implies the feasibility of using two replicas of the attosecond pulse from ALS both as a pump pulse and as a probe pulse in one interaction. Attosecond XUV-pump/XUV-probe spectroscopy will – for example – open the door to direct time-resolved studies of electronic processes deep in the interior of atoms. The characteristic time scale for these dynamics is dictated by the atomic unit of time, which amounts to 24 attoseconds. ALS will be able to access this time domain. Attosecond pump-probe experiments at ALS will allow real-time investigation of multi-channel relaxation cascades of inner-shell-excited and hollow atoms, electron-electron times in inner shells, and the influence of ultra-strong light fields on these dynamics. The temporal evolution of inner-shell populations in the presence of strong external fields, which is highly relevant to X-ray laser research, will become experimentally accessible for the first time.

The speed of electron-electron interactions inside atoms is also dictated by the atomic unit of time. Hence their direct observation will also rely on ALS. One of the numerous questions of fundamental importance in atomic physics is the time response of the remaining electrons of an atom to photoionization. If, for instance, the two-electron He atom is ionized by a single 45-eV photon, is the remaining bound electron instantly projected onto the He^+ ground state? This would imply that a second 45-eV probe photon can liberate the second bound electron only if its delay is “essentially zero”. Recent calculations predict universal ~50-as relaxation behaviour for the electronic system of atoms and molecules following abrupt ionization. ALS may allow the first experimental tests.

In highly-charged ions lifetimes of even forbidden transitions reach the *fs* to *as* regime and could be determined with high precision providing unprecedented information on the bound-state wave functions. Such experiments would constitute never-before-available tests of QED, relativistic and nuclear contributions in a hitherto inaccessible regime.

B.I.3.4 Control and real-time observation of electron dynamics in molecules and clusters

Much of our present-day understanding of physical, chemical and biological processes stems from studies where dynamics in these systems is triggered by photoexcitation. A sound example is the tremendously successful field of femtochemistry, which was honoured with the award of Nobel Prize to Ahmed Zewail in 1999. Importantly, in a molecule light fields interact primarily with electrons, whose motion subsequently drives nuclear dynamics resulting in structural changes and possibly in chemical reactions. Femtochemistry was able to access this nuclear motion only. The recent advent of the experimental tools and techniques of attosecond physics has – for the first time – opened the door to observing in real time how the motion of electrons drives structural dynamics. Just as *femtochemistry* is the science of “making the

molecular movie", *attophysics* will allow zooming in on the most fundamental molecular building block, the electron.

Currently available laboratory-scale attosecond technology offers sub-femtosecond XUV pulses for probing but is unable to provide energetic attosecond pulses for exciting a substantial fraction of the irradiated specimen. Intense attosecond UV and VUV pulses from ALS will constitute ideal tools for setting – with attosecond precision – dynamics going in a large fraction of identical molecular systems under study. Attosecond pulses at carefully selected (filtered) wavelengths will allow triggering reactions by excitation localized to a selected atomic constituent and thereby to a selected geometric site within the molecule, opening the way to site-selective time-resolved chemistry through VUV/XUV excitation. Furthermore, frequency-domain shaping of the energetic attosecond UV/VUV pulses from ALS will allow simultaneous population of several excited electronic states (rather than only the LUMO state) in a well-controlled single-photon excitation process (in contrast to strong-field control, where several laser photons are involved in the transitions to higher electronic states). These intense sub-fs-to-few-fs UV/VUV pulses will not only launch an electron wavepacket on molecular orbitals but – due to their controlled waveform – also be able to steer its subsequent motion within the molecule.

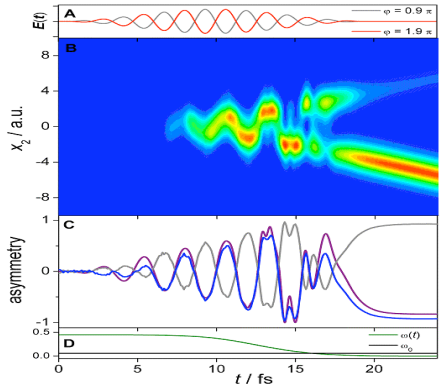

Fig. 7: *Modelling of dissociative ionization of D2 into D^+ + D: after the formation of $D2^+$, the remaining electron oscillates back and forth between the two nuclei before getting trapped on one of them. On which one was experimentally shown to be controllable by the carrier-envelope phase of the few-cycle driver laser.*

These technical capabilities may revolutionize physical chemistry. A few examples of unprecedented research opportunities are listed, below.

Photoionizaton of molecules such as C_{60} reveals the presence of broad resonances thought to be due to collective excitation of the 240 delocalized electrons with lifetimes in the range of 0.5-1 fs. Both the collective excitation and the subsequent decay mechanisms are barely understood. Direct insight into the underlying physics can be gained by means such as XUV pumping and VUV probing at ALS. In addition, the high brightness of ALS would allow resonant multi-photon excitation through the plasmon resonance, providing a unique signature of the collective nature of the excitation process.

Recent experiments have shown that control of the waveform of a few-cycle laser pulse can be used to control the motion of electrons in small molecules such as hydrogen (Fig. 7). ALS will permit extension of this capability to complex systems by creating a localized electron wavepacket with a VUV-UV trigger pulse and steering its subsequent motion in the molecule with the controlled electric field of an ultrabroad-band UV-VIS-IR control pulse. Real-time observation will be accomplished by a time-delayed attosecond VUV/XUV pulse.

These investigations will provide – for the very first time – direct insight into the influence of electron motion on chemical and biochemical reaction pathways.

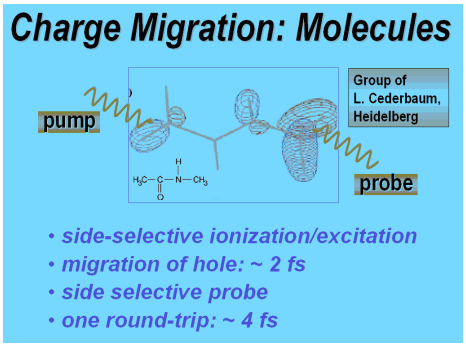

Fig. 8: *Illustration of ultra-fast charge migration due to electronic correlation in a small molecule as predicted by theory and schematic of a side-selective experimental pump-probe scheme.*

A topic of great current interest is, for instance, charge migration in biomolecules, which is believed to occur due to purely electronic rearrangement following localized excitation. Calculations indicate (Fig. 8) that a (positively-charged) localized hole state can migrate over the whole molecule within a couple of femtoseconds and lead to breakage of a chemical bond far away from the site where the hole was originally created. ALS will provide ideal opportunities for studying these and related processes, which are believed to play a fundamental role in bioenergetics, in real time.

B.I.3.5 Real-time observation of electron transfer processes at interfaces

Electron transfer processes of valence electrons constitute the fundamental step in photochemistry, electrochemistry, and electron transport across boundaries. Understanding the underlying mechanisms has important implications for a range of fields from material to life sciences. The time scale of electron transfer is determined by the interaction strength of the donor and acceptor states. For weakly interacting states, e.g. image potential states at metal surfaces, the electron transfer dynamics has been studied in the last decade by femtosecond laser pulses. For stronger covalent interactions, electron transfer occurs on an attosecond time scale and has been inaccessible in the time domain so far. Frequency-domain experiments using high-resolution resonant X-ray spectroscopy indicate transfer times well into the attosecond regime, e.g. for sulphur covalently bound on a transition metal substrate. However, this method does not provide real-time resolution as in pump-probe experiments and is based on assumptions about the relaxation dynamics.

A question highly relevant to fundamental physics is the dynamics of electron correlations and screening of charge carrier excitations in solid-state materials with high electron density. Theoretical estimations show that the screening is built up within the inverse plasma frequency, i.e. well below 1 fs. ALS with its attosecond VUV-pump/VUV-probe capability offers a unique opportunity to address these problems experimentally. Figure 9 illustrates possible generic schemes for probing electron transfer and screening processes at interfaces in a wide range of systems in real time.

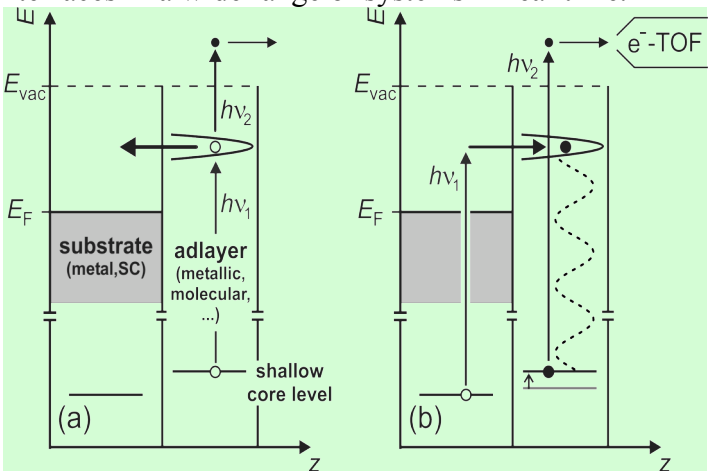

Fig. 9: *Proposed schemes for attosecond real time observation*

In a more general context, these studies aim at probing the evolution of non-stationary electron wave functions in condensed matter. In scheme (a) a VUV laser pulse $h\nu_1$ resonantly populates an occupied state in an adlayer. A subsequent pulse $h\nu_2$ monitors the ultrafast electron transfer to the substrate, which provides a sink for electrons. The electron transfer between the solid (acceptor) and the adlayer (donor) is thereby analyzed. Various model interfaces such as Bi/Si, CO/Pt, and H_2O/metal allow addressing key questions for material science, catalysis, and life science. On the other hand, scheme (b) shows that charge screening can be studied by probing the change in binding energy upon electron injection into an unoccupied state of the adlayer. Due to electron-electron interaction the binding energy of a shallow core level will be renormalized upon electron injection. This change in binding energy is monitored in the photoelectron kinetic energy by a time-delayed second VUV pulse.

B.I.3.6 4-dimensional microscopy of electron dynamics with nanometer-resolution in space and attosecond resolution in time

Beyond a broad range of electron dynamics in isolated atoms and molecules, a rich variety of ultrafast electronic motion, important for many ongoing and future developments, occur on surfaces and in solids. Emphasis in surface science and nanotechnology is shifting towards ever more complex architectures. These include layers of large organic molecules and biomolecules, self-assembly of monolayers and of supramolecular structures on surfaces and nanoparticle formation. In all applications, ranging from functionalized surfaces of nanoparticles to solar cells based on dyes on surfaces, bio sensors and molecular electronics, insight into electronic dynamics is a prerequisite for modelling and optimizing surface-based systems.

In the field of semiconductor nanostructures, the realization of fully-quantized systems has allowed the development of optoelectronic devices that have true quantum mechanical functionality. Probing these systems with attosecond temporal resolution will provide direct access to the processes responsible for quantum state dephasing, the origin of which is ill-understood. Insight into the nature of such processes is essential to the development of solid-state coherent quantum devices such as hardware for utilization in quantum information technologies.

ALS-based attosecond techniques will grant access to even the fastest electronic processes on surfaces and in solids, including those relating to the motion of electrons as well as their spin dynamics. Selecting its radiation at the highest photon energies (~1 keV) will offer attosecond temporal resolution combined with nanometre spatial resolution by means of attosecond soft-X-ray diffraction. This 4D microscopy will allow – for the first time – recording of movies of electronic dynamics in nanometre-scale molecular and solid-state structures with truly electronic attosecond time resolution.

B.I.3.7 Objectives of time-resolved attosecond Science

We now summarize the main goals expected on ELI at different intensity levels.

1. Inner-shell nonlinear optics and coherent control, relativistic atomic and molecular physics
2. Real-time observation of intra-atomic electron dynamics
3. Control and real-time observation of electron dynamics in molecules and clusters
4. Real-time observation of electron transfer processes at interfaces
5. 5 4-dimensional microscopy of electron dynamics with nanometre resolution in space and attosecond resolution in time
6. Laser generation of relativistic proton beams
7. Electron acceleration in wake field bubbles
8. Relativistic electron transport beyond the Alfven limit
9. Application to chemistry, radiolysis

Time-resolved plasma physics with ELI (see section Plasma Physics)

10. Electron acceleration in wake field bubbles
11. Relativistic electron transport beyond the Alfven limit

Time-resolved in material science (see section Material Science)

12. Time-resolved defect creation with laser-produced ions

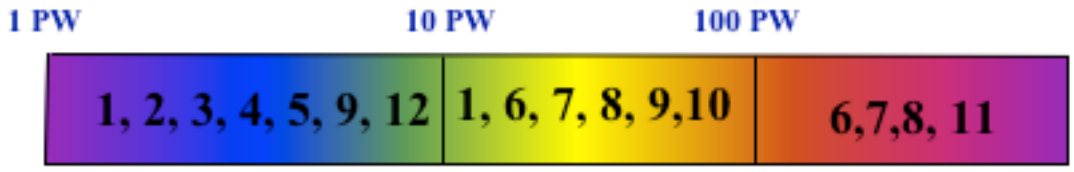

B.II Beam Physics: Laser plasma accelerators and high energy physics

B.II.1 Status of relevant research, scientific context, objectives and planned achievements

Particles and radiation have many applications in several fields of activity. Today, particles are produced by linacs, synchrotrons, X-ray tubes or radioactive nuclei. They are used in, for example, medicine (radiotherapy, imaging by PET), chemistry, agro-alimentary, material science, nuclear physics and many other domains. The parameters of these sources (energy range, cost, brightness, duration etc…) are limited. It has been demonstrated very recently - both experimentally and theoretically - that particles and radiation sources can be produced by intense lasers.

Extremely high electric fields, with values in excess of 1 TV/m (Malka 2002), have recently been produced by focusing ultrashort high-intensity laser pulses onto targets. Depending on the target (gas jets, thin foils, clusters, etc…), it is possible to generate radiation (from X-ray to γ-ray) and energetic particles (ions and electrons). The pulse duration and brightness of these beams make them unique and different from conventional accelerator sources. Since the value of the electric field is more than 10,000 times greater than electric fields generated in RF cavities, the length required to generate these sources (less than one millimetre) is orders of magnitude smaller than that required by conventional means. Ultra-intense laser systems thus allow the realization of new physics with potentially important applications in the near future. ELI will serve as a research centre for development and application of laser-based particle acceleration in both the intense and ultra-intense regimes.

B.II.2 Electron beam produced by laser

B.II.2.1 State-of-the-art

The state of the art of laser plasma accelerators is the bubble regime, in which quasi-monoenergetic electron beams with high charge and low emittance can be achieved. Laser Wake Field Acceleration (LWFA) works for laser pulses shorter than the plasma wavelength. When driven into the highly non-linear wave-breaking regime, the wake field takes the form of a solitary bubble (Pukhov 2002). In the bubble regime, ultra-short bunches of electrons with superior properties are produced. Large amounts of electrons are self-trapped and accelerated to relativistic energies (γ-factors of 100 - 1000) with high efficiency. Very dense low-emittance pulses are created and, most importantly, quasi-monoenergetic electron spectra are obtained.

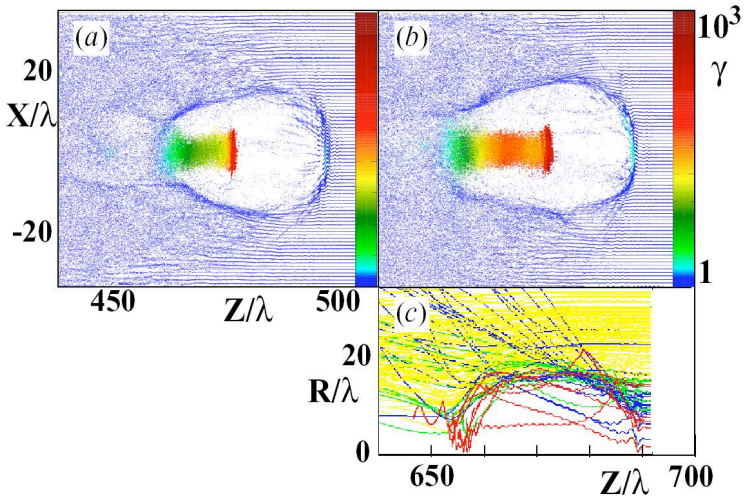

Fig. 1: *3D particle-in-cell simulation. Solitary laser-plasma cavity produced by 12-J, 33-fs laser pulse. (a) ct/λ=500, (b) ct/λ=700, (c) electron trajectories in the frame moving together with the laser pulse. Trapped electrons are coloured red.*

Currently, the parameters of the electron beam are as follows: energy up to 175 MeV, total charge of 0.5 nC, divergence of a few mrad, and ~10 fs duration.

The trapping of electrons and the evolution of their energy distribution are continuous (Fig. 2). At time ct/λ=350, the high-energy branch of the spectrum corresponding to the stem of Fig. 1 still has a plateau structure. However, the spectra shown in Fig. 2 change at time ct/λ=450 and develop a distinct peak which grows in time. This peak starts to appear when the total charge of the stem becomes equal to the charge expelled from the cavity by the driving laser pulse. The cavity then elongates, this having the consequence that the front and rear sides of the cavity move at different speeds. The base at which the stem is fed by fresh electrons then lags behind, this producing the monoenergetic spectral feature. Clearly, there is an accumulation of electrons with $\gamma \approx 600$, which explains the peak in the spectrum.

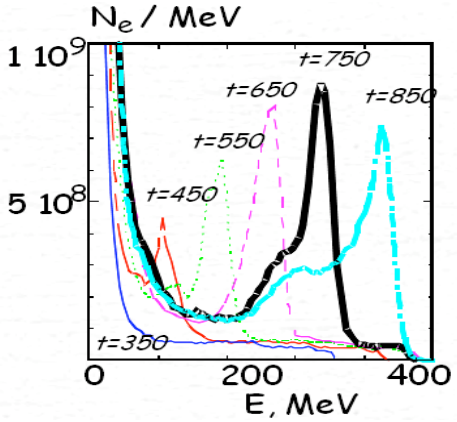

Fig. 2: *Time evolution of the energy spectrum: 1: ct/λ=350, 2: ct/λ=450, 3: ct/λ=550, 4: ct/λ=650, 5: ct/λ=750, 6: ct/λ=850.*

In the very first experiments conducted in the bubble regime, monoenergetic electron beams in the range from 70 to 170 MeV were measured [Mangles 2004; Geddes 2004; Faure

2004]. The experiment done at LOA shows the sharp dependence of the beam quality on the laser and plasma parameters. The laser pulse with an energy of 1 J and a duration of 30 fs was focused onto a 3 mm long gas jet. The focal spot size was chosen such that the Rayleigh length of the laser pulse corresponded to the plasma size. Figure 3 shows the transverse quality of the electron beam as a function of the plasma density.

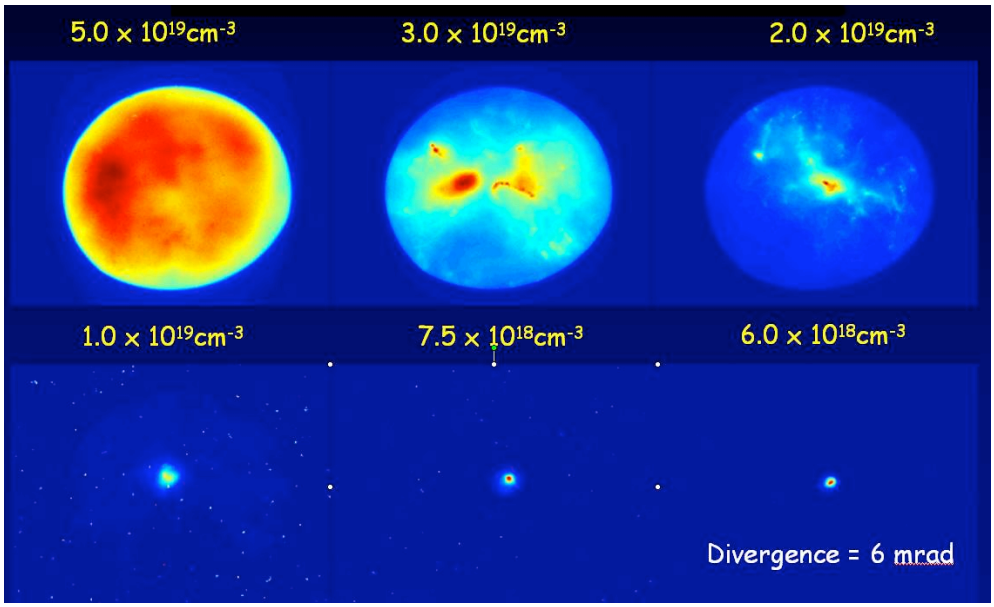

Fig. 3: *Spatial quality of electron beam obtained in the LOA experiment as a function of the plasma density [Malka 2005].*

One sees that the beam spatial quality improves abruptly at densities below 10^{19} cm^{-3}. At this density, the laser pulse duration becomes equal to the plasma period. The same behaviour is seen in the energy distribution of the electrons: the electron beam spectrum evolves from quasi-thermal to monoenergetic once the laser pulse duration becomes smaller than the plasma period (Fig. 4). The LOA experiment has been simulated with the 3D PIC code VLPL. The simulation results confirm that the wake field of the laser pulse takes the form of the solitary cavity.

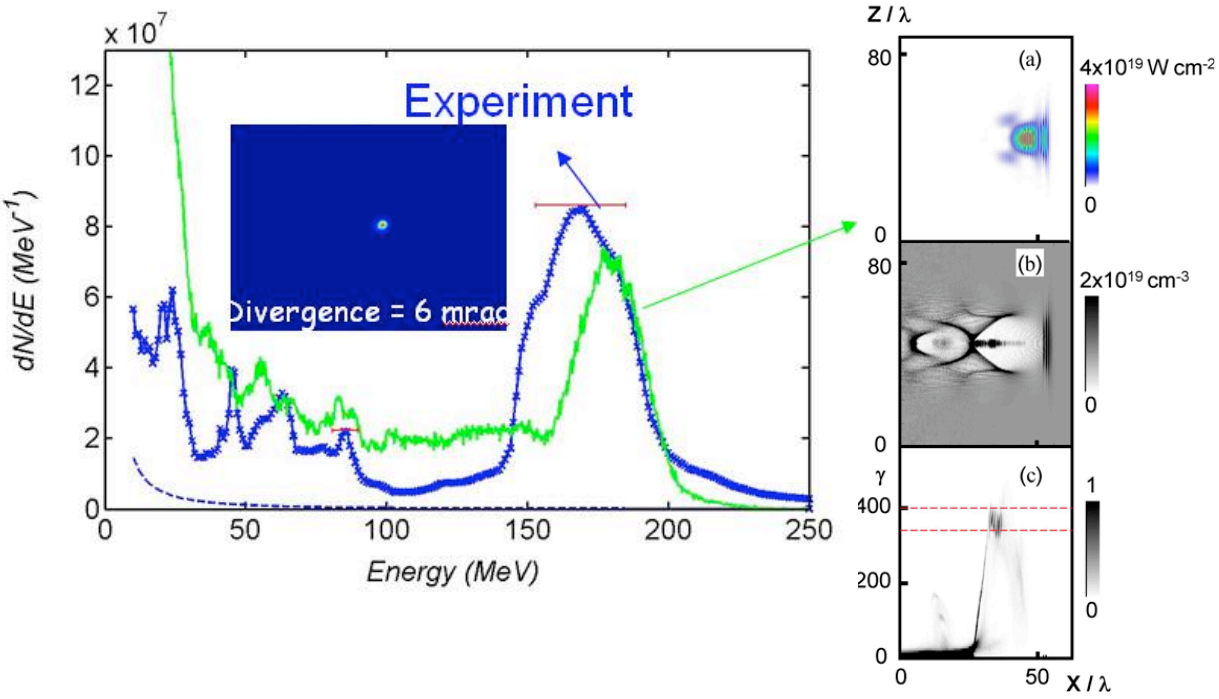

Fig. 4: *Comparison of the 3D PIC simulation with the LOA experiment [Faure 2004].*

B.II.2.2 Future developments and applications

Several ideas have been proposed to improve the parameters of the electron beam: an ultra-short and mono-energetic electron beam can be produced by using two laser beams with moderate intensity in combination with a plasma channel. Another solution is to use a more powerful laser system. Successful workshops dedicated to the application of laser-based accelerators, funded by the European Science Foundation, offer possibilities of considering different approaches and generating new collaborations between the different European groups. Since mono-energetic electron beams can be used for the future generation of photo-injectors, this research is also of importance to the accelerator physics community.

New science has already been performed with these sources, which extend the well-known parameter regimes of electron beams to ultra-short durations. It has been shown that ultra-short electron beams generated with a laser are perfectly synchronized with the laser and can be used for pump-probe experiments. Such experiments can provide a fundamental understanding of the first events occurring in radiolysis with particles (Brozek-Pluska 2005).

The availability of relatively inexpensive, compact accelerators for a wide range of electron energies (0.1-2 GeV) or proton energies of (10-200 MeV) should make them affordable to universities and industries. The first part of the ELI project is to demonstrate significant progress towards the achievement of compact laser plasma accelerators in the GeV range and to offer these sources to users.

B.II.2.3 Particle beam generation experiments at the PW (first stage of ELI) level

The aim is to promote new science and applications with new particle beams with a PW-class laser:

- Electron beam line for applications of the quasi-monoenergetic electron beam at 200-300 MeV for fast chemistry, radiotherapy (Glinec 2005) and material science (see Applications section).

To improve particle beam parameters:
- Quasi-monoenergetic electron beam produced in the bubble regime, with energies of up to 1.5-2 GeV, charge in the nC range, duration less than 30 fs and few-percent energy spread. Numerical simulations done with 3D PIC codes by different groups indicate that such achievement will be realized with such as lasers (Tsung 2004, Gordienko 2005).

- Monoenergetic electron beam with energies of up to 1 GeV, charge in the nC, duration less than 30 fs, produced in a two-stage approach, 1 % energy spread. To control and reduce the bandwidth of the electron beam, we will consider injection of a low-energy electron beam into a long plasma wave in the cm scale length; this plasma wave will be excited in the weakly non-linear regime. Such a scheme will permit one to avoid self-trapping of electrons and benefit from the focusing of the plasma wave arch. According to particle simulations, the GeV level and low energy spread (1%) will be achieved at this stage (Malka 2005, Lifshitz 2005). We present in the figure below the final electron distribution of the beam produced in the bubble regime and accelerated into a long plasma wave structure produced in homogenous plasma and into a plasma channel.

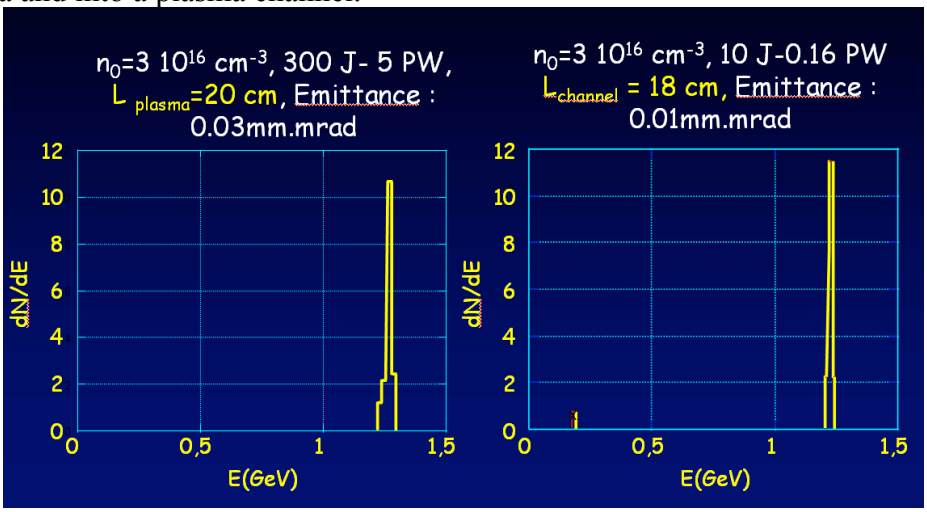

Fig. 5: *Simulation of a staged acceleration [Malka 2005]*

The injected electron beam will be produced in the bubble regime and/or by using the state of the art of conventional accelerators as performed in the Netherlands by the group of M. Van der Wiel (TUE), in Scotland by the group of D. Jaroszynski (Strathclyde), in France by the group of T. Garvey (LAL) and in Frascati by the group of L. Serafini (INFN).

Special tasks will be dedicated to the development of targets such as capillary discharges, capillary, gas-filled chambers and gas jets in order to increase the potential interaction length.

The very important quality of the bubble acceleration regime is its scalability. This is shown in the similarity theory (Gordienko 2005). Using a fully kinetic approach, it was shown that the similarity parameter $S=n_e/a_0\ n_c$ exists, where $a_0=eA_0/m_ec^2$ is the relativistically normalized laser amplitude, n_e is the plasma electron density and $n_c = m_e\ \omega_0^2\ /4\pi e^2$ is the critical density for a laser with the carrier frequency ω_0. The basic ultra-relativistic similarity states that laser-plasma interactions with different a_0 and n_e/n_c are similar as soon as the similarity parameter $S= n_e/a_0 n_c$ =const for these interactions. The basic S-similarity is valid for both over- and underdense plasmas. In the special limit $S<<l$, the parameter S can be considered as a small parameter and quite general scalings for laser-plasma interactions can be found. It follows from the theory that in the optimal configuration the laser pulse has the focal spot radius $k_pR\sim a_0^{1/2}$ and the duration $\tau < R/c$. Here, $k_p=\omega_p/c$ is the plasma wave number and ω_p is the plasma frequency. This corresponds to the "bubble" acceleration regime.

The central result of the theory is that the bubble regime of electron acceleration is stable, and scalable, and that the scaling for the maximum energy E_{mono} of the monoenergetic peak in the electron spectrum is

$$E_{\text{mono}} \approx 0.65\ m_ec^2\ [P/P_{\text{rel}}]^{1/2}\ c\tau/\lambda$$

Here, P is the laser pulse power, $P_{\text{rel}}=m_e^2c^5/e^2 \cong 8.5$ GW is the natural relativistic power unit and $\lambda=2\pi c/\omega_0$ is the laser wavelength. This scaling assumes that the laser pulse duration satisfies the condition $c\tau < R$. The scaling for the number of accelerated electrons N_{mono} in the monoenergetic peak is

$$N_{\text{mono}} \approx 1.8/k_0r_e\ [P/P_{\text{rel}}]^{1/2},$$

where $r_e=e^2/m_ec^2$ is the classical electron radius, and $k_0=2\pi/\lambda$. The acceleration length L_{acc} scales as

$$L_{\text{acc}} \approx 0.7\ c\tau/\lambda Z_R,$$

where $Z_R=\pi R^2/\lambda$ is the Rayleigh length.

The parametric dependences in these scalings follow from the analytical theory. The numerical pre-factors are taken from 3D PIC simulations. These pre-factors may change, depending on the particular shape of the pulse envelope. However, as soon as the envelope of the incident laser pulse is defined, the pre-factors are fixed. The parametric dependences are universal and do not depend on the particular pulse shape.

a_0=4

P(PW)	τ (fs)	n_e(cm^{-3})	W_0 (μm)	L(m)	E(J)	Q(nC)	E(Gev)
0.12	30	2e18	15	0.009	3.6	1.3	1.12
1.2	100	2e17	47	0.28	120	4	11.2
12	300	2e16	150	9	3.6k	13	112
120	1000	2e15	470	280	120k	40	1120

Table 1: *Numerical examples of the electron beam energy scalings (W. Mori et al., UCLA).*

B.II.2.4 Objectives for the second stage at laser power levels in the 10 PW range (with laser pulses of a few 100 fs)

Efficient electron acceleration in the 10-100 GeV range is expected to be reached in the bubble regime (Gordienko and Pukhov 2005). The same range of energy can also be reached by using a multi-stage approach. Both approaches will be considered.

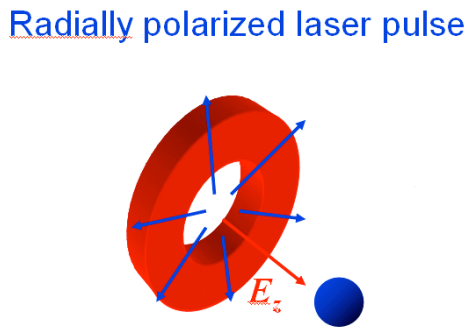

Fig. 6: *Radially polarized laser pulse has zero transverse and maximum longitudinal electric field on-axis.*

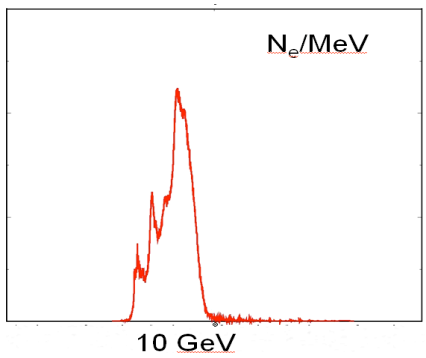

Fig. 7*: Electron spectrum (a.u.) from the 3D PIC simulation of electron acceleration in vacuum.*

ELI will also permit exploration of direct laser acceleration in vacuum, which can occur in the case of intense laser pulses with amplitude a_0>>1. To keep the electron bunch spatially confined, one should use the radially polarized laser pulse shown in Fig. 6. The radial electric field focuses the electrons, while the strong longitudinal component accelerates them forward. 3D PIC simulations suggest that a nanobunch of electrons can be accelerated in vacuum to multi-GeV energies in this way. The electron spectrum obtained in the simulation for a 100-J, 5-fs laser pulse is shown in Fig. 7.

B.II. 3 Proton beam produced by laser

B.II. 3.1 State-of-the-art

Until now, proton beams with energies of up to tens of MeV (Clarks 2000, Snavely 2000) and very low emittance (0.01mm.mrad) have been produced by focusing a laser beam onto a thin foil target (Cowan 2004). More recently, it was experimentally demonstrated that quasi-monoenergetic ions (Hegelich 2006) or proton beams (Schwoerer 2006) in the MeV range can be achieved. Ions can be accelerated at the front surface of an overdense plasma by a short laser pulse. In this configuration, the laser ponderomotive pressure pushes the background electrons, and a double layer is produced at the boundary of the overdense region. The ions are accelerated by the electrostatic field of the double layer. If the laser intensity is so high that the plasma becomes relativistically transparent, then ion trapping in the running double layer and acceleration to relativistic energies are possible. Ion acceleration is especially efficient in two-component plasmas. In this case, the ions with the largest charge-to-mass ratio get the highest energies.

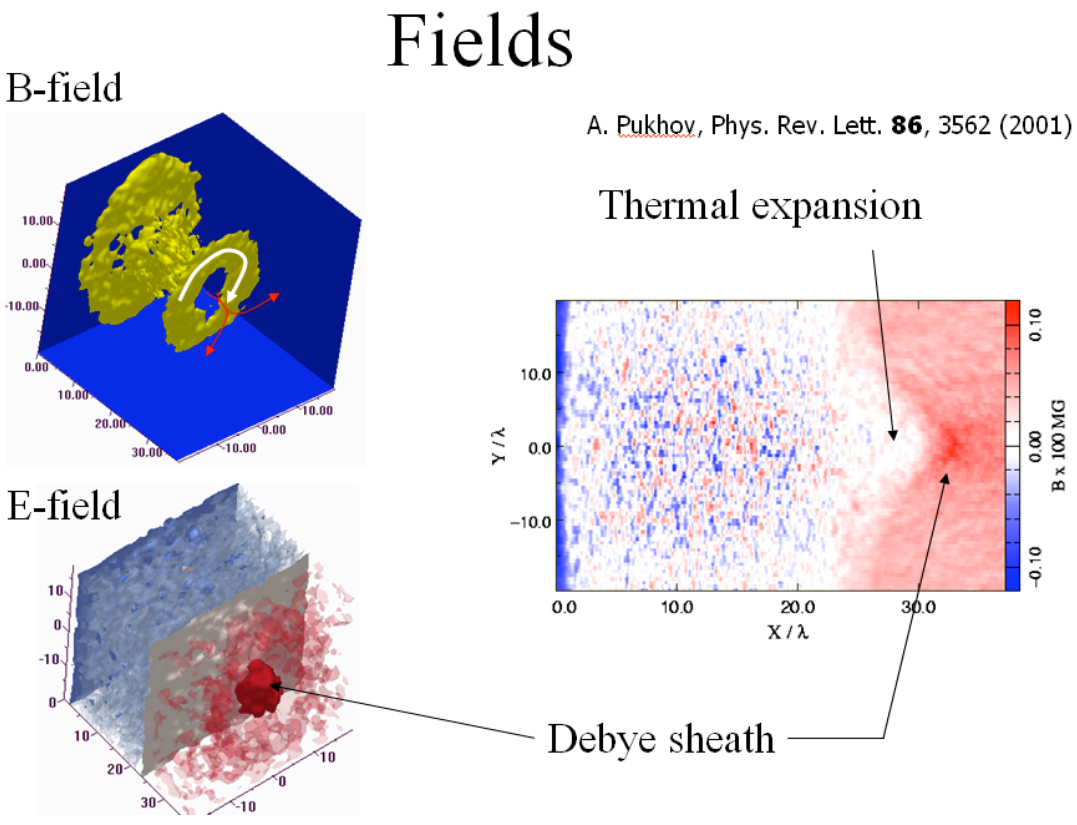

Fig. 8: *Electric fields surrounding a plasma foil irradiated by a short-pulse laser. The red colour marks the Debye region, where the uncompensated spatial charge of the hot electrons accelerates ions.*

Another possibility of ion acceleration is plasma expansion at the rear surface of a plasma foil. In this case, the ions are accelerated in the Debye layer produced by the spatial charge of the hot electrons, produced by the laser pulse (Fig. 8). The hot electrons travel through the overdense plasma region and exit in vacuum, where the ion accelerating field is generated. One can expect quasi-monoenergetic ion spectra if one exploits double-layer targets. In this case, a foil made of high-Z material is covered by a monolayer of protons. All the protons in the monolayer experience the same electric field and are accelerated to the same energies. This leads to a quasi-monoenergetic proton spectrum (Fig. 9).

B.II. 3.2 Future developments and applications

B.II. 3.2.1 For the first stage with current laser technology: 1 PW

Proton production and acceleration can be improved on several fronts. First, increasing the 30-fs laser power to the PW range will make it possible, according to theoretical simulations, to extend the maximum energy to 200 MeV. Second, the number of protons with moderate energy (few MeV) can be increased by optimizing the laser and target parameters. Both high and modest energy protons are of interest for medical applications. Since the source beam quality is very good, one can consider using these beams as proton (ion) injectors. For medicine, two main applications will be considered:

First, proton therapy assisted by lasers. Here, the proton energies ought to be within the therapeutic window: between 70 and 250 MeV. To reach this goal, compact high-repetition-rate PW lasers need to be developed (Malka 2003, Bulanov 2002). This would offer an economical proton source for hospitals to treat cancer tumors. This scheme will therefore feature several major advantages: *(i)* Thanks to a major scale reduction (as compared wuth vast stand-alone cyclotron sites), it brings the treatment facility to a normal hospital environment. *(ii)* It enables easy beam orientation without expensive isocentric gantries. *(iii)* It could reduce cost and thus make this superior treatment more widely available. *(iv)* Simultaneous in-beam imaging with the same device could be envisioned (generation of radionuclides). For this purpose, proton beams with a Maxwellian-like or a quasi-monoenergetic distribution will be produced. The quasi-monoenergetic proton beam was predicted on the basis of numerical simulations (Esirkipov 2002) and was recently measured, as published in “Nature” this year. Ion beams, such as carbon or lithium beams, will also be produced, since they appear to be of major interest for hadron therapy. One can expect quasi-monoenergetic ion spectra if double-layer targets are exploited. In this case, a foil made of high-Z material is covered by a monolayer of protons. All the protons in the monolayer experience the same electric field and are accelerated to the same energies. This leads to monoenergetic proton spectra (Fig. 9).

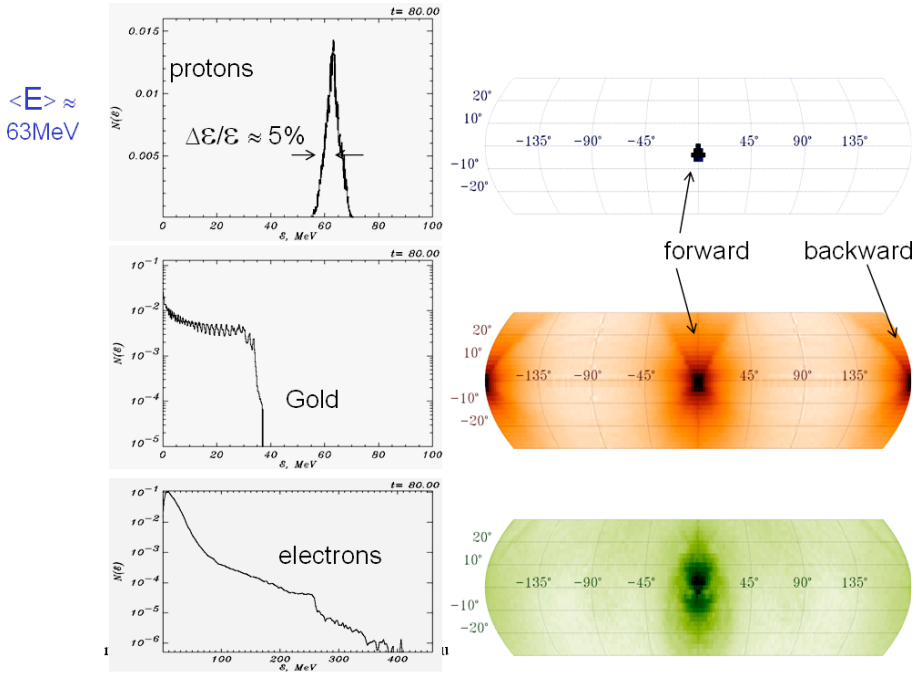

Fig. 9: *Electric fields surrounding a plasma foil irradiated by a short pulse laser. The red colour marks the Debye region, where the uncompensated spatial charge of the hot electrons accelerates ions (Eserkipov 2002).*

The use of particle beam selectors (Fourkal 2003) will be considered for all these schemes since they relax the constraint of stability and reproducibility of the particle beam from shot to shot.

Secondly, medical applications are also envisaged with the production of short-lifetime radioisotopes for PET (Ledingham 2004). For this purpose, it was concluded from the existing data that a 100-TW laser operating in the kHz regime will be needed, whereas theoretical work indicates that by optimizing laser plasma parameters the laser constraints will be relaxed (Fritzler 2003).

ELI will allow estimation of the cost and optimization of the source through the guidance of radiotherapists. Interaction with laser and cyclotron companies will be encouraged to study the economics (cost, development, industrialization, market) and reinforce links between industry and research. Electron and proton beams with a pulse length in the ps or fs time scale will provide a unique opportunity to study new and important biological radiation effects.

B.II.3.2.2 For the second stage with laser power in the 10 to 100 PW range

Efficient proton acceleration in the 1-10 GeV range in a new (piston) regime would be investigated. Here, about 10^{12} protons in the 5-6 GeV range are expected (Pukhov 2003) and

will be used for laser-driven heavy-ion collider experiments with about 1 million events per laser shot (Ersikepov 2004).

B.II.4 High-energy Physics

The particle physics community is almost ready to start the Large Hadron Collider at CERN with proton beams of up to 7 TeV in a circular machine. But the composite character of the proton and its drawbacks, such as unknown initial-state energy and huge backgrounds, makes an electron collider still a must. Unfortunately, the small mass of the electrons makes them radiate heavily in a magnetic field and it is therefore not possible to use circular accelerators above an energy of around 100 GeV. Linear electron accelerators on the TeV scale are currently under design and the International Linear Collider (ILC) project is proceeding. Here the limitation is no longer the field needed to curb the trajectories but the accelerating gradient. For ILC, a technique with superconducting accelerating cavities was chosen but it is intrinsically limited to about 50 MVm^{-1}. Other techniques, such as the double accelerator technique, under development at CERN, could lead to more than 100 MVm^{-1} but no classical technique seems to promise the gradient needed for the further steps. Under these circumstances, there is a strong interest in high-energy particle physics for novel techniques such as plasma or laser-plasma acceleration.

It is to be noted that the idea in this project is not that a TeV electron accelerator be immediately proposed, but that ELI make an experimental evaluation of the main issues:

- To reach the TeV range, should linear or highly non-linear modes be used?
- What should be the properties of the beam to be injected in a plasma cavity?
- What impact do very short electron bunches have on luminosity?
- How monochromatic can the beams be?
- What emittances can be obtained and what repetition rates?
- Is the power efficiency of a laser system acceptable?
- What about producing and accelerating positrons?
- What about electron and positron polarization?
- Etc...

There are numerous questions to work on in parallel in order to establish the realism of such a project.

These studies will be organized in steps with clear milestones taking into consideration sub-projects which could make some valuable contributions to the community. Some are under consideration, such as a compact and energetic injector. A challenging realization would be a compact and efficient positron source. Such sources are currently obtained from electron beams by creating photons through collisions with matter (bremsstrahlung) and subsequently electron-positron pairs. More recently, sources where the photons are obtained from electrons passing through undulators have been considered, or sources using Compton backscattering. Powerful lasers play an important role in the latter but plasma undulators could also bring a very interesting solution.

Even simpler developments can be extremely useful. For the development of detectors, for their calibration, electron (or proton) beams of up to a few GeV are needed. Finding them at the large accelerator centres is becoming difficult with the closing of many utilities in the world. This need would be met by having, close to laboratories developing detectors, facilities delivering medium-energy beams, but the way of using these beams for this purpose has to be found. More generally, the beams obtained by laser-plasma acceleration have properties quite different from those of classical beams. Does this really mean drawbacks or rather new opportunities? Some studies and some imagination are needed.

It should be clear that the interest expressed here is not a European singularity. Programmes along the same lines are being considered in many other places bringing laser and plasma specialists into conjunction with high-energy physics people. In the HEP community, the interest in a detector testing facility would be rather local, involving about a hundred physicists and engineers from surrounding laboratories, depending on the performance of the beam. The interest in a positron source or even more in a high-energy accelerator would be much wider, on an international scale, and involve thousands of physicists.

B.II.4.1 Laser-produced pions, muons, neutrinos

At much higher intensities, of 10^{23} W/cm^2, and 15 fs duration, PIC simulations performed by Pukhov *et al*, 2003, show that the interaction with a solid 50 μm, target with an electron density of n= 10^{22} cm^{-3} leads to an electron beam of 5GeV followed by a proton beam of 5GeV. It should be noted that the electrostatic field gradients involved are of the order of the laser transverse field gradients of 500 TeV/m at 10^{23} W/cm^2. Bychenkov 2001, carried out 2DPIC simulations to determine the laser intensity threshold for pion production by protons accelerated by relativistically strong, short laser pulses acting on a solid target. The pion production yield was determined as a function of the laser intensity. It was shown that the threshold corresponds to s laser intensity exceeding 10^{21} W/cm^2. The pion has a rest mass of ~140 MeV and a lifetime at rest of only 20ns. This short lifetime prevents acceleration of the low-energy pions.

At and acceleration rate of 10 MeV/m, the pions will disintegrate into muons and neutrinos before they have time to be significantly accelerated. Prompt acceleration offers a completely new paradigm for high-energy physics. Over a distance of the order of only a mm, the pions can be accelerated to many times their mass, say 100 times (Bychenkov 2001). This decay will provide collimated muon and neutrino beams.

B.II.4.2 Increasing the τ-lepton lifetime

It is interesting to see that the next lepton would be the tau with a mass of 1784 MeV and a lifetime of 300 fs. It should be noted that 300fs corresponds to100 μm, a very short distance for conventional acceleration. This distance would, in principle, be sufficient for prompt acceleration to accelerate a τ lepton to several times its mass and increase its lifetime accordingly.

B.II.5 Objectives for beam physics/high-energy physics

Summarized below are some of the main goals at each intensity level.

Electron
e1 quasi-monoenergetic 1-1.5 GeV
e2 two-stage generation and acceleration
e4 100GeV beam

Proton
p1 generation of 200 MeV protons
p2 generation of 1-10 GeV protons

High-energy physics questions:

E1. TeV accelerator, should linear or highly non-linear modes be used?
E2. Can we inject a beam in a plasma accelerator?
E3. What impact do very short electron bunches have on luminosity?
E4. How monochromatic can the beams be?
E5. What emittances can be obtained and what repetition rates?
E6. Is the power efficiency of a laser system acceptable?
E7. What about producing and accelerating positrons?
E8. What about electron and positron polarization ?

Pion **π pion generation**
τ **τ generation, increasing its lifetime**
Positron **P1 positron generation**

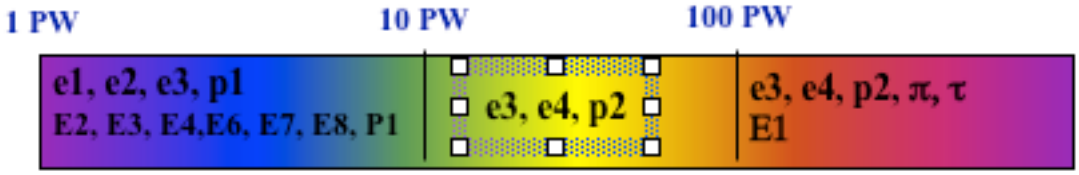

B.III. Laser-produced X-Ray Beam

B.III.1 State-of-the-art

Hundreds of fs Kα lines are commonly produced by focusing an ultrashort laser on a solid target (Rischel 1997, Rousse 2001). Recently, synchrotron-type X-ray radiation has been efficiently produced by focusing an ultra-short laser pulse on a gas jet. Millimeter-scale laser-produced plasma is used to create, accelerate and wiggle ultrashort and relativistic electron bunches. As they propagate in an ion channel produced in the wake of the laser pulse, the accelerated electrons undergo betatron oscillations and generate a femtosecond pulse of broadband radiation in the few-keV spectral range within a narrow 10-mrad cone (Rousse 2004).

B.III.2 Future developments and applications

One of the main goals in our scientific community is to producte femtosecond beams in the X-ray spectral range, which would open an entirely new field of research in multidisciplinary fields. In the detailed characterization of atomic processes, the shortest time of interest is of the order of the elementary atomic vibration (100 fs). Studying the very first steps of reactions and probing ultrafast transient structures in solid-state physics and bio-chemistry then call for production of 100-fs X-ray flashes to probe each ultrafast event. The full movie of the reaction can be reconstructed by means of instantaneous pictures of the matter, recorded at different time delays following excitation, using a so-called “pump-probe” experiment for which the pump beam is used to excite the sample.

Energetic and ultrafast electron beams produced from laser-matter interaction may have dramatic applications in the field of X-ray production. Promising ideas for developing and improving X-ray sources based on laser-accelerated electrons have been proposed in recent years. Several schemes can be efficiently used to produce ultrafast X-rays. First, a second intense femtosecond laser beam could be focused on the relativistic electron bunch to produce X-rays by Compton scattering. Very hard X-ray beams, in the few-100 keV spectral range, could be generated by this method. Second, electrons can be wiggled in an ion cavity produced in the plasma and generate few-10 keV X-rays. Third, with appropriate electron bunch parameters, which could be obtained with ELI, ultrabright free-electron laser radiation can be produced in the X-ray range. The possibility of combining synchrotron features and femtosecond duration place these sources well beyond the limitations of existing large-scale instruments and laser-based sources. In the laser plasma community, three types of laser-based sources have been developed. They were demonstrated more than 10 years ago: high-harmonic generation and XUV lasers (collimated but not in the X-ray range); and the plasma X-ray tube (in the X-ray range but not collimated). Since that time there has been a race to group - in one source – the capabilities provided independently by the three existing ones: X-ray spectral range, collimation (a beam of radiation), polychromaticity and ultrashort pulse duration. However, none of these sources could at present offer all the capabilities cited above. The use of ultrafast electron bunches combined with the various wiggling methods proposed therefore represents a fully novel concept towards this goal. Here, the contribution of the

synchrotron physics community will allow the best strategy to be defined since these new sources have complementary parameters.

The project will have a tremendous impact in the X-ray field, opening unique opportunities for applications in science and technology. In particular, the high laser intensity will provide access to intense ultrafast X-ray beams of radiation with the following features:

- Ultrafast durations: 10 femtoseconds to a few attoseconds
- Spectral range: 1 nm to 0.01 nm
- Collimation: down to a few 10 μrad
- Production of spatially and temporally coherent beams
- Full synchronization with an ultrafast laser pulse for pump-probe investigations
- Brightness comparable to the forthcoming large-scale and costly X-ray infrastructures.
- Compactness and in expensive tool leading to high and wide dissemination in the user's community.

The possibility of producing X-ray beams with laser systems was recently shown. We demonstrated a first proof-of-principle experiment showing that relativistic electron bunches accelerated in laser-produced plasma could be efficiently generated and used for X-ray production. The laser intensity envisaged in the project will provide an invaluable jump in the X-ray beam characteristics as already quoted. Thanks to the strong laser and laser-produced plasma fields, the generation of X-ray radiation will enter a novel regime in which manipulation of the relativistic trajectories of energetic electrons plays a central role.

B.III.3 Compact X-ray beam

The overall goal of this ELI subproject is to provide *intense, ultra-short X-ray beams*. We thus propose using the ELI laser systems in order first to generate highly relativistic electron beams with unprecedented features and secondly to convert them into femtoseconds-short, brilliant X-ray pulses. Since there is no “ideal light” source for all applications together, we will develop complementary sources. We will realize laser-assisted synchrotrons, linear and non-linear Compton scattering, betatron radiation, and a free-electron-laser. With the help of the latter we will be able to provide an ultra-brilliant X-ray light source whose output parameters are comparable to those of the large-scale XFELs planned world-wide. Our concept has the tremendous advantage of being of only table-top size. Our table-top X-ray free-electron laser (TT-XFEL) could thus even be used in hospitals, e.g. for phase-contrast imaging or small-angle X-ray scattering (SAXS).

The success of this enterprise will critically depend on the feasibility of generating an ultra-short ($\tau_e \leq 10$ fs), monoenergetic ($\Delta E/E < 1\%$), low-emittance (<1 mm·mrad), high-current (≥150 kA) electron bunch, for which the ELI front-end petawatt laser creates ideal

prerequisites. Our goal is to develop this new X-ray laser technology and use it – in collaboration with other groups – for first proof-of-principle experiments.

The TT-XFEL project has already been proposed as an EU NEST project utilizing petawatt lasers at Max Planck Institute of Quantum Optics (Garching, Germany) and LOA. The key difference to the ELI project will be a much higher repetition rate and higher power with the ELI lasers. Only this advance would enable SAXS applications with reasonable exposure times and X-ray photon energies in the medically relevant energy region.

B.III.3.1 Motivation

So-called 4D imaging with spatial and temporal resolution on atomic scales allows structural and dynamic studies of atoms and molecules to be conducted. X-ray light has the advantageous property of wavelengths equal to or smaller than typical distances in molecules. Furthermore, X-ray photons have such high energies that they can ionize deeply bound electrons, opening the possibility of temporal studies of inner-shell ionization processes. Single molecule imaging, which is probably the most prominent scientific case for all XFELs planned world-wide, could provide a key tool for the structure-function relationship of all proteins which cannot be crystallized in practice. Another key application could be SAXS, which could provide medical information on normal, benign, or cancerous tissue**.** The high photon flux required could be provided with the TT-XFEL on a time scale and with a size suitable for clinical application. Medical imaging requires photon energies above 20 keV, which could only be reached with ELI lasers.

With the other light sources we can produce much higher photon energies, up to 100 keV, for various multidisciplinary applications such as in pump-probe experiments on a femtosecond time scale (ultrafast zooming on the atomic landscape) and in plasma physics (for probing dense matter). We will also be able to produce efficiently ultrafast beams of gamma rays for particle physics (γ-γ-colliders, neutron production).

B.III.3.2 Concepts

B.III.3.2.1 Laser-assisted synchrotrons

First of all, ELI lasers could be used solely for electron acceleration. The enormous accelerating fields in the range of TV/m allow electrons beams with up to 100 GeV to be generated (see Particle Beams section). Accelerated electrons thus have ultrashort bunch lengths (<10 fs) and large charges (>1 nC), and hence, ultrahigh beam currents (several 100 kA). The electrons can be efficiently used to produce innovative ultrashort X-ray radiation sources.

B.III.3.2.2 Compton scattering

In so-called Inverse Compton Scattering (ICS) a laser pulse collides with an electron bunch and forces the electrons to wiggle. This wiggle motion makes the electrons emit, just as in a conventional insertion device in a synchrotron, highly collimated synchrotron radiation in

the forward direction. The Doppler energy upshift allows one to reach high photon energies, e.g. 100 MeV γ-rays with a 10-GeV electron beam. ICS radiation produced with the 10-fs ELI laser systems has a duration comparable to the electron bunch duration, which in turn is expected to be on the same time scale as the laser pulse duration. While in linear Compton scattering only the fundamental wavelength is generated, non-linear ICS allows one to produce higher harmonics where the critical harmonic number scales with the third power of the dimensionless laser amplitude a: $n_c \sim a^3$ (TaPhuoc 2003). The laser amplitude provided by ELI can be as large as 280 (in the case of 150 PW) and can provide intense beams of ultrafast radiation in the MeV energy region.

B.III.3.2.3 Betatron

Laser-plasma accelerators not only generate highly relativistic electrons, but also force these electrons to wiggle around the laser axis, forming betatron oscillations. These oscillations, equivalent to oscillations in static wigglers, produce synchrotron radiation (Rousse 2004). The key advantage here is the small size of these laser-plasma betatrons and output parameters comparable to those of large synchrotrons. Again, the ultra-short electron bunch length implies ultrashort synchrotron pulses (10 fs) – much shorter than in any large-scale synchrotron.

B.III.3.2.4 Free-Electron Laser (FEL)

Any FEL requires an undulator, which is an arrangement of magnets with alternating transverse magnetic field orientation. Electrons in an undulator are forced on a sinusoidal trajectory and can thus couple with a co-propagating radiation field. The induced energy modulation yields a current modulation due to the dispersion of the undulator. This modulation is called **micro-bunching**, expressing the fact that the electrons are grouped into small bunches separated by one wavelength. Due to this micro-bunching electrons emit **coherent** radiation on this wavelength, which is determined mostly by the relativistic Doppler effect. In a **SASE FEL** there is no initial radiation field and the seed has to be built up by the spontaneous (incoherent) emission (SASE = Self-Amplification of Spontaneous Emission) (Bonifacio 1984).

Attaining sub-nm wavelengths calls for electron energies in the GeV range as those supplied by the proposed ELI lasers. While the large-scale XFELs planned require kilometre-long linear electron accelerators, our TT-XFEL can thus be realized in table-top size with revolutionary impact, such as providing XFELs to hospitals.

Though only a few metres in size, its peak brilliance, which is the measure of a light source's quality, is comparable to that of large-scale XFELs. This was found by the same simulation technique as used for all XFELs planned world-wide (Reiche 1999). The requirement for realizing a TT-XFEL is to generate GeV electron beams with low energy spread (<1%), low emittance (<1mm.mrad), and high currents (several 100kA). In our case the desired energy spread can be two orders of magnitude larger than the values of large-scale XFELs, because our TT-XFEL has a larger Pierce parameter (Bonifacio 1984), which defines the tolerance of an FEL. The same holds for, for instance, wake-field-induced additional

energy spread. Laser-plasma-accelerated electrons thus have just the right features to make a TT-XFEL, possible.

By comparison, our project will provide in expensive and compact table-top synchrotrons and XFELs providing intense and ultrafast X-rays for multidisciplinary applications. It will, in particular, constitute a decisive technological step towards the advent of powerful and compact X-ray infrastructures that will meet the demands of user's community: combination of ultrafast (femtosecond or shorter), intense and collimated X-rays perfectly synchronized with optical laser pulses to tackle the new scientific realms emerging in multidisciplinary fields. Time-resolved pump-probe investigations will be used to record ultrafast snapshots of matter, opening new areas of research, as well as tremendous applications in a broad area of science:

- the fundamental time scale of atomic motion will be accessible; elementary structural events will be captured by zooming in time and space
- structural dynamics of matter in solid-state physics and biochemistry
- biomolecular imaging of single molecules to extend investigations of non-crystallizable compounds
- imaging of nanoscale objects (including biological samples)
- high-field physics and non-linear optics generated by intense XUV and X-ray pulses will open the door to investigations of hot, dense matter relating to astrophysical and fusion studies.

Several of these applications have been addressed in great detail in various projects involving free-electron lasers and temporal slicing of synchrotrons conducted by the accelerator community.

B.III.4 X-ray beam work plan at different power levels

- Laser-assisted synchrotrons
- Compton scattering

Betatron

- Free-Electron Laser (FEL)

B.IV Laser-plasma Interaction

Plasma physics at extreme laser intensities

The new extra-high intensity and ultra-short pulse laser facility opens very interesting and unexplored horizons for the plasma physics and inertial confinement fusion community. We address here the following problems:

- Propagation of intense laser pulses in dense matter
- Electromagnetic solitons
- Limited mass targets, multiple ion species acceleration
- High-current electron beam transport
- Hot dense matter

B.IV.1 Propagation of intense laser pulses in dense matter

The penetration of non-relativistic laser pulses is limited by the critical density n_c, which is of the order of 10^{21} cm^{-3} for lasers in the optical range. However, increasing the laser intensity makes the medium transparent (Lefebvre 1994). This relativistic transparency allows propagation and energy transfer between the laser and electrons deep in the irradiated target. For intensities above 10^{24} W/cm^2 the laser pulse can penetrate to densities above 10 times the solid density.

ELI will allow the propagation of laser pulses under such conditions to be investigated. Although the laser pulse cannot deliver the energy needed for ignition to the core of the thermonuclear target, it might create a deep density channel which survives a long time (picoseconds) after the end of the pulse, and can guide another pulse of lower intensity but higher energy. This channel formation effect was observed and explained for underdense plasma and relatively low laser intensities (~10^{18} W/cm^2) (Sarkisov 1999) and then applied to the ICF fast-ignition problem (Mulser 2003). The problem is that channel formation leads to significant energy losses of the beam :

$$dE/dx \approx \varepsilon_0 e^2 n_e^2 R^4 \approx 10 \text{ kJ/mm}$$

Energies of the order of 100 J are thus needed to make a channel 100 μm long. It might happen that the intense laser propagates into densities even higher than n_{max} by pushing the electrons aside by its strong light pressure.

Proving the efficiency of channel formation by ultra-intense laser pulses could constitute an important step in the fast-ignitor approach to the ICF.

B.IV.2 Electromagnetic solitons

Parametric instabilities are well investigated for non-relativistic laser intensities but they are usually ignored for high intensities because of the very short pulse duration. However, stimulated Brillouin and Raman scattering at high intensities could create the

conditions for trapping laser light and formation of relatively long-lived electromagnetic solitons.

These solitons have been observed in three-dimensional PIC simulations (Esirkepov 2003) and more recently in the nonlinear stage of SBS evolution (Weber 2005). They can stay in the same place for a sufficiently long time (of about tens of ps) or slowly drift if the ambient plasma is inhomogeneous.

ELI will allow such structures to be manipulated, and used for studies of long-term effects of extremely high electric and magnetic fields on isolated nuclei.

B.IV.3 Limited-mass targets, multiple ion species acceleration

The ELI project relies on production of ultra-high electromagnetic fields by using very short pulses of relatively low energy. The interaction of such pulses with massive targets will not be too efficient, because the energy delivered to charged particles will be quickly spread out over large distances and redistributed between many secondary particles. One possibility of limiting this undesirable energy spread and achieving high energy density deposition is to use mass-limited targets. For example, deposition of 1 J in a droplet 10 μm in diameter would correspond to deposition of about 10 keV for each particle. Since the expansion time of such a droplet is more than 1 ps, during this time period one can study matter in a quite unusual state of very high density and temperature in the same time.

The limited-mass targets made from transparent materials allow one to avoid negative effects associated with prepulses and they could be used in many applications, in particular for efficient ion acceleration to high energies. The latter was demonstrated in recent experiments at Max Born Institute in Berlin.

B.IV.4 High-current electron beam transport

The problem of efficient transport of intense current of relativistic electrons is at the heart of the fast-ignitor scheme for the ICF. One has to transport these energetic electrons through relatively hot and low-density plasma without significant losses and then deposit all their energy in the small volume of a dense and cold core. These processes cannot be studied confidently without using high-intensity multi-petawatt laser systems. The beam of hot electrons needs to be neutralized by the return current of the cold electrons and the resistivity of these cold electrons provides the major source of the energy losses and the instabilities in the transport region. It is therefore interesting to increase the density of cold electrons in order to reduce the beam energy losses. The target ionization by the electric field of the fast-electron beam and the heating process might improve the transport process and make it possible to control the beam characteristics.

Studies of ionization effects in relativistic beam transport were started very recently (Manclossi 2006) and must be continued with higher-energy pulses. The important point is that the observed instability of the electron beam in a plastic target strongly depends on the beam density and can be suppressed at higher beam currents.

Another attractive possibility of efficient current neutralization is to use positrons. Qualitative estimates show that production of several nC of positrons is possible by a μC of 10 MeV electrons within a 300-μm-thick Z ~80 target. Generation of positrons was recently reported (Gahn 2002), but much higher laser intensities of the order of 10^{20} W/cm^2 are needed for studies of various channels of positron production and their utilization for current neutralization.

B.IV.5 High-energy-density matter

Hot, dense matter defines part of the density-versus-temperature plane between the solid and plasma, where the physics is quite complicated due to strong interaction between individual particles. In this domain, typically found in the interiors of planets, in cool dense stars, and in inertial confinement implosion, standard theories of condensed-matter physics and/or plasma statistical physics are questionable. Knowledge of strongly coupled plasmas opacity is therefore a crucial point. The difficulty of performing accurate measurements of this quantity in this particular regime makes theory the main source of information, which remains untested in most cases.
Extreme laser intensities will open a new opportunity to study hot, dense matter in the laboratory using direct laser-solid interaction or a secondary source. In fact with very high intensity we can produce hot dense plasma before any hydrodynamic motion, which will allow us to study this very important state of matter. A laser of very high intensity will also permit as to produce a secondary source such as laser harmonics or ion beams with high efficiency. These two types of sources are also very promising for producing very dense and hot plasma. A very short and high-intensity laser will afford an unprecedented new opportunity to study hot, dense matter, which is crucial to understanding the interiors of planets, cool dense stars, and inertial confinement implosion.

B.IV.6 Time-resolved relativistic plasma physics with ELI

The goal of ELI is to build a laser delivering exawatt = 10 kJ/10 fs pulses, using a petawatt = 10 J/ 10 fs laser as front-end. Relativistic plasma physics accessible with ELI can be studied within attosecond dynamics with ultra-short photon and particle probes. They can be produced by the PW front-end pulses. As probe beams one can use either portions of the few-cycle laser pulse itself or secondary electron, ion, or X-ray pulses of similar time duration or even much shorter, attosecond XUV pulses that can be generated by means of laser harmonics. Attosecond time scales govern electron motion not only in atoms and molecules, but also in metals and solid-density plasmas.

Three examples of relativistic plasma physics requiring time-resolved attosecond diagnostics are given below.

(i) Laser generation of relativistic proton beams

ELI pulses can be focused to intensities of 10^{25} W/cm^2 and more, corresponding to normalized light amplitudes above a_0 = 1000, and will produce ultra-relativistic electrons and

even relativistic protons. Interacting with gas and solid targets, the pulses ionize the material and generate dense plasma. A most outstanding goal is wake field acceleration of particle beams. Proton acceleration in a solid foil is illustrated in Fig. 1. The laser pulse (not seen) pushes target electrons to the front and to the sides, separating them from the ions and creating huge electric fields (Fig. 1a). These accelerate large amounts of ions to relativistic energies (Fig. 1b). The ion energy spectrum shows a mono-energetic peak at 4 – 5 GeV. In the ion density plot (Fig. 1a), a large crater is seen and a compression wave propagating sidewards. The whole structure moves to the right at almost the velocity of light. These are results obtained from 3DPIC simulation. They need to be verified experimentally with sub-femtosecond diagnostics, in particular the density and E-field structure at $z = 20 – 25$ μm.

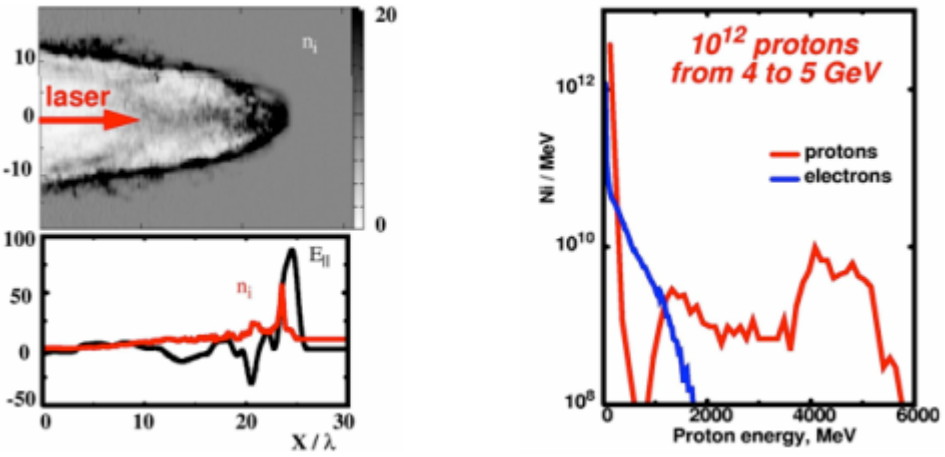

Fig. 1: *A 1 kJ, 15 fs , 10^{23} W/cm^2 laser pulse, incident on 10^{22} cm^{-3} hydrogen plasma, produces 10^{12} protons at energies of 4 -5 GeV (3D-PIC simulation by A. Pukhov (2000)) (Habs2001)*

(ii) Electron acceleration in wake field bubbles

Relativistic electron dynamics already occur at lower laser intensities above 10^{18} W/cm^2 ($a_0 > 1$). A most prominent application is bubble acceleration of electron bunches to energies of 100 MeV and higher over distances of a few 100 μm. A simulation is shown in Fig. 2 for a gas jet target. The action of the 5-fs laser pulse is apparent in the electron plasma density on the right-hand side, where electrons bunch in the ponderomotive troughs of the laser wave, separated by half the laser wavelength, $\lambda_L/2$. These electrons are expelled to the sides, leaving behind a region void of electrons and filled only with ions. The electrons swing back to the laser axis at a distance equal to the plasma wavelength, $\lambda_p = 2\pi c/\omega_p$, where they accumulate and create a high electric potential; electrons scattered upstream are trapped in the first bucket of the wake field, the so-called bubble. They are then accelerated in the longitudinal E-field of the bubble, forming nano-coulomb, low-emittance, ultra-relativistic (γ = 100 – 1000) electron bunches. This mechanism is of great importance for converting the few-cycle laser pulses into ultra-bright electron and X-ray pulses and will have many applications.

Quasi-monoenergetic electron bunches have been detected experimentally (Faure 2004), but so far all we know about details of the amazingly stable dynamics involved is

derived from 3DPIC simulations alone. A lot of structure is observed in Fig. 2, not only at the laser front but also at the bubble boundaries, at the rear vertex, and in the high-energy stem of accelerated electrons inside the bubble. This fine-structure appears on a sub-femtosecond timescale and needs to be investigated experimentally. We anticipate that the 50 as VUV pulses generated by means of relativistic surface harmonics (see section ALS) will be best suited to probing these structures, but also side-lighting with charged-particle pulses (electrons and ions) may be useful for investigating the E- and B-fields of the bubble. At the ELI facility, small portions of the front-end laser pulses will be sufficient to generate these probe pulses, time-locked to the driving pulse. This means that these pulses may be used to study the mechanism involved in their generation.

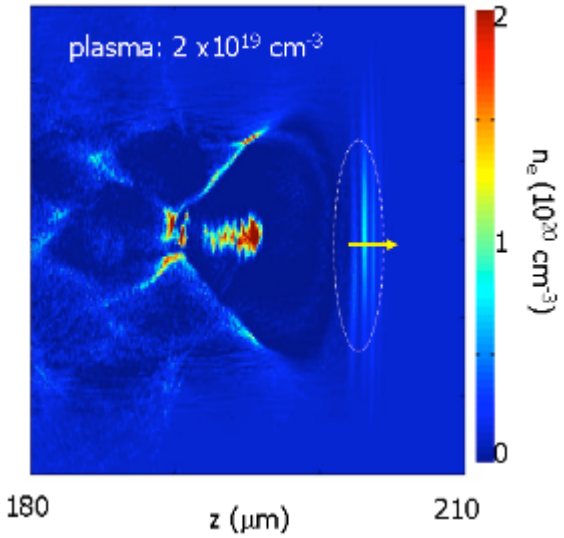

Fig. 2: *Bubble wake field driven by a 5-fs, 115-mJ laser pulse in a gas jet plasma and accelerating a nC electron bunch to 70 ± 10 MeV with 15% efficiency (Geissler 2006)*

(iii) Relativistic electron transport beyond the Alfven limit

The ELI laser pulses will drive relativistic electron currents of the order of giga-amperes in overdense plasma targets. Ultra-short high-power laser pulses are unique for studying electron transport in plasmas beyond the Alfven limit (I_A = 17 $\beta\gamma$ kA). In vacuum, electron current transport is limited by I_A due to magnetic self-interaction. But in plasma return currents tend to suppress B-fields. The system of counter propagating beam and plasma currents, however, is unstable and leads to beam filamentation and a host of secondary filament dynamics and merging events. Understanding these plasma dynamics is crucial for many applications (e.g. fast ignition of inertial fusion targets), because it may lead to anomalous beam stopping and collective plasma heating. This is demonstrated in Fig.3, which shows snapshots of the current distribution of a 1 GA beam injected from the right-hand side into a dense plasma layer. In Fig. 3a, the corresponding electron temperature distribution is also depicted, showing plasma temperatures of up to 30 keV. Here the choice of parameters and density profile relate to fusion applications. At present, it is unclear to what extent beam energy can be transported to the compressed cores of fusion targets. The filamentation instability may be reduced by transverse beam heating and other effects. Again, the present predictions are based only on 3D simulation and require experimental verification. The

filamentary structures evolve and change on the microscopic plasma time scale, which is in the attosecond regime at these densities.

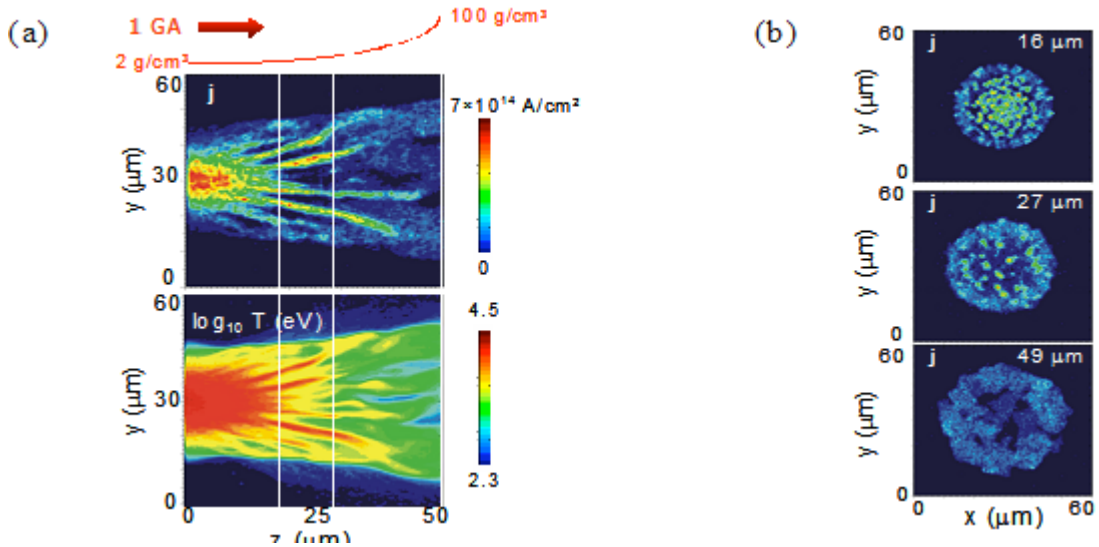

Fig. 3: *Transport of a 1 GA current of 1 MeV electrons in a hydrogen plasma with density varying from 2 to 100 g/cm3; (a) longitudinal cuts through current density and plasma electron temperature, (b) transverse cuts through current density at given z-positions (3D hybrid simulation by J. Honrubia (2005), (J. Meyer-ter-Vehn 2005).*

The ELI facility will provide broad access to the full spectrum of relativistic laser plasma physics and be unique for addressing key questions important for applications.

B.IV.7 Laser-plasma interaction: work plan

-s1, s2 electromagnetic soliton

-m1, m2 limited mass target

-ri3 relativistic ions

-i1, i2, i3 high-current electron beam transport

-h1, h2, h3 high energy density matter interaction

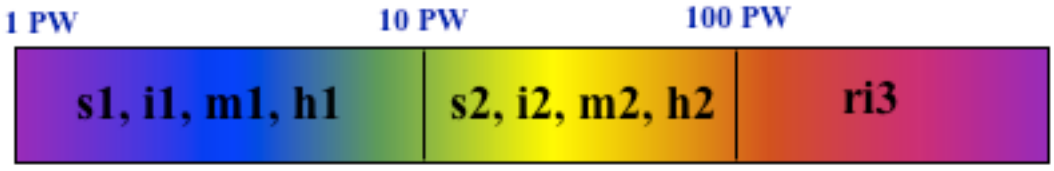

B.V Nuclear Physics and Astrophysics

During the last five years it has become possible to induce almost all known low-energy nuclear reactions either with large laser facilities (Ledingham 2000, Cowan 1984), or with table-top terawatt-class lasers (Schwoerer 2001, Schwoerer 2003, Magill 2003). The intensities necessary for these experiments are in the range 10^{19}-10^{20} W/cm². The laser intensities in the 10^{24}-10^{26} W/cm² range that will be possible with ELI, will allow a number of exciting, innovative experiments in nuclear physics.

B.V.1 Direct interaction

With sufficient laser intensity, the electromagnetic field will interact directly with the nucleus. If ELI can generate photon intensities of up to 10^{26} Wcm^{-2}, then this would result in protons gaining energies of up to about 100 eV. For high-Z nuclei, energies of up to 10 keV could be deposited in the nucleus. These energies would be sufficient to modify the nuclear levels and characteristic gamma emission above detection thresholds. Nuclear polarization effects could be visible at lower laser intensities.

B.V.2 Changing the nuclear level lifetimes

At intensities two orders of magnitude lower than those required for direct interaction (10^{24} W/cm²), the ponderomotive energy of the electrons amounts to 500 MeV. We may then completely strip ions and observe effects such as inhibition of internal conversion. Two orders of magnitude lower in intensity (10^{22} W/cm²), the electron ponderomotive energy of ~10 MeV is sufficient to observe effects on the nuclear decay involving atomic core electrons. For example, modification of the levels of the electrons involved in the internal conversion processes, in the presence of a high external field, will change the corresponding nuclear level lifetimes.

B.V.3 Neutron-rich nuclei

With coherent harmonic focusing of an exawatt laser (Gordienko 2005) it appears possible to generate fields which accelerate protons with fields equivalent to 1-10 MeV/fm. Let us assume that we can superimpose such an electric field of 1-10 MeV/fm on a uranium nucleus. In the single-particle picture, the majority of protons that leave the nucleus are accelerated at this rate, and we can produce extremely neutron-rich nuclei at the neutron dripline. The picture is similar to the ionization of an atom in a laser field where one superimposes the electric field and the Coulomb field and lets the electrons freely leave the atomic potential. The nucleus typically has a 50 MeV deep potential with an edge diffusivity of 0.5 fm. When the field is superimposed at the edge of the nuclear potential, the protons stay trapped and all neutrons will collect around these few protons. The dynamics of this process is most likely determined by whether it is impulsive or adiabatic. The highest harmonics are probably in the MeV range, corresponding to times of 10^{-21}s. On this time scale many protons probably gain more energy than their binding energy and leave the nucleus. The nuclear pn-force will be typically of the order of 100 MeV/fm, leading to the situation, where after some evaporation of protons, the remaining neutrons will retain the protons.

B.V.4 Decay of neutron-rich nuclei

The process may also be discussed in a collective picture. One superimposes the electric field and studies the collective dynamics of the nucleus. It will elongate until it fissions. A very proton-rich fission fragment such as the doubly magic ^{100}Sn will occur, while the rest corresponds to a very neutron-rich fission fragment. In such a process, neutron-rich nuclei at the neutron dripline can be produced which are totally inaccessible even with newly planned radioactive beam facilities (FAIR or RIA). Here one would produce at a very low rate (e.g. only one exotic nucleus per laser shot) but could track the events by means of the long sequence of β-decays before stability is reached. Studying the decay of such nuclei would be extremely interesting for the nuclear physics community and would lead to a large user community.

The properties of heavier nuclei (lead and above) are essential to studying the astrophysical r-process and the waiting point nuclei. We are currently studying the nuclear dynamics in these high fields more carefully to make better predictions regarding the nuclei produced. Another possibility is to form a standing wave from two laser pulses to generate ultrashort and extremely large magnetic fields (10^{12} T). The larger the field is the shorter the pulse it becomes. As very high fields occur on the surface of white dwarves (10^{2}-10^{4} T) or neutron stars (10^{7}-10^{9} T), ELI-generated high magnetic fields are of particular relevance to laboratory astrophysics. If atoms are placed in such strong magnetic fields, the Lorentz force dominates the Coulomb force and the electrons are confined to small Landau cycles. Here the quadratic Zeemann effect becomes important. In this way elongated knitting-needle-like atoms form. They have been studied in detail in theory (Ruder 1994), but the investigations were stopped because experimental results were lacking.

B.V.5 Developing new detector technology

Exciting new laser-driven physics in the field of nuclear and particle physics on the ELI laser facility will require new detector technology. At present most of the experiments carried out on single-pulse and high-repetition-rate lasers at high intensity (10^{21}Wcm^{-2}) use time consuming CR plates and simple magnetic and electric field technology. Advanced nuclear detector technology should register data within the laser pulse or very shortly after. All of this technology is at present being used on advanced accelerators. The ultra-intense laser interaction with the solid target will generate extreme gamma flashes, thus necessitating radiation-hard detectors. Conventional magnetic and electric field technology must be developed to focus and control the intense particle beams generated by the laser.

B.V.6 Electron-positron pair production

Another interesting and exciting research programme using counter-propagating laser beams could be set up. Initial experiments have already been carried out on the high-intensity single-shot facility at Rutherford Appleton Laboratory. Two intersecting laser beams interacted with a thin high-Z target at an angle of 145^{o}. The object of the exercise was to generate positrons which would be detected with a specially designed pairs spectrometer. Unfortunately, this experiment proved inconclusive due to the fact that the two beams had to overlap with great precision both spatially and temporally. However, at the University of Jena it was shown that counter-propagating laser beams can be made to generate non-linear Thomson scattering radiation. This radiation emitted at right angles to the laser beams only exists when the beams overlap spatially and temporally. This provides a robust diagnostic for

these difficult experiments. On the ELI facility the programme would start with positron generation from thin high-Z targets and then proceed to the lasers generating high electron beams which would collide and produce electron-positron pairs in vacuum without a target. This could be carried out at laser intensities of the order of 10^{23} Wcm^{-2}. Finally, at higher intensities, photon-photon scattering experiments would be carried out in vacuum to produce initially electron/positron pairs and then muon pairs. Vacuum requirements represent an important challenge to these experiments. Experiments would begin at 10^{-12} torr and then be extended with local particle-reducing technology. The technology developed could be applied to $\gamma\gamma$ colliders for high-energy physics.

Besides this programme, here are also some ideas that nuclear physicist are ready to explore:

1. fast ignition with e^+ e^- beams
2. production of meson, muon and neutrino beams
3. production of heavy-ion beams at energies around the Coulomb barrier, nuclear photo-excitation processes.

B.V.7 Objectives for nuclear physics and astrophysics

In addition to the nuclear physics experiments described here, which all rely on the direct action of the strong electromagnetic field of the laser on the nucleus, numerous other experiments are possible that use advanced laser accelerators for nuclear physics. In general, an innovative laser facility such as ELI would be highly attractive to the nuclear physics community. At least ten experimental and theoretical working groups are at present involved with laser-induced nuclear physics in Europe and approximately twenty world-wide. Since this is a very young field, interest is expected to grow further, in particular when advanced applications of laser nuclear physics in medical isotope production or nuclear waste transmutation prove technologically feasible.

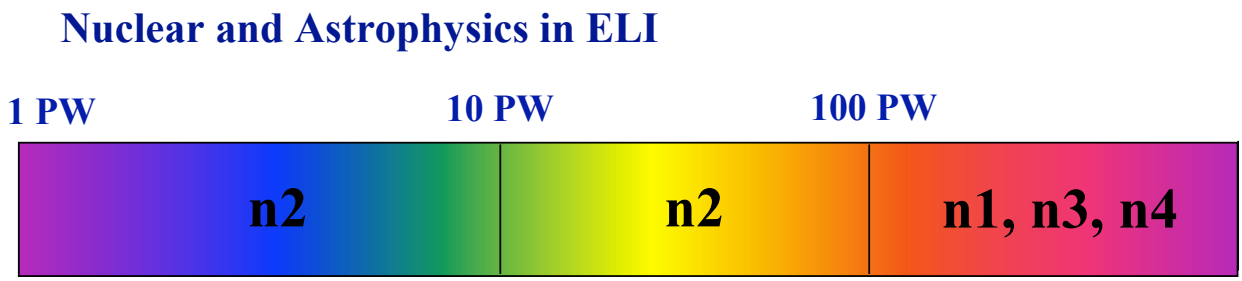

B.VI "Exotic Physics"

Ultra-high fields of high-power short-pulse lasers pose important possibilities for fundamental physics (Mourou 1998). At present we are approaching focused intensities of 10^{22} W/cm^2 (Bahk 2004), but significantly higher fields are needed (Tajima 2001, Mourou 2006). Such fields can be attained when ultra-relativistic laser fields are further intensified and shortened via non-linear relativistic effects.

Making use of such effects, e.g. relativistic plasma mirrors (Bulanov 2003, Gordienko 2005, Nees 2005), one can envisage higher field strengths than in future X-FELs. In these proposed XFELs, field strengths of 10^{17}V/m are expected and fundamental physics with these fields constitutes an important research area (Ringwal 2001). As well, with peripheral relativistic heavy-ion collisions very intense quasi-real photon fields can occur, but these conditions would be markedly less controlled than those of direct laser experiments (Hencken 2004).

B.VI.1 Exploring the fundamental properties of vacuum

Experimentally exploring the fundamental properties of the vacuum and its fluctuations is challenging. The breakdown of the vacuum in high fields via pair creation is a fundamental process in QED (Schwinger 1951) and represents a general process of quantum field theory (Itzykson 1980). It is also related to the quantum evaporation of black holes (Hawking 1975). A deeper understanding of the vacuum touches many fundamental questions such as the unsolved origin of dark energy. Naive estimates of the contributions of quantum vacuum fluctuations to the dark energy of the universe are wrong by many orders of magnitude (Perkin 2003).

In ultra-strong fields the breakdown of the vacuum into e^+e^- pairs can be studied. The characteristic field strength is the Schwinger limit of 1.3 10^{18} V/m, where an electron gains its rest mass energy over its Compton wavelength, resulting in the breakdown of the vacuum into e^+e^- pairs. The Schwinger field corresponds to a laser intensity of 5 10^{29} W/cm^2. With weaker fields the sub-threshold production can be studied, where in the oscillating fields enhanced production of e^+e^- pairs and their annihilation radiation are predicted. For a strongly focused laser pulse pair production is predicted already at 10^{27} W/cm^2 (Popov 2004), while for two counter-propagating pulses the threshold should occur at 10^{26} W/cm^2 (Narozhny 2004, Alkofer 2001, Roberts 2002, Blaschke 2002).

In this sub-threshold field strength region theoretical predictions differ by many orders of magnitude (Marinov 1977, Popov 2002, Popov 2004, Avetissian 2002). Experimental clarification of these conflicting predictions is required.

B.VI.2 Observing vacuum polarization

The observation of vacuum polarization effects is feasible in laser fields significantly weaker than the Schwinger field. The detection of vacuum birefringence is already possible by the available laser technique with 10^{22} W/cm^2 intensities if X-rays are employed as a probe. Light-by-light scattering processes may also become experimentally accessible. When the

scattering of a laser beam by another laser beam is stimulated with a third laser beam (Moulin 1999), the scattering probability becomes measurable. The observation of γ-photon splitting in a laser field (Affleck 1987) may require XUV lasers with 10^{26} W/cm^2 intensity. Meanwhile, in fields exceeding the Schwinger critical field, high-harmonic generation from the laser field may become possible (Dipiazza 2005, Dubeis 1992).

The process of e^+e^- pair creation can be studied in the region of overcritical field strengths where most theoretical predictions agree by reaching the Schwinger limit with coherent focusing of harmonics of a petawatt laser. In this case the total energy density of the fermion pairs created becomes comparable to that of the laser field. The usual approach where the laser is considered as a classical external field will be inapplicable.

B.VI.3 e^+e^- annihilation and the evolution of the universe

Back-reactions of the electron-positron plasma created possibly limit a further rise in the laser beam intensity when 10^{31} W/cm^2 is reached. A state of light and matter can be prepared under controlled laboratory conditions which mimicks the e^+e^- annihilation era during the evolution of the early universe.

Muon or pion pairs can be generated from positronium atoms submitted to a strong laser field, which leads to coherent electron-positron (re)collisions at microscopic impact parameters (Henrich 2004) with substantial enhancement of the collision luminosity.

Studying the QED vacuum requires separation of the effects from the residual vacuum. Since a prepulse of the strong laser field already ionizes the remaining ions, we can pull the charged particles out of the interaction zone by clearing fields and thus prepare an ultrahigh vacuum for a short time in the region of interest.

Electron-positron pair creation can also occur in the collision of an intense laser beam with a relativistic nucleus (Mueller 2003). In the nuclear rest frame, the laser field strength as well as the photon energy are considerably enhanced and can approach the Schwinger limit or the electron rest mass, respectively. Both the free and bound-free pair creation channels could become accessible experimental observation in the near future.

B.VI.4 Observing Unruh radiation

Ultra-strong laser fields allow unprecedented acceleration of electrons with more than 10^{30} g, giving access to investigation of the interplay between general relativity (equivalence principle) and quantum field theory in the laboratory (Mcdonald 1985). From the point of view of a non-inertial observer co-moving with the accelerated electron, a horizon occurs at a typical distance of $d=c^2/a$, resulting in many exotic and seemingly paradoxical effects (Unruh 1984). Such an observer experiences the usual (inertial) vacuum state as a thermal bath with apparent temperature $T_{\mathrm{unruh}}=ha/4\pi^2c$, the Unruh temperature (Unruh 1976). This Unruh effect has hitherto not been directly observed. The high acceleration occurring in the laser focus should allow the first observation of the Unruh effect (Unruh 1976), where previous proposals (Bell 1987, Rogers 1988, Yablonovitch 1989) have (so far) been unsuccessful. The much larger acceleration accessible with high-power lasers causes the Unruh temperature to increase and hence makes the Unruh radiation much stronger. The competing classical process, Larmor radiation, has a blind spot in the forward direction in the laboratory system where the Unruh radiation has its maximum (Chen 1999). Another possibility of discriminating the two types

of radiation is provided by their different spectral distributions. Due to the entanglement of the vacuum state across the horizon, the scattering of a photon from the thermal bath from the accelerated electron in the non-inertial frame corresponds to the emission of two photons in the inertial (laboratory) frame (Unruh 1984).

These two emitted photons are maximally entangled (Einstein-Podolski-Rosen state) and can be detected by measuring their polarizations. More detailed questions of the photon statistics for Unruh radiation can thus be studied experimentally. For this quantum radiation we expected fully entangled photon pairs and not the Poisson distribution of classical radiation.

B.VI.5 Extra dimensions

In this way, we will achieve a better understanding of the non-perturbative rearrangement (Bogoliubov transformation) of the creation and annihilation operators of the vacuum, when going from the inertial Minkowski frame to the non-inertial (accelerated) Rindler frame. The small horizon size $d=c^2/a\approx10^{-12}$ m also allows one to address questions of "large" extra dimensions or contributions from a 5th force and to test certain classes of models for new physics. The Unruh effect is closely related to Hawking radiation, i.e. black-hole evaporation with a temperature $T_{hawking}=hg/4\pi^2c$, where g is the gravitational acceleration at the Schwarzschild radius (surface gravity) measured by an observer at infinity (Hawking 1975). The occurrence of an event horizon is again important, separating the interior of the black hole from the outside observer.

When going to even higher fields, the e^+e^- pair creation shifts to higher lepton energies due to Pauli blocking in the small space-time volume and enhanced production of π's in a condensate will start. Sub-threshold production should again be observable at lower fields. This gives access to, totally new questions of QCD with the interaction and condensation of the Goldstone bosons of chiral symmetry breaking of QCD. One obtains situations very different from the nuclear reactions in present hadron physics. In the case of the experiments suggested with ELI, the vacuum of QCD, potentially exposing both quarks and gluons, will be studied.

B.VI.6 Quark-gluon and neutrino oscillations

In the extremely-high intensity limit the laser pulse-plasma interaction acquires new properties, ranging from the effects of the radiation friction force and QED effects to nonlinear vacuum polarization and electron positron pair creation (Mourou 2006). In this limit novel mechanisms of the ion acceleration come into play. Since the energy of the resulting ion bunch can be over 100 GeV per nucleon, this ion acceleration regime is suitable for quark gluon plasma studies (Esirkepov 2004) and in connection with an application to the investigation of neutrino oscillations (Bulanov 2005).

B.VI.7 “EXOTIC PHYSICS”; objectives

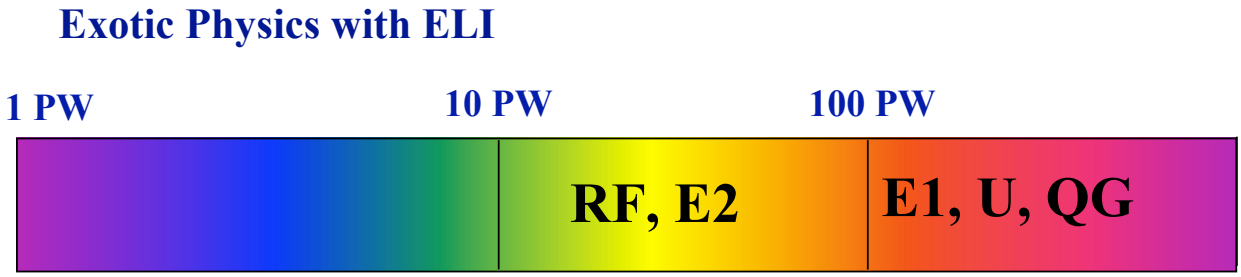

B.VII An exawatt class high-repetition-rate laser design for interaction physics for interaction physics at extreme intensities

As part of the process of identifying novel European research infrastructures, the European Strategic Forum for Research Infrastructures (ESFRI) are considering ultra-high-power infrastructures as possible future research platforms for Europe.

One of these is the so-called Extreme Light Infrastructure (ELI). It will host an exawatt class laser. The ultra-high peak power will be achieved by extending current high-energy laser technology (kJ energy level) to support extremely short pulse durations of the order of 10 fs. This will enable ELI to study light-matter interaction in the ultra-relativistic regime. The design of the ELI laser system delivering peak powers in the exawatt (10^{18}W) range is presented here. As a first step, a front-end delivering pulses in the petawatt (10^{15}W) regime at a repetition rate of up to 1 kHz could be constructed. This front-end could be complemented with a power amplifier in a single beamline to deliver 70 PW at 1 shot/minute, and later up to 1Hz. This beam would deliver peak intensities of 10^{25}W/cm^2 when focused. As a last step, coherent combination of 10 such laser lines could allow to exawatt peak powers to be attained and would make a hitherto completely unexplored research field accessible, spanning physics, material science, biology, chemistry and medical research. This laser will serve as the backbone of a future European experimental facility called Extreme Light Infrastructure (ELI).

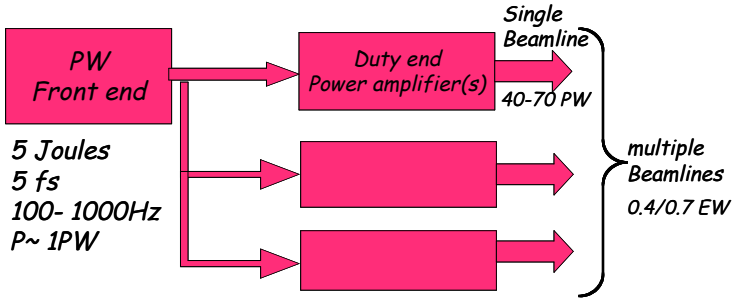

***Fig. 1**: Schematic picture of the exawatt system starting with a front-end producing 5-fs pulses at the joule level (PW). A power amplifier chain will boost this energy to the tens of petawatt level in a single beam. Coherent combination of 10 to 12 beams will lead to an exawatt-class output power.*

In the following, we discuss our proposed approach for designing such a laser, starting with an upscaled version of MPQ's Petawatt Field Synthesizer (PFS) project as a front-end. Pulses from this system can then be further amplified in a chain of power amplifiers, f or which purpose two promising strategies are discussed. The first, more conventional, approach is based on established Ti:sapphire (Ti:Sa) technology, but, the pulse duration achievable in this case will be limited to 15-20 fs. The second, more novel, approach will draw on a modification of the concept of optical parametric chirped-pulse amplification (OPCPA), which will in principle allow generation of few-cycle pulses with durations as short as 5 fs, and may greatly facilitate pulse compression. Moreover, it will allow the carrier-envelope phase to be controlled and thus provide completely controlled light pulses for experiments. This second approach is also used in the aforementioned PFS project, allowing us to gather experience with this technique. A hybrid design using both techniques will also be investigated. These

studies will serve as a basis for choosing the final amplifier design. Finally, we will discuss possible ways of pulse compression.

B.VII.1 Frontend development

In order both to provide a suitable seed pulse for the ELI high-energy amplifiers, and to conduct experiments on the PW scale with high repetition rate, we plan to develop a front-end based on the concepts of the 10-Hz PFS project under construction at MPQ. Most applications of such a PW-scale system will require rapid scanning of parameters and accumulative data collection during the experiment, and therefore a repetition rate of 1 kHz is envisaged for the fully evolved state of the system.

In a first development stage, a copy of MPQ's 10-Hz PFS laser will be adapted to the particular wavelength requirements of the ELI amplifier chain. Later extensions will reach a repetition rate of 100 Hz … 1 kHz. At every stage, the system will provide absolutely phase-controlled, few-cycle light pulses with unprecedented intensity and repetition rate:

Pulse duration: < 5 fs
Pulse energy: > 3 J
Repetition rate: 10 Hz – 1000 Hz
Peak power: > 500 TW
Carrier wavelength: 0.8 µm
Spectral range: 0.5-1 µm
Intensity: $>10^{22}$ W/cm^2

The development of this front end will draw on experience gathered with the 10-Hz PFS system at MPQ, but its fully developed state with 1-kHz repetition rate can at present only be anticipated by using established scaling laws. However, our stepwise approach allows back-up solutions to be applied where necessary. The concept outlined therefore follows the PFS design, and changes to be introduced for higher repetition rate/different wavelength will be emphasized in the text.

B.VII.1.1 System layout

The proposed layout of a first 10-Hz system is depicted in Fig. 2. For accurate temporal synchronization between the OPCPA line and the pump, both lines will be seeded from a common 1-kHz Ti:sapphire oscillator/amplifier system, which will be spectrally broadened inside a hollow fibre. Seed pulses for the OPCPA chain will be derived in their respective spectral region from this ultra-broad continuum and stretched to 2 ns for the pump and 1 ps for the OPA chain. The pump laser consists of a chain of Yb:KGW/Yb:YAG amplifiers, a compressor and frequency-doubling crystals. It will pump a succession of non-collinear OPA (NOPA) stages up to 80 mm in diameter. Final compression of the amplified signal pulses will be performed in a slab of fused silica and an array of chirped mirrors. In the following, we discuss in more detail the novel OPCPA concept and the pump laser design, including possible upgrades for 100 Hz and 1 kHz operation.

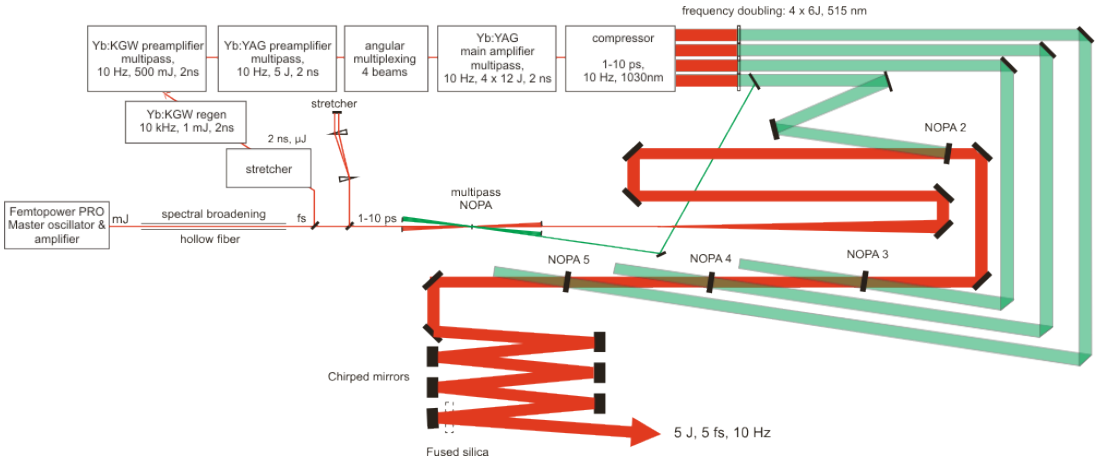

***Fig. 2**: Schematic layout of the ELI 10-Hz front-end*

B.VII.1.1.1 Short pulse OPCPA

Known laser materials do not provide enough bandwidth to support the amplification of few-cycle pulses to high energies. A promising alternative is optical parametric amplification (OPA) (Dubietis 1992), an intensity-dependent, nonlinear mixing process of a pump, a signal, and an idler wave in an anisotropic crystal. If a high-energy pump pulse and a low-energy signal pulse overlap in the crystal, energy is transferred from the pump to the signal, while a third wave, the idler, is generated to maintain energy and momentum conservation. With a monochromatic pump wave, the signal wave can be amplified with a very large bandwidth, since the idler wave adjusts itself in frequency and wave vector (i.e. momentum) to obey the two conservation laws.

However, the properties of the nonlinear crystal have to ensure that all three waves stay phase-matched within the crystal length, which poses restrictions on the material, crystal thickness and wavelength ranges used. Generally, the thinner the crystal, the broader a spectrum can be amplified. In special cases, the gain bandwidth of the OPA can be extended to one octave in the optical spectrum, which is sufficient to support almost single-cycle pulses.

OPA provides additional benefits such as negligible heat dissipation since no absorption and energy storage takes place in the crystal, facilitating scaling to high repetition rates, and high spatial beam quality since any wavefront aberrations of the pump are only transferred to the idler.

Through their high power high-energy ultra-short light pulses can lead to nonlinear propagation effects and damage to optical components. To counter these problems, the pulses are stretched in time before and compressed again after amplification, a technique called CPA (chirped-pulse amplification) (Strickland 1985). The combination of this principle with OPA is called OPCPA.

OPCPA systems have been demonstrated for both the generation of few-cycle, low-energy optical pulses (Balutska 2006) and longer (~100 fs) high-energy (30 J) pulses (Ross 2006).

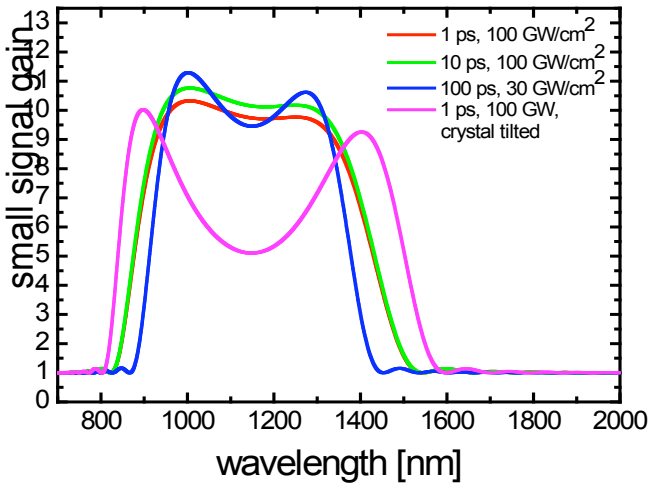

***Fig. 3**: Comparison of DKDP amplification bandwidth, pumped by 1, 10 and 100 ps pulses. The crystal thickness was adjusted to obtain the same small-signal gain.*

In all these systems, relatively long (>100 ps) pump pulses (as readily available from commercial pump lasers) are used, requiring that the few-cycle signal pulses be stretched by factors of 10^5 or more. Apart from this inconveniently large stretching factor, several other problems are inherent to this standard approach: Crystals with high nonlinearity and good phase-matching properties such as BBO and LBO are only available in sizes up to 30 mm and may have to be arranged in a mosaic pattern for generation of PW-scale pulses. On the other hand, crystals available in larger sizes, such as deuterated potassium dihydrogen phosphate (DKPD), cannot support the necessary bandwidth.
Changing the pump pulse duration to the order of a few picoseconds dramatically changes this unfavourable situation. Due to the high intensity of the short pulses, for achieving a given gain, even a crystal with low nonlinearity such as DKDP can now be made thin enough to support a bandwidth suitable for nearly single-cycle optical pulses (see Fig. 3). DKDP can be fabricated in large enough sizes to support petawatt light pulses without optical damage.

The smaller stretching factor makes it much easier to compress the signal pulse after amplification. Since parasitic processes leading to generation of incoherent light (e.g. parametric fluorescence) are limited to the pump duration, short pulses will also enhance the overall pulse contrast.

Short pump pulses have the drawbacks of increased complexity of the pump laser, larger beam sizes and demanding synchronization requirements.

The choice of crystal will also depend on the choice the final amplifier. If a Ti:Sa system is chosen, only BBO or LBO will allow amplification of pulses around 800 nm to match the Ti:Sa amplification band. This will require a mosaic arrangement of 4 crystals in the final amplifier of the front-end, unless larger crystals become available in the future. In the case of OPCPA power amplifiers, which can only be made from DKDP of a suitable size, the bandwith lies between 900 nm and 1500 nm (Fig. 3), and so the front-end has to be based on DKDP as well.

In the former case, the front-end OPCPA chain will be directly seeded from the hollow-fibre-broadened output of the Ti:Sa oscillator/amplifer. In the latter case, a suitable signal can be generated by difference frequency generation of such a hollow-fibre supercontinuum.

B.VII.1.1.2 Pump source

The perhaps greatest technological challenge lies in the development of a suitable pump source capable of delivering 20 J of green light in short pulses (approx. 1 ps) at

ultimately up to a repetition rate of 1 kHz. Assuming 50 % conversion efficiency into the second harmonic, this translates to 40 J per pulse at the fundamental wavelength (~1μm). Picosecond pulses at that energy level can only be created by the CPA technique. As an amplifying medium for the 10-Hz stage, we have chosen a combination of Yb:KGW and Yb:YAG, for reasons of high energy storage capability, efficient diode pumping, small quantum defect (all required for low heat load and efficient cooling), resistance to damage, size, and amplification bandwidth. The laser will be built as a chain of amplifiers, where, in spite of the favorable properties of Yb:YAG, realization of an output energy of 40 J at 10 Hz in the last stage still poses a great technological challenge. However, pumping and heat transport calculations show the feasibility of our concept of a face-cooled slab amplifier (for schematic layout see Fig. 4).

In order both to reach the saturation fluence for high extraction efficiency and stability and stay below the damage limit for the laser crystal, the beam is split into four rectangular beams which are sent to the main amplifier in a temporally multiplexed fashion, as shown in Fig. 4. Each beam will thus contain only 10 J of energy.

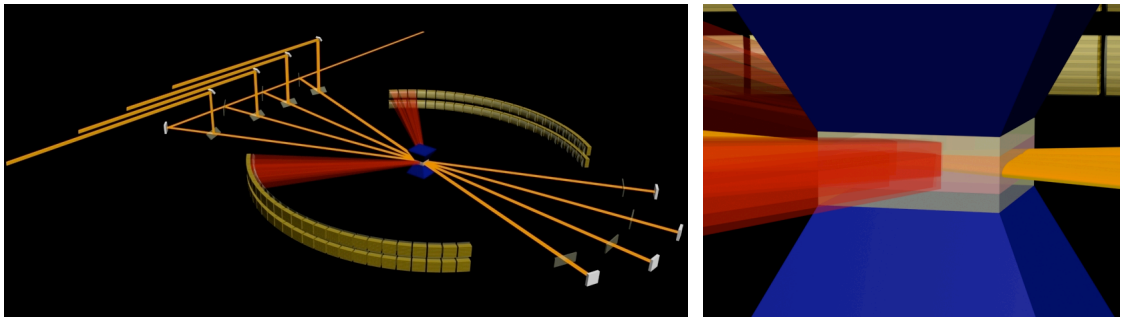

Fig. 4*: Left: layout of the Yb:YAG amplifier: The pulse is split into four, which are angularly and temporally multiplexed and pass the amplifier twice after polarization rotation in a quarter-wave plate. Right: close-up view of the crystal: The amplifier is arranged in a slab geometry for efficient cooling.*

This design allows later scaling of the repetition rate by reducing the thickness of the amplifier crystals, in which case the pulse energy drops linearly with thickness, whereas the average power grows with the inverse of the thickness. This will ideally lead to an increase of the repetition rate proportional to the inverse thickness squared. For instance, a 50 mm x 50 mm x 1 mm crystal can thus produce 4 J of laser energy at 1 kHz, using $1/10^{th}$ of the diodes of the 40-J amplifier. Ten such amplifiers have to be parallelized to produce 40 J in 40 beams. The limits of this scheme are given by the large aspect ratio of the beams (50:1), the complexity of 40 beams and the associated pumping geometry for the OPCPA stages. It should be noted, however, that multibeam pumping of a single OPA stage is in principle feasible and can even be used to increase the signal amplification bandwidth (Dubietis 1998, Marcinkevicius 1998). A 100-Hz system of greatly reduced complexity can be realized with only 3 - 4 parallel amplifiers and 12 - 16 beams.

Each of the Yb:YAG amplifiers will be diode-pumped at a wavelength of 940 nm. This is a prerequisite for achieving high repetition rates, since the heat deposition in Yb:YAG is two orders of magnitude lower than in flashlamp-pumped materials. At 10 Hz, the diode stacks will be operate in pulsed mode with a duty cycle of 1.5×10^{-2}. The 1-kHz stage will

therefore need only 1.5 - 2 times the total number of diodes needed by the single 10 Hz of the triple 100-Hz stages.

For the compressor of the 10-Hz system, a design based on small individual gratings for each beam and one big, shared grating has been developed. This will minimize the cost and allow individual fine-tuning of the compression parameters for each beam. By using dielectric gratings in the compressor a throughput of 80% can be achieved. Scaling to 100 Hz and 1 kHz requires further work, but can in principle follow the same lines.

B.VII.2 Power amplifier development

Using the frontend described in the previous section, we can now turn to investigation of the main amplifier stages necessary to reach first the 100-petawatt level and later, in a combination of multiple beams, the exawatt level. Two main phases of the project are necessary in order to minimize risk and make the right choice for the final design. The first step consists in studying the maximum energy we can extract from a *single* beamline, considering different key issues such as transverse lasing, gratings, amplifying crystal dimensions and pump laser technology. This first step, using already validated technology and pushing everything to the limit, should lead to a peak output power in the range of 10 to 20 PW; 70 PW at a repetition rate of 1 Hz in a single beam seems feasible. The second phase will then be dedicated to combining and focusing 10 identical beamlines in a coherent way to reach the exawatt level at 10^{26}W/cm² and a repetition rate of 1 Hz.

B.VII.2.1 The Ti: sapphire approach

By virtue of recent developmentsat several laboratories around the world (JAERI in Japan, CUOS in USA, LIXAM/LOA in France, etc.), petawatt-class lasers delivering 20 J in 20 fs are now available at relatively high repetition rates (up to 0.1 Hz with the LASERIX system under construction at LIXAM/LOA). This level of performance relies on several key points, which have been successfully resolved:

Large-size Ti:Sa crystals: High-quality Ti:Sa crystals 110 mm in diameter are at present available from commercial suppliers. When pumped on each side at a 2J/cm² pump fluence on a pumping area of 25 cm², 100 J of green pump light can be converted to an amplified pulse with an energy content of more than 40 joules.

The past rate of increase in crystal size makes it realistic to assume the availability of Ti:Sa discs 200 mm in diameter at the start of the project. However, due to non-uniformities in the doping concentration, the useful aperture is typically limited to 80% of the disc diameter (160 mm). Assuming a pump fluence of 5 J/cm², 1000 J of green light per side can be used to pump the power amplifier. At these fluences, an extraction efficiency of up to 50% can be achieved, which translates to an amplified pulse energy of 1000 joules. This value is in agreement with the 6-grating compressor design described above.

Operating an amplifier at these fluence levels requires special care in smoothing the pump profile in order to avoid damage to the crystals, ensure homogeneous gain, and suppress the onset of transverse parasitic lasing, as discussed below.

Pump energy distribution: In order to achieve a smooth pump profile without hot spots leading to damage and uneven gain, the traditional relay-imaging method has been replaced by beam homogenization using refractive and/or diffractive micro-lens arrays. With careful control of both the temporal and the spatial coherence of the nanosecond pump lasers, this technique leads to a very homogeneous energy distribution on the amplifying crystal (see Fig. 5). It can be readily adapted to a large number of pump beams, as will be necessary to provide the required energy and repetition rate.

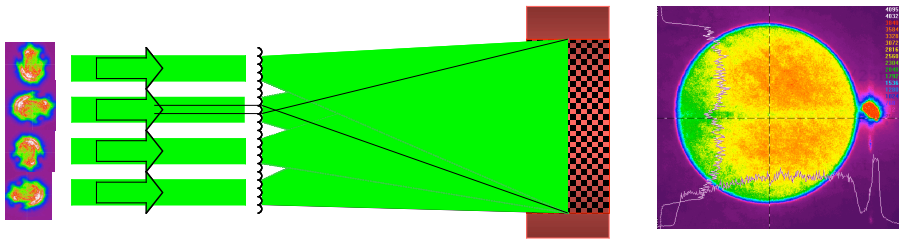

Fig. 5: *Schematic picture of a homogenizer which mixes four beams and leads to a flat-topped pump beam.*

Parasitic transverse lasing: Parasitic transverse lasing occurs when a thin disc-shaped amplifer is pumped very hard. In this case, the single-pass gain in the plane of the disc can overcome the losses at the reflection from the internal circumference of the disc, leading to lasing action in the plane of the disc. This quickly leads to depletion of the stored energy and limits the gain for the signal beam. Several strategies have been used to prevent this from happening, e.g. with an index-matched absorbing liquid flowing around the crystal perimeter (Patterson 2002). When a Ti:Sa amplifier is pumped with 2 kJ delivered by exactly synchronized pump lasers, the transverse gain can be 50 times higher than the above limit. However, it is possible to overcome this problem with different timing for the individual pump lasers. By this sequential pumping technique the transverse gain can be kept below the lasing threshold, permitting almost 1000 J, to be extracted.

High-performance pump lasers: Currently, 100 J of green pump light can be routinely delivered to a Ti:Sa amplifier at a repetition rate of 0.1 Hz by a set of 4 frequency-doubled Nd:glass lasers, each delivering 25 J in 2 beams.

The main limitations for this conventional technique are the constraints on beam quality imposed by the image-relaying technique. These constraints can be strongly relaxed by using homogenizers as discussed above, and so 150 J in a single beam at 523 nm may be within reach. Such a system would employ Nd:phosphate glass rods 90 mm in diameter pumped by flashlamps at a rate of 1 shot/min. In accordance with our needs, 12 of these beams could then deliver energies of close to 2 kJ.

Recently, new developments using phase-conjugated mirrors and Nd:glass slabs have also demonstrated energies of up to 65 J at 3Hz (LLNL 2004) and could deliver 100 J of green light at 1Hz, which may open the road to a later upgrade of the laser's repetition rate.

New results can also be expected from ongoing developments in the fields of YAG or ceramics as host materials and of diode-pumped ytterbium-doped materials (Mercury project at LLNL, LUCIA at LULI, Polaris at Jena and PFS at MPQ)

Gain narrowing and spectral shaping: In principle, Ti:Sa can support an amplification bandwidth of 160 nm, which would support laser pulses of sub-10 fs duration. However, this

is at present only possible with in low-energy (μJ) laser systems since the non-uniform gain across the laser bandwidth leads to narrowing of the amplified spectrum. Spectral shaping based on suppressing the peak of the amplification curve after each amplifier stage has been successfully used to broaden the spectrum of amplified pulses in the mJ range to 80 nm. Since this principle involves loss modulation, its implementation would be too costly in terms of energy for a high-power system. However, it is possible to use an active spectral shaper based on OPCPA technology where a small part of the pump light of each Ti:Sa amplifier stage is used to broaden the spectrum in a second OPCPA amplifier and regain the bandwidth. This approach would then lead to a hybrid system with high design flexibility.

If current technology is pushed to the limits, it seems feasible to design a single beam Ti:Sa laser chain delivering 10 - 15-fs pulses with an energy in the range of 700 joules (50 to 70 PW). This estimate is based on a crystal diameter of 200 mm, available in the near future, and gold gratings in commercially available sizes. The repetition rate will be limited by the pump laser performance to 1 shot/minute when established techniques are used, and up to 1 Hz with innovative developments, now being validated. Active phase control for the amplified beams in conjunction with large-aperture optics, yielded **intensities as high as 10^{25} W/cm²**.

B.VII.2.2 The OPCPA power amplifier option

Given the rapid progress in OPCPA-related work over the past few years, this technique is worth considering not only at the front-end level, but also as a possible multi-petawatt power amplifier for ELI. As outlined in the description of the front-end, OPCPA offers the unique feature of gain bandwidths large enough to support light pulses even shorter than 10 fs. This also implies that less total energy is sufficient to achieve a given laser power. To date, pulse energies of up to 30 J have been generated with such an amplifier which were compressed to sub-100 fs, using a relatively conservative design and a standard, multipurpose Nd:glass laser as pump. With a more specialized design for pumping and signal generation, this result will most likely be greatly surpassed in the near future. As a power amplifier, OPCPA also offers several major advantages over Ti:Sa technology:

Single-pass amplification leads to low pulse distortion by dispersion or intensity-dependent nonlinear effects.

Negligible absorption virtually eliminates the thermal load in the power amplifiers, leading to high-repetition-rate potential. The maximum shot frequency is therefore given by the constraints of the pump laser.

Large high-quality nonlinear amplifier crystals are available, which is a prerequisite for low spatial phase errors. Furthermore, spatial fluctuations in the phase of the pump beam within certain limits are not transferred to the signal wave, thereby relaxing constraints on the pump beam quality.

Improved pulse contrast can be achieved due to the absence of spontaneous emission outside the temporal width of the pump pulse.

The main OPCPA crystals will approach sizes of 60 cm or more, which is at the limit of present-day fabrication capability. However, mosaic configurations might be a solution to this problem, these being similar to NOVA frequency conversion crystals.

In addition to simplifying the design and operation of the whole system, these features may be of crucial importance for pulse-to-pulse carrier phase control. Since no energy storage takes place in the OPCPA process, the pump and signal pulses have to be precisely matched in space and time to achieve best results. Hence, increased complexity of the pump laser is the price to be paid for all the above simplifications in the power amplifier chain. Here, all the considerations outlined in the front-end description remain valid. One important point has to be kept in mind: In order to attain large bandwidth and high energy, short (<few ps) pump pulses are needed, which will also warrant high temporal contrast.

The most promising approach is therefore a CPA pump laser delivering pulses in the few-ps range. For 1 kJ the output energy of the frequency-doubled pump pulses will have to reach 3 kJ. That energy does not have to be delivered in a single beam, since both pump multiplexing and separate OPA stages for each beam can couple the energy from many pump pulses into a single signal pulse.

Present-day Nd-glass petawatt lasers reach about $1/10^{th}$ of the required energy in a single beam, this being mainly limited by the damage threshold of the gold-coated compression gratings, but a number of systems now under construction aim at tripling this value by using dielectric gratings (and different amplifier architecture).

The main drawback of all these systems is their inherently low repetition rate of typically 1 shot/hour. For the OPCPA approach a pump laser very similar to that for the Ti:Sa option therefore seems more appropriate. 20 Nd:glass amplifier chains as described above, seeded by a chirped-pulse front-end and each complemented by a moderate-size compressor, would deliver sufficient energy for pumping the OPCPA amplifiers. The seed can be derived from the same broadband oscillator that provides the seed pulses for the OPCPA petawatt front-end, thus ensuring perfect synchronization. As in the case of Ti:Sa, we would also investigate possible new gain materials, such as Yb:YAG crystals or ceramics, which could be diode-pumped to increase the repetition rate. In that case, the pump laser chain could simply be an extension of the already synchronized petawatt front-end pump lasers.

Compression of these ps-scale pulses to the femtosecond range could be achieved, as in the front-end, with scaled-up bulk glass and chirped mirrors.

In summary, OPCPA can provide an alternative route to achieving exawatt powers at high repetition rate. Although the technology has not yet been fully validated for generating high-energy, few-cycle pulses, first experiments and theoretical calculations have shown promising results. The experience gathered with the PFS system currently under construction at MPQ will allow a decision between Ti:Sa and OPCPA. If either concept is chosen for the power amplifier, the design of the front-end will be adapted accordingly to match the amplifier's spectral bandwidth.

B.VII.3 Multiple beam power OPCPA

One of the distinct advantages of the optical parametric amplifier (OPA) as compared with conventional quantum (laser) amplifiers is that the OPA permits the use of multiple pump beams. This possibility is predefined by the nature of the parametric amplification process. The phase difference between the pump and the signal pulses is transferred to the idler pulse, thus compensating for random differences between the pump pulses. In the more general case, multiple-beam pumping can be accomplished by using several mutually uncorrelated, but properly synchronized laser sources. The only requirements to be met are the phase matching condition and proper timing with a single signal beam. The major benefit of using the multiple-beam pump is that synchronized incoherent low-to-medium power pump sources can be used to amplify a single signal beam, thus potentially increasing the repetition rate of the overall laser system. In practice, many low-energy pump sources can replace one high-energy, but low-repetition-rate pump laser, usually used in powerful OPCPA systems. The proposed scheme could therefore be potentially useful in designing systems with high energy, short pulse duration and high repetition rate, thus yielding very high average output power. Originally, the multiple-beam pumped OPA was proposed for narrowing the spectral and the spatial bandwidth of the emitted parametric superfluorescence (Baltuska 1995). In seeded OPA configuration, multiple-beam pumping yields several practical benefits as compared with a single beam pump: (i) A multiple-beam pump allows efficient energy combining and ensures that the energy of the amplified signal exceeds that of a single pump pulse. The proof-of-principle has hitherto been demonstrated with a remarkable 80 % energy conversion efficiency without distortions of the temporal pulse profile (Dubietis 1992). In the more general case, a multiple-beam pump might be accomplished by using several mutually uncorrelated, but properly synchronized laser sources (Marcinkevicius 1998); (ii) Another relevant feature of the multiple-beam pumped OPA is that the multiple pump beams, if used in a proper geometry, could notably extend and shape the amplification bandwidth in the case of the chirped broadband seed (Zeomskis 2002). This approach constitutes an improvement of the multipass OPA, where each pass was independently tuned to amplify a different spectral portion of the broadband seed pulse (Sosnowski 1996). Most recently, two-beam pumping was shown to support more than an octave-spanning gain bandwidth for OPCPA systems (Wang 2004).

In the frame of the project, various properties of nonlinear OPA crystals have to be evaluated prior to choosing the right one for the multiple-beam pumped OPCPA configuration in terms of the damage threshold and nonlinear index of refraction, which leads to self-phase modulation, group velocity mismatch and dispersion, supported bandwidth for the appropriate pump wavelength, figure of merit and the ability to be grown in large sizes. The optimum number of separate pump channels is to be determined. Increasing the number of pump beams allows the pulse repetition rate, to be increased, but the spatial and temporal overlap can result in an interference profile within the nonlinear crystal subjected to crystal damage. The spatio-temporal shape of the pump beam also has to be estimated for the highest possible energy conversion. The matrix-type combining of the multiple-beam pump in OPCPA will be investigated as well.

B.VII.4 Compressor grating issues

A major impediment to both approaches is the limited availability of large gratings needed at the compression stage after CPA amplification. For Ti:Sa, the broadband amplified beam has to be compressed by means of gratings. The only technology today supporting large spectral acceptance linked with ultra-short pulse duration (>100 nm) consists in using metal-coated gratings (gold or silver). Such gratings are commercially available in sizes up to 94 x 75 cm². Assuming diffraction efficiencies in the range of 92 - 94% per grating, one can expect an overall compressor efficiency in the range of 70%. The drawback of such gratings is their low damage threshold limiting the fluence in the range of 100 to 200 mJ/cm².

In a conservative design (100 mJ/cm²) and assuming a 240 nm spectral window centred around 800 nm, it would be possible for 94x75 cm², 1480 l/mm gratings to support input pulse energies of up to 300 J when using elliptical pupils in order to cover the whole grating area as shown in Fig. 6a.

If the energy distribution on the grating surface is smooth enough, the fluence can be increased to 200 mJ/cm². In that case, an unfolded four-grating compressor can be envisioned: The first and last gratings are standard (94x75 cm); the intermediate gratings need to phase-lock 2 pairs of large gratings as already demonstrated at LLE Rochester and now under study at LULI (Fig. 6b) . This design could support a 1000-J input pulse, leading to an output of 700 J after compression (10-fs pulses, beam diameter 72 cm²) .

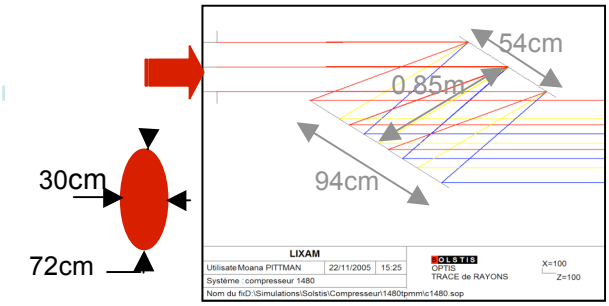

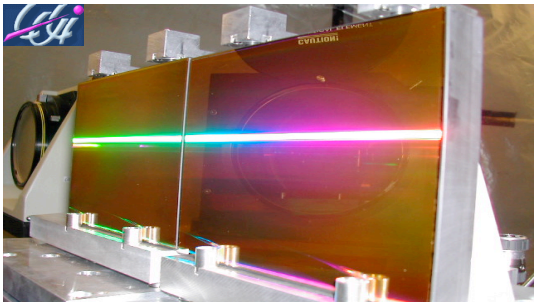

Fig. 6a ***Fig. 6b***

Fig. 6 a: *Compressor arrangement to support a 300-J input beam (210 J after compression in 10 fs). The spectral window is 240 nm and the pupil is elliptic (30x72 cm). The maximum fluence on the 1480 l/mm gold gratings is 100 mJ/cm²*

Fig. 6 b: *Demonstration of phase-locking 2 gratings at LULI. The accuracy of piston control must be better than 35 nm. With such a design and a fluence of 200mJ/cm² one can obtain 700-J, 10-fs pulses with an aperture 72 cm in diameter aperture.*

For the OPCPA approach, a large number of smaller gratings will be needed for compressing the multiple pump beams. Fortunately, the bandwidth is rather limited in that case (few nm), permitting the use of dielectric multilayer gratings.

These exhibit two major advantages: (i) higher damage threshold than gold gratings (factor 2 or more), leading to a smaller beam size, and (ii) higher diffraction efficiency (up to 98%), leading to higher throughput (80-90%), which will reduce the primary cost for generating pump energy.

B.VII.5 Multi-beam strategy for reaching exawatt peak power

To reach the exawatt level it is necessary to combine 10 to 12 beams on target in a coherent manner. This has been demonstrated in preliminary experiments with four fibre lasers as shown in Fig. 7. A similar combination of 10 single 50 – 70-PW beamlines could lead to peak power of 500 – 700-PW and corresponding intensities on target in the range of 10^{26} W/cm².

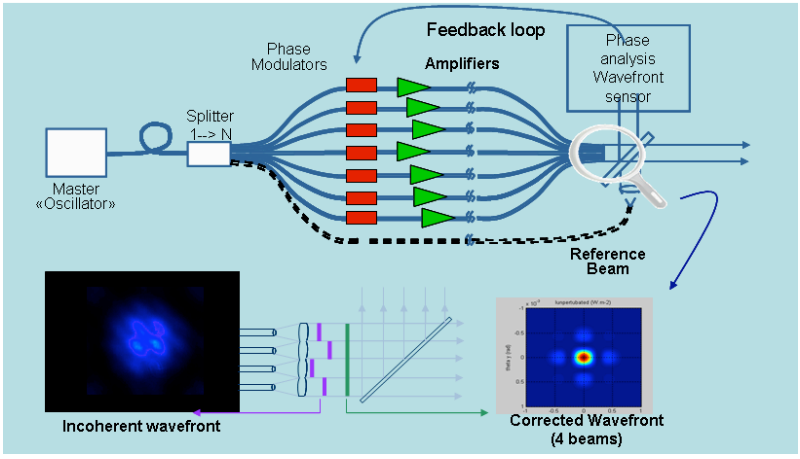

Fig. 7: *Phase-coherent addition of 4 different fiber amplifiers (LCFIO and Thales RT)*

B.VII.6 Conclusion

We have investigated solutions and schemes for a new high-potential light source based on the latest technologies which can deliver in a single beam up to 700 J in 10 to 15 fs at 1 shot per minute. The main technical and theoretical impediments have been identified and a two alternative schemes relying on either parametric amplification or laser amplification in Ti:sapphire have been proposed and dimensioned. Combining a dozen of such beam lines through coherent summation could be a path towards reaching the exawatt level.

Such an extremely high-intensity laser facility will provide a versatile range of repetition rates and energies ranging from kHz repetition rates at the joule level to 0.1-Hz repetition rate at the kJ level and will afford exceptional potential for the most challenging laser-matter interaction experiments described in the science case for ELI.

B.VIII : BIBLIOGRAPHY

Affleck 1987 Affleck, I. and Kruglyak, L., Phys. Rev. Lett. **59**, 1065 (1987).

Akama, 1983 Akama., K, *Gauge Theory and Gravitation*, Vol. **176**, Berlin: Springer-Verlag, p. 267 (1983)

Alkofer 2001 Alkofer, R., et al., Phys. Rev. Lett. **87**, 193902 (2001)

Akama, 1983; Akama., K, *Gauge Theory and Gravitation*, Vol. 176, Berlin: Springer-Verlag, p. 267 (1983)

ArkaniHamed 2000 Arkani-Hamed, *et al*., Phys, Rev. Lett. 84, 586 (2000).

ArkaniHamed 1998 Arkani-Hamed, N., *et al*., Phys. Lett. B 429, 263 (1998).

ArkaniHamed 2002 Arkani-Hamed *et al*., Phys. Today 55, 35 (2002).

Avetissian 2002 Avetissian, H. K., et al., Phys. Rev. E **66**,016502 (2002)

Bahk 2004 Bahk, S.-W *et al.*, Opt. Lett. **22**, 2837 (2004).

Baltuska 1995 Baltuska A. *et al.*, Opt. Lett. **20**, 2174 (1995).

Baltuska 2003 Baltuska A. *et al.*, Nature 421, 611-615(2003).

Baltuska 2006 Baltuska, A., private communication

Blaschke 2002 Blaschke, D. B., *et al.*, nucl-th, 0511085 (2003).

Bell 1987 Bell, J. S., *et al.*, Nucl. Phys. B **284**, 488 (1987).

Bonse 1983 Bonse, U., and Wroblewski, T., Phys. Rev. Lett. **51**, 1401 (1983).

Brozek-Pluska 2005 Brozek-Pluska, B., Radiation and Chemistry, **72**, 149-159 (2005).

Bulanov 2002 Bulanov, S.V., *et al.*, Physics Letters A **299**, 240–247 (2002).

Bulanov 2003 Bulanov, S. V., *et al.*, Phys. Rev. Lett. **91**, 085001 (2003)

Bulanov 2004 Bulanov, S. V., *et al.*, Phys. Lett. A **330**, 1 (2004)

Bulanov 2005 Bulanov, S. V., *et al.*, Nucl. Instrum. Methods A **540**, 25 (2005)

Bychenkov 2001 Bychenkov, V., et al., Plama Phys. Rep. **27**, 1017 (2001).

Chen 1999 Chen, P. and Tajima, T., Phys. Rev. Lett., **83**, 256 (1999)

Chen 2002 Chen, P., *et al.*, Phys. Rev. Lett. 89, 161101 (2002).

Cerullo 2003 Cerullo, G., De Silvestri, S., *Rev. Sci. Instr.* **74**, 1 (2003)

Clark 2000 Clark, E., *et al*., Phys. Rev. Lett. **84**, 670-673 (2000).

Cowan 2004 Cowan, T., *et al.*, Phys. Rev. Lett. **92**, 204801 (2004).

Dawson 1984 Dawson, J. M., and Lin, A. T., 1984, in: Basic Plasma Physics, Vol. 2, p. 555 (1984).

Dipiazza 2005 Di Piazza, A., *et al.*, Phys. Rev. D **72**, 085005 (2005).

Dubietis 1992 Dubietis, A. *et al.*, 1992, Opt. Comm. 88, 437 (1992).

Dubietis 1998 Dubietis, A. *et al*., J. Opt. Soc. Am. B **15** 1135 (1998)

Euler 1936 Euler, H., Ann. Phys. (Leipzig) **26**, 398 (1936).

Esirkepov 2002 Esirkepov, T., *et al.,* Phys. Rev. Lett. 89, 175003 (2002).

Esirkepov 2004 Esirkepov, T., *et al.,* Phys. Rev. Lett. 92, 17 (2004).

Faure 2004 Faure, J., *et al.,* Nature **431**, 541 (2004).

Faure 2005 Faure, J., *et al.,* to be published in PRL

Fourkal 2002 Fourkal, E., *et al.*, Med. Phys. **29**, 2788-2798 (2002).

Fourkal 2003 Fourkal, E., *et al.*, Med. Phys. **30**, 1660-1670 (2003).

Fradkin 1985 Fradkin, E. S., *et al.*, *Quantum Electrodynamics with Unstable Vacuum*, (Springer-Verlag, Berlin) (1985).

Fritzler 2003 Fritzler, S., *et al.*, Appl. Phys. Lett. 83, 15 (2003).

Gahn 2002 Gahn, C., et al., Phys. Plasmas **9**, 987 (2002).

Geddes 2004 Geddes, C. G. R. *et al.,* Nature **431**, 538 (2004).

Geissler 2006 Geissler, M., *et al.*, submitted to New Journal of Physics (2006).

Glinec 2005 Glinec, Y., *et al.,* Phys. Rev. Lett. 94 025003 (2005).

Glinec 2005 Glinec, Y., *et al.*, to be published in Med. Phys.

Gordienko 2005 Gordienko, S., and Pukhov, A., Phys.of Plasmas, 12 (2005).

Gordienko 2004 Gordienko. S. *et al*. Phys. Rev. *Lett*. **93**, 115002 (2004)

Gordienko 2005 Gordienko, S., *et al.*, Phy. Rev. Lett. **94**, 103903 (2005)

Greisen 1966 Greisen, K., Phys. Rev. Lett. 16, 748 (1966).

Habs 2001 Habs, D., *et al.*, Progr. Part. Nucl. Phys. 46, 375 (2001).

Halpern 1933 Halpern, O., Phys. Rev. **44**, 855 (1933).

Hawking 1975 Hawking, S. W., Nature, **248**, 30 (1975)

Hawking 1975 Hawking, S. W., 1975, Commun. Math. Phys. **43**, 199.

Hegelich Hegelich, B. M., *et al.*, Nature 2006.

Hencken 2004 Hencken, K., *et al.*, Czewch. J. of Phys. **54**, A21 (2004)

Henrich 2004 Henrich, B., *et al.*, Phys. Rev. Lett. **93**, 013601 (2004)

Hentschel 2001 Hentschel M. *et al.*, Nature 414, 509-513(2001)

Heisenberg 1936 Heisenberg W., and Euler, H., Z. Phys. **98**, 714 (1936).

Ishii 2005 Ishii, N., *et al.*, *Opt.Lett*. **30** 567 (2005)

Itzykson 1980 Itzykson, C., and Zuber, J.-B., Quantum Field Theory, Mc.Graw-Hill, 1980, ISBN 0-07-032071-3.

Kienberger 2004 Kienberger R. *et al.*, Nature **427**, 817(2004), Science **305**, 1267 (2004).

Klein 1964 Klein, J. J., and Nigam, B. P., Phys. Rev. **135**, 1279 and Phys. Rev. **136**, 1540 (1964).

Ledingham 2003 Ledingham, K., *et al.*, Science **300**, issue 5622, 1107-1111 (2003).

Ledingham 2004 Ledingham, K., *et al.*, J. Phys. D: Appl. Phys. **37**, 2341–2345 (2004).

Lefebvre 1994 Lefebvre, E and Bonnaud, G, Phys. Rev. Lett. **74**, 2002 (1994).

Lewis 2000 Lewis, R., *et al.*, J. Synchrotron Rad., **7**, 348 (2000).

Lifschitz 2005 Lifschitz, A., et al., Phys. Plasmas **12**, 0931404-0931412 (2005).

LLNL 2004 LLNL and Metal improvement company, ICUIL conference, **28**, 14 15 July (2004).

Mcdonald 1985 McDonald, K.T., Fundamental physics during violent acceleration, DOE/ER/3072-21 (1985).

Magill 2003 Magill, J., et al., *Appl. Phys.* B. 77, 387-390 (2003)

Malka 2002 Malka, V., *et al.*, Science **298**, 1600 (2002).

Malka 2003 Malka, V., Europhysicsnews, Feb. (2004).

Malka 2004 Malka, V., *et al.*, Med. Phys. **31**, 1587-1592 (2004).

Malka 2005 Malka, V., *et al.*, Plasma Physics and Controlled Fusion **47** (2005).

Manclossi 2006 Manclossi, M. *et al.*, Submitted to Phys. Rev. Lett.

Mangles 2004 Mangle, S. P. L., *et al.,* Nature **431**, 535 (2004).

Marcinkevicius 1998 A. Marcinkevicius et al., Opt Comm. **158** 101 (1998)

Marinov 1977 Marinov, M. S., and Popov, V. S. Fortschritte der Physik, **25**, 373 (1977)

Meyer-ter-Vehn 2005 Meyer-ter-Vehn, J., *et al.*, Plasma Phys. Control. Fusion **47**, B807 (2005)

Moulin 1999 Moulin, F., and Bernard, D. Opt. Commun. **164**, 137 (1999).

Mourou 1998 Mourou, G. A., *et al.*, Phys. Today 51, 22 (1998).

Mourou 2002 Mourou, G. A., *et al.,* Plasma Phys. Rep., **28**, 12 (2002).

Mourou 2006 Mourou, G. A., Tajima, T., and Bulanov, S. V., Rev. Mod. Phys. **78**, 1 (2006).

Mueller 2003 Müller, C., *et al.*, Phys. Rev. A **67**, 063407 (2003),

Mueller 2003 Müller, C., *et al.*, Phys. Rev. Lett. **91**, 223601 (2003).

Mulser 2003 Mulser, P., & Schneider, R., Laser & Particle Beams 22, 157 (2003).

Narozhny 2004 Narozhny, N.B., *et al.*, JETP Lett. **80**, 382 (2004).

Naumova 2004 Naumova, *et al.*, Phys. Rev. Lett. **92**, 063902 (2004).

Naumova 2004 Naumova, *et al.*, Phys. Rev. Lett. **93**, 195003 (2004).

Naumova 2005 Naumova, N., Nees, J., Mourou, G., Phys. Plasmas **12**, 056707 (2005).

Nees 2005 Nees, J., *et al.*, J. Mod. Optics **52**, 305 (2005) 305

Parker 1969 Parker, L., Phys. Rev. **183**, 1057 (1969).

Patterson 2002 Patterson, F. G., *et al.*, Optics Letters **28**, 14 (2002)

Popov 2002 Popov, S.V., Phys. Lett. **A298**, 83 (2002)

Pukhov 2002 Pukhov, A. and Meyer-ter-Vehn, J., Appl. Phys. B: Lasers Opt. **74**, 355 (2002)

Pukhov 2003 Pukhov, A., 2003, Reports on Progress in Physics **66**, R47.

Reiche 1999 Reiche, S., Nucl. Instrum. and Methods in Phys. Research A, **429**, pp. 243 (1999).

Ringwald 2001 Ringwald, A., Phys. Lett. **B510**, 107 (2001)

Rischel 1997 Rischel, C., *et al.*, Nature (London) **390**, 490 (1997).

Roberts 2002 Roberts, C. D., *et al.*, Phys. Rev. Lett. **89**, 153901 (2002).

Rogers 1988 Rogers, J. , Phys. Rev. Lett. **61**, 2113 (1988)

Rousse 2001 Rousse, A., *et al.*, Nature (London) **410**, 65 (2001).

Rousse 2001 Rousse, A., *et al.*, Rev. Mod. Phys. **73**, 17 (2001).

Rousse 2004 Rousse, A., *et al.*, Phys. Rev.Lett. **93**, 135005 (2004).

Ross 1997 Ross, I. N., *et al.*, Opt. Comm. **144** 125 (1997).

Ross 2000 Ross, I. N., *et al.*, Applied, Optics 39, 2422 (2000).

Ross 2002 Ross, I. N., *et al., J. Opt. Soc. Am. B* **19** 2945 (2002)

Ross 2006 Ross, I. N., private communication

Rubakov 2003 Rubakov, V. A., Uspekhi Phys. Nauk 173 (2003).

Rubakov 1983 Rubakov, V. A., and Shaposhnikov, M. E., Phys. Lett. B 125 (1983).

Ruder 1994 Ruder, H., *et al.*, Atoms in strong magnetic fields, Springer (1994).

Sarkisov 1999 Sarkisov, G., *et al*., Phys. Rev. E **59**, 7042 (1999)

Snavely 2000 Snavely, R. A., *et al*.. *Phys. Rev. Lett.* **85**, 2945-2948 (2000).

Strickland 1986 Strickland, D., and Mourou, G., Opt. Commun. **56**, 212 (1986).

Schwinger 1951 Schwinger, J., Phys. Rev. **82**, 664 (1951)

Schwoerer 2001 Schwoerer, H., *et al.*, Phys. Rev. Lett. 86 (11), 2317 (2001)

Schwoerer 2003 Schwoerer, H., *et al.*, Europhys. Lett. 66 (1), 47-52 (2003)

Schwoerer 2006 Schwoerer, H., *et al.*, Nature 2006

Sosnowski 1996 Sosnowski, T. S., *et al.*, Opt. Comm. **21**, 140 (1996).

Ta Phuoc 2003 Ta Phuoc, *et al.*, J. Opt. Soc. Am. B **20**, 221-223 (2003)

Ta Phuoc 2005 Ta Phuoc, *et al.*, Physics of Plasmas **12**, 023101-8 (2005)

Tajima 1979 Tajima, T., and Dawson, J. M., Phys. Rev. Lett. **43**, 267 (1979)

Tajima 1989 Computational *Plasma* Physics (Addison-Wesley, Reading) (1989).

Tajima 2001	Tajima, T., *Advanced Accelerator* Concepts (2001).
Tajima 2002	Tajima, T., and Mourou, G., Phys. Rev, STAB **5**, 031301 (2002).
Tsakiris 2006	Tsakiris, G., *et al.*, New Journal of Physics, **8,** 19 (2006).
Tsung 2004	Tsung, F. S., Phys. Rev. Lett. **93**, 185002 (2004).
Wang 2004	Wang, C., *et al.*, Opt. Comm. **237**, 169 (2004).
Weber 2005	Weber, S., *et al.*, Phys. Rev. Lett. **94**, 055005 (2005).
Weber 2005	Weber, S., *et al.*, Phys. Plasmas **12**, 112107 (2005).
Unruh 1984	Unruh, W.G., and Wald, R., Phys. Rev. D **29**, 1047 (1984).
Wilczek 2000	Wilczek, F., *et al.*, Phys. Rev. Lett. **85**, 5042 (2000)
Yablonovitch 1989	Yablonovitch, E., Phys. Rev Lett. **62**, 1742 (1989).
Zatsepin 1966	Zatsepin, G., and Kuzmin, V., JETP Lett. 4, 78 (1966).
Zel'dovich 1974	Zel'dovich, Ya. B., 1974, in Proceed IAU Symp. 63: Confrontation of Cosmological Theories with Observational Data, vol. 63, p. 329.
Zeromskis 2002	Zeromiskis, E. *et al.*, Opt. Comm. **158**, 435 (2002).

B.IX Scientific Programme of "*EUROPEAN EXTREME LIGHT INFRASTRUCTURE: SCIENTIFIC PROSPECTS*", ENSTA, Paris, December 9-10, 2005

⏭ Friday, 9 December 2005

	Registration
8.30 • 9.00	*Inscription*
9.00 • 9.45	**Introduction : G.-A. Mourou**
9.45 • 10.15	**Attosecond Physics Part I : F. Krausz**, G. Tsakiris, Ph. Balcou
10.15 • 10.45	*Coffee break*
10.45 • 12.00	**Attosecond Physics Part II : F. Krausz**, D. Charalambidis, K. Kompa, U. Bovensiepen, M. Vrakking, J. Ullrich
12.00 • 13.00	*Lunch*
13.00 • 14.15	**Medical Applications : A. Brahme**, D. Schardt, R. Ferrand, J. Freudenberger
14.15 • 15.15	**Particle Beams Part I : V. Malka**, A. Pukhov, J. Scrheiber, M. Roth
15.15 • 15.45	*Coffee break*
15.45 • 16.45	**Particle Beams Part II : V. Malka**, H. Videau, D. Bernard
16.45 • 18.15	**Femto X and X FEL : F. Gruener**, A. Rousse, F. Sette, S. Sebban

20.00 *Dinner*

⏭ Saturday, 10 December 2005

8.30 • 10.00	**New Physics Frontiers : S. Bulanov**, D. Habs, D.-B. Blaschke, R. Shützhold, Hatsagortsyan, F. Pegoraro
10.00 • 10.30	*Coffee break*
10.30 • 11.30	**Nuclear Physics : R. Sauerbrey**, F. Hannachi, K. Ledingham
11.30 • 12.30	**Plasma physics : J. Meyer-ter-Vehn**, V. Tikhonchuck, O. Willi
12.30 • 13.30	*Lunch*
13.30 • 14.30	**Relativistics Engineering : J.-P. Brasile**, H. Backe
14.30 • 15.30	**Material Science : G. Petite**, G. Dollinger
15.30 • 16.00	*Coffee break*
16.00 • 17.30	**Laser Technology : J.-P. Chambaret**, S. Karsch, J. Collier, A. Piskarskas
17.30 • 18.00	**Academic Formation : D. Hulin**
18.00	**Concluding Remarks : G. Mourou**

	List of participants	In the scientific programme	Country	Number
1	BACKE Hartmut			
2	BLASCHKE David			
3	BOVENSIEPEN Uwe	Freie Univ. Berlin		
4	DOLLINGER Günther			
5	FREUDENBERGER Joerg			
6	GRUENER Florian	MPQ		
7	HABS Dietrich	MPQ		
8	HATAGORTSYAN Karen	MPK		
9	KARSCH Stefan			
10	KOMPA L.K.	MPQ		
11	KRAUSZ Ferenc	MPQ		
12	MEYER TER VEHN	MPQ		
13	OSTERHOLZ Jens			
14	PUKHOV Alexander	Univ Dusseldorf	Germany	28
15	ROTH Markus			
16	SANDNER Wolfgang	MBI		
17	SAUERBREY Roland	Friedrich-Schiller-Universitat		
18	SCHARDT Dieter			
19	SCHRAMM Ulrich			
20	SCHREIBER Joerg			
21	SCHUETZHOLD Ralf			
22	SEWTZ Michael			
23	TARASEVITCH Alexander	Univ Essen		
24	TSAKIRIS George	MPQ		
25	ULLRICH Joachim			
26	WILLI Oswald	Univ. Düsseldorf		
27	WITTE Klaus	GSI		
28	MUELLER Carsten			
	LEDINGHAM Ken	University of Strathclyde	Scotland	1
1	ALBERT Olivier		France	88
2	ALEONARD Marie Madeleine	CENBG		
3	AMIRANOFF François	LULI		
4	ANTONETTI André			
5	ANTONUCCI Rahul			
6	ARTEMIEV Nikolay			
7	AUBOURG P.	QUANTEL		
8	BALCOU Philippe	LOA		
9	BEN ISMAIL Ahmed			
10	BOSCHETTO Davide	LOA		
11	BOYKO Olga			
12	BRASILE Jean-Pierre	THALES Laser		
13	BURGY Frédéric			

14	CHAMBARET Jean-Paul	LOA
15	COTEL Arnaud	
16	COUPRIE Marie-Emmanuelle	CEA Saclay
17	CROS Brigitte	LPGP
18	D'AMICO Ciro	
19	DESRUELLES Bruno	
20	DOUMY Gilles	
21	ETCHEPARE Jean	LOA
22	EWALD Friederike	
23	FAURE Jérôme	LOA
24	FERRAND Régis	CPO Orsay
25	FLACCO Alessandro	LOA
26	FRANCO Michel	
27	GARL Thomas	
28	GAUTHIER Jean-Claude	CELIA
29	GLINEC Yannick	LOA
30	GLORIEUX Pierre	
31	GODET Nathalie	CNRS
32	GOSSELIN Gilbert	
33	GOUNAND François	
34	GUEMNIE TAFO Alain	LOA
35	GUIGNARD Gilbert	
36	HOUARD Aurélien	
37	HUIGNARD J.P.	THALES Laser
38	HULIN Danièle	
39	KLISNICK Annie	LIXAM
40	KOVACS Francis	CEA CESTA
41	LABAUNE Gérard	THALES Laser
42	LAVOCAT Philippe	IN2P3
43	LE BLANC Catherine	
44	LEBLANC	LULI
45	LEFEBVRE Erik	CEA
46	MALKA Gérard	
47	MALKA Victor	
48	MANCLOSSI Mauro	
49	MAQUET Alfred	
50	MARTEAU Jean-Michel	QUANTEL
51	MAYNARD Gilles	LPGP
52	MEOT Vincent	
53	MERANO Michele	
54	MERDJI Hamed	CEA
55	MIGUS Alain	IOTA
56	MORA Patrick	CPHT
57	MOREL Pascal	
58	MOUROU Gérard	
59	MULLER Sophie	THALES Laser
60	NAUMOVA Natalia	
61	PAPALAZAROU Evagellos	

62	PETITE Guillaume			
63	PETROFF	ESRF		
64	PITTMAN Moana	LIXAM		
65	PLE Fabien	LIXAM		
66	PRADE Bernard			
67	QUERE Fabien			
68	RAOUX D.	SOLEIL		
69	RENAULT Amandine			
70	ROS David	LIXAM		
71	ROUSSE Antoine			
72	SAUTERET Christian			
73	SEBBAN Stéphane			
74	SETTE Francesco	ESRF		
75	SHAH Rahul			
76	SHEVCHENKO Oleg	LOA		
77	SOMEKH Guy	ENSTA		
78	TA PHUOC			
79	TARISIEN Medhi			
80	TIKHONCHUK Vladimir	celia		
81	TOURNOIS Pierre			
82	TRISORIO Alexandre			
83	VIDEAU	LLR		
84	VIGROUX L.	Amplitude Technologies		
85	WATTELIER B.	Phasix		
86	ZOU Ji Pong	LULI		
87	HANNACHI Fazia			
88	THAURY Cédric			
89	COLLIER J.L.	CLF		
90	DUNNE Mike	CLF	GB	3
91	NEELY David	CLF		
92	ZEPF Matthew		Ireland	1
93	GIULIETTI Danilo	CNR		
94	PEGORARO Francesco	Univ Pisa	Italy	3
95	TURCHETTI Giorgio	Univ Bologna		
96	BULANOV Sergei		Japan	1
97	PISKARSKAS Algis	VULRC	Lithuania	1
98	UBACHS Wim	LCVU	Netherlands	2
99	VRAKKING Marc	FOM-AMOLF		
100	BADZIAK Jan		Poland	2
101	WOLOWSKI	IPPLM		
102	RUS	PALS	Czech Republic	1
103	NORLIN Andréas			
104	WAHLSTROM Claes-Göran	LLC	Sweden	3
105	BRAHME Anders			

PART C: IMPACT ON SOCIETY AND ON NEW TECHNOLOGY FOR INDUSTRY

C.I Medicine: Application to HadronTherapy

High-power laser systems as proposed in the ELI project afford new and unique possibilities of producing of intense particle beams with energies in the MeV to GeV region. Particular advantages of laser-driven accelerators are their compact size ('table-top' devices) and low cost – both investment and operation costs – which would significantly reduce the size and cost of hospital-based proton and light-ion cancer treatment facilities. Furthermore, laser technology may offer much more elegant and cost-saving solutions for the rotating gantry structures, which at present are very heavy and bulky devices allowing beam delivery to the patient at all angles. For these reasons, laser technology is expected to revolutionize the field of particle radiotherapy and make very compact treatment units available. As a result, much more patients would benefit from highly precise and effective radiation treatment with energetic particle beams.

At present, twenty-five proton and three carbon-ion treatment units are in operation world-wide, these using either cyclotron or synchrotron RF accelerators. In Europe a number of new facilities are coming up soon or in the near future: RPTC Munich (protons), HIT Heidelberg (light ions), CNAO Milan (light ions), MED-AUSTRON Vienna (light ions), ETOILE Lyon (light ions), and RKA Marburg (light ions). These facilities will be the first clinical-based ion therapy centres in Europe. In view of the promising clinical results recently obtained with carbon-ion radiotherapy at HIMAC/Japan and GSI Darmstadt/Germany, there is a strong demand for new treatment facilities with much higher patient capacity. Laser-driven accelerators are therefore expected to have a strong impact on the next generation of treatment facilities.

The typical and most critical requirements for particle beams used for cancer treatment are briefly discussed in the following:
The major physical advantage of charged-particle beams in radiotherapy is their excellent inverted depth-dose profile (Bragg curve) offering most favourable conditions for the treatment of deep-seated tumours. In contrast, to photons the energy deposition increases for particles with depths up to a pronounced maximum (Bragg peak) at the end of range. For example, the Bragg peak of a 330 MeV/u monoenergetic carbon-ion beam penetrating 20 cm into tissue has a half-width (FWHM) of only 5 mm and the peak dose is a factor of about 4.5 higher than the plateau dose. The width of the Bragg peak is mainly caused by the unavoidable energy-loss straggling. By varying the particle energy, the depth of the Bragg peak in the target volume can be precisely adjusted to the location prescribed by the treatment plan. With scanning systems, the target volume is irradiated slice-by-slice in steps of typically 1 - 2 mm in depth by moving pencil-like ion beams over each target slice in strict accordance with the prescribed contour and dose pattern.

Both the absolute kinetic energy and the energy spread of the incident ion beam are of key importance for radiotherapy applications. In the example above, an energy shift of ±1% would shift the Bragg peak location by ±3.3 mm. At least at higher energies, the energy spread

of the primary beam should therefore be better than 1%. The recent finding of narrow peak structures of laser-generated electron beams (Nature Vol. 431, Sept.2004) was an important step demonstrating that favourable beam characteristics such as narrow beam energy spectra can be achieved by the laser-foil technology. Laser-generated carbon-ion beams with an energy spread of 25% at 3 MeV/u have been produced experimentally. PIC-simulations predict a much smaller energy spread (order of 1%) at higher laser power.

The treatment of deep-seated tumours requires beam energies in the range of about 50 – 430 MeV/u for carbon-ions. Ideally, the selected energy is delivered directly by the accelerator. Alternatively, passive degraders (range-shifters) can be used for energy selection, but this causes contamination of the primary beam by secondary fragmentation products, in particular neutrons, with long ranges. These particles can be removed by proper shielding and cleaning magnets before reaching the treatment area, but only at the expense of increased space and cost requirements.

Another important question is how to control the beam intensity and number of ions delivered, which is directly related to the dose deposited in a patient. Scanning beam systems (such as operational at GSI) require intensities in the range of 10^6 – 10^8 carbon ions per second, the scanning speed being limited by the magnet power supplies. Such systems require beams with a well-defined average intensity and can tolerate only small fluctuations. For a laser-driven system, control and regulation of the dose rate would require either a sufficiently high pulse repetition rate (100 – 1000 Hz) or stretching of the ultra-short pulses. This could be achieved by injecting the short particle pulses into a stretcher ring which would also serve as an accumulator ring. From this ring particle beams with well-defined beam energy could be slowly extracted and distributed to several treatment rooms.

Table 1 Basic requirements for ion beams used in radiotherapy

Type of ion	proton, He, Li, B, C, O contamination level < 1%
Energy range	p, He 30 – 220 MeV/u C 50 – 430 MeV/u O 50 – 500 MeV/u
Energy spread	0.1 – 1%
Intensity range	10^6 – 10^8 ions/s selectable intensity levels, small fluctuations
Time structure	100 – 1000 Hz rep. cycle required for dose control or pulse stretching
Beam interrupt	fast (< 1 ms)

Table 1 lists the basic requirements for particle beam applications in radiotherapy. Although these requirements can not yet be fully met by laser-driven systems, solutions to specific problems might be possible in the near future. The requirements for scanning beam systems are higher than those for passive beam delivery systems. However, scanning beam systems are clearly superior, giving optimum three-dimensional conformation of the dose to the target volume and thus taking full advantage of the clinical benefits of light-ion beams.

Replacement of the LINAC section by a laser-driven accelerator (as proposed by M. Roth) will represent a very important first step towards laser-generated ion beam applications in radiotherapy and is essential for demonstrating the feasibility and potential advantages of such systems. This would require particle beams of a few MeV/u, which have already been produced by existing laser-driven systems. Such a test facility would permit thorough investigations of all beam parameters relevant to applications in radiotherapy, in particular the stability and reproducibility of the particle energy as well as long-term behaviour and safety aspects.

This programme will permit multidisciplinary activities in a very new and promising field of research and will lead to the strengthening of European leadership.

C.II Secondary sources for material science studies

C.II.1 Understanding fundamental aging processes in nuclear power plant material

ELI will be a powerful tool for generating secondary beams, among which intense, ultra-short particle bunches may prove particularly useful for material sciences. Let us recall that with present-day lasers it has already been demonstrated that electrons with hundreds of MeV, protons and carbon ions with several MeV, and even 2.5-MeV neutrons can be obtained in short (sub-picosecond) and intense ($>10^{12}$ particles) pulses. It is reasonable to expect that a x1000 increase of the power available will result in much more intense pulses for such particles, higher energies, and also the possibility of accelerating heavier ions.

Obviously, however, having access to short pulses of high-energy ions synchronized with laser pulses affords hope o realizing a brand new type of experiments, viz. ion (pump)-laser (probe) experiments. Indeed, the mechanisms leading to defect creation or phase transformation in materials subjected to low or high-energy ions involve as initial steps ultra-fast processes whose elucidation is still a challenge: in the case of elastic scattering, collision cascades – at present observed only through atomistic simulations – or intense and short-lived electronic excitation in the case of high-energy ions – for which essentially two models were proposed long ago; and there is no clear answer yet concerning their respective validity. It is essential in both cases to obtain observations of the state of the target in the first few picoseconds after passage of the particles, and only laser-based sources can make such observations possible. It would, in principle, be possible either to observe directly the instantaneous electron distribution just after irradiation (in laser-laser experiments, time resolutions of a few 10^{-14} s are currently being achieved) or, with the use of a second derived source as a probe (e.g. an X-ray source, for X-ray diffraction experiments), to observe the

onset of the disorder induced in the material with unequalled resolution. It must be clear, however, that, if demonstration experiments can be started very soon, clean experiments will require such control of the ion beam quality as is still beyond reach for the time being. In particular, it will be necessary to control the ion charge state and the energy spectrum, while keeping the pulse as short as possible – i.e. well below one picosecond - at the sample position. This is a serious challenge the ion-beam community, and the availability of intense sub-picosecond ion pulses resulting from the completion of the ELI project could thus boost technical progress way beyond the laser community. In this respect, it is not too early to start thinking of solutions for recompressing an ion pulse to durations of less than one picosecond. A final remark concerning experiments of this type is that they should bring decisive progress in a field (radiation physics) that is at the heart of the economic and environmental performances of major technologies, such as the production of electronuclear energy, and the associated fuel cycle.

C.II.2 Positron microscope

Intense and short pulses of positrons could also be particularly interesting. Positrons are used in several techniques of material analysis: The lifetime of the positrons in solids, this being in the range of picoseconds, is inversely proportional to the electron density. Positrons are easily trapped at vacancy-type defects, where the positron lifetime is prolonged. The lifetime spectrum, therefore, tells about the type and density of the defect distribution in solids. On this basis, it has been possible, for instance, to build a positron microscope able to observe inside a material the appearance of clusters of vacancies located at the head of a scratch. In addition, the chemical surroundings can be analyzed from the Doppler shift of the annihilation radiation. The Doppler effect can also be used to analyze the momentum distributions of the electrons in the solid in great detail.

Many of the techniques associated with positrons rely on measurement of their lifetime, which … in the range of hundreds of picoseconds. It is usually measured as the time elapsing between a start signal associated with penetration of the positron into the solid and detection of the gamma photons emitted in their annihilation with one material electron. This works because of the low intensity of the positron beams used so far (on the nanosecond time scale, they can be considered as isolated). This is also true in the case of the short bunches of positrons generated in existing machines, as well as in those still being planned (there are several such projects in Europe as well as in Japan), which produce pulses with durations of typically 100 ps at a high (tens of MHz) repetition rate, but with on average one positron only per pulse.

C.II.3 Positron sources for Bose-Einstein condensate

The progress that can be expected from a laser-produced positron source does not, however, arise mainly from the pulse shortness, since this will be extremely difficult to maintain in the necessary handling of the beam (which, in particular requires a “moderation” stage followed by re-bunching of the positrons), but from the opportunity of obtaining intense pulses. One can consider first extensions of the applicability of present applications. For example, if it is possible to saturate all vacancies and vacancy clusters in the irradiated zone,

the lifetime measurements could provide not only identification of the type of defects present in the sample but also, by virtue of the change in the lifetime occurring on saturation, a measurement of their absolute density. But entirely new physics could also emerge from high-intensity positron sources, e.g. the possibility of realizing Bose-Einstein condensates of positronium: in a cavity with a volume of 1000 nm^3, such a condensate could be obtained with 100 positronium "atoms" only. But if 10^{10} positronium atoms could be trapped in a 1-cm-long cavity 1 μm in diameter, some recent theoretical predictions suggest the possibility of realizing in this way a 511-keV X-ray laser.

C.II.4 Improving environment: transmutation and nuclear waste treatment

Transmutation, i.e. using nuclear reactions to change very long-lived radioactive elements into less radioactive or shorter-lived products – is a concept for nuclear waste management being developed in several countries. Very long-lived iodine-129 has a half-life of 15.7 million years, high radiotoxicity and mobility, and is an important constituent of nuclear waste – making it one of the primary risk considerations in the nuclear industry. It currently has to be sheathed in glass and buried deep underground. Handling of iodine is also difficult since it is corrosive and volatile. Through the laser-induced photo-transmutation process, this long-lived isotope is transmuted first to the short-lived isotope, iodine-128, which then decays with a half-life of 25 minutes to the stable inert gas, xenon-128. The experiments demonstrate the feasibility of transmuting radioactive iodine-129; limitations to scaling up this technique may be the high energy consumption of the laser and the low cross-sections of the elements in question, resulting in low transmutation efficiencies. By focusing the high-power laser onto a tantalum metal target, the beam generates a plasma with temperatures of ten billion degrees. The electrons in the plasma generate gamma radiation intense enough to induce nuclear reactions in the iodine target.

Medicine:
1 Application to hadron therapy

Secondary sources for material science studies:
2 Understanding fundamental aging processes in nuclear power plant materials
3 Positron microscope
4 Positron source for Bose-Einstein condensate
5 Improving environment: transmutation and nuclear waste treatment

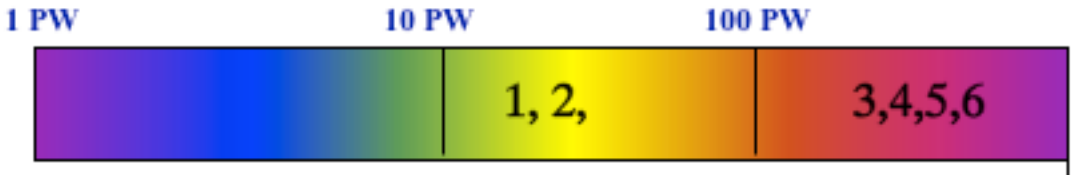

PART D: EDUCATIONAL AND TRAINING PERSPECTIVES IN THE ELI PROJECT

An ambitious project such as ELI should give Europe world leadership in ultra-intense lasers and in the corresponding new physics; this is a unique opportunity in terms of tuition and training within the well-known triangle linking research, education and innovation.

We identify two levels of training activities, defined in accordance with the unified Bologna course of studies in the EU:

D.I Training at the Master's Degree and Engineering School Levels

The Master's degree plays a vital role in national training programmes. It is at this stage that young post-graduates will in fact choose their career and this is therefore the ideal time to attract the brightest of them to laser and plasma physics. Different Master's degree courses in these fields are already available Europe-wide, but they suffer from limited publicity on the European level, which tends to restrict them to a purely national audience in each case; furthermore, such Master's degree programmes are also provided in larger domains.

In the wake of the ELI project, there is the possibility of launching an international Master's degree dedicated to the physics of matter in extreme light interactions. The visibility of this Masters's degree programme would be very strongly enhanced in relation to current national programmes, allowing it to attract students from all over Europe and, as a consequence, to diffuse the know-how in many EU countries.

A broad range of scientific subjects should be proposed within this European Master's degree programme; this, of course, is in line with the many scientific application realms of the ELI project.

At a later stage, benchmarking actions will be necessary in each participating country to estimate and improve the added valued of the Master's degree programme.

D.II Training at the Doctorate (PhD Thesis) Level

Pre- and post-PhD training courses enable students to confirm their choice while at the same time providing essential additional training in the extremely complex field of physics with ultra-high-intensity lasers. At the doctorate level, pre- and post-PhD "summer schools" are envisioned. It should be emphasized that the aim of a PhD programme accompanying ELI is by no means to duplicate the efforts of national educational systems or Marie Curie activities. On the contrary, the Marie Curie training site programme can be considered as an ideal framework for performing PhD work along with ELI.

In every respect, the necessity of using the ELI project as a basis for tuition and training should be kept in mind at all stages in the project definition. The pronounced visibility of such a project is a unique opportunity to highlight to the accompanying tuition and training

programmes, thus contributing therefore to attracting bright students either from Europe or worldwide and improving Europe's scientific and technological manpower.

PART E: STRATEGIC IMPORTANCE OF ELI

E.I Why ELI?

ELI will be the first facility of this kind. Its scientific scope is vast, ranging from eV to possibly 100 GeV in energy and femtosecond to attosecond in time scale. ELI appeals to a broad-based scientific community. This was evidenced by the workshop on ELI's scientific case, to which many European researchers representing almost all the European laboratories came to contribute and participate. With ELI, the high-field community will move from the relativistic to the ultra-relativistic regime.

The relativistic regime (10^{22} - 10^{23} W/cm^2) of laser-matter interaction is quite mature. Twenty major laboratories outside Europe and approximately fifteen within Europe are now or soon will be in this regime. The success of this field has prompted the International Union of Pure and Applied Physics (IUPAP) to create a working group, the International Committee on Ultra-high Intensity Lasers (ICUIL) with the mission to promote the field. At the moment, the field is subject to an intensity ceiling imposed by the size and cost of the individual systems that a country can support. In contrast, the scientific possibilities call for the higher intensities of the ultra-relativistic intensity regime (>10^{24} W/cm^2), attosecond time durations, and high-energy secondary beams. To explore the ultra-relativistic regime, the next laser generation must be implemented. This system will enable scientists from Europe and rest of the world to congregate and perform the first experiments in the ultra-relativistic regime. Once the field is partially explored and new directions outlined separate countries could then develop their own system.

Time domain: For example, the unique combination of ultra-fast, high brilliance and beam compactness forecasts numerous breakthroughs in the X-ray domain for wavelengths below 10 Å. These will be used to probe structures on the atomic scale but with time resolutions superior to synchrotron sources. As indicated by the success of synchrotrons around the world, shorter and intense X-ray pulses are in high demand by most branches of science. Ultra-short snapshots of nuclear positions in many-body systems have the power to reveal the elementary steps of atomic motion, thus opening new areas of research to novel applications in fields as diverse as condensed matter physics, plasma physics, chemistry, biology, and material sciences.

Beam physics and high-energy physics: The expressed interest of these communities is reflective of the world-wide situation. Programmes along the same lines are being considered in many other places, associating laser and plasma specialists with high-energy physics people. In the HEP community the interest in a detector testing facility would be rather local, involving physicists and engineers from surrounding laboratories at the level of a hundred people, depending on the performance of the beam. The interest in a positron source or even more in a high-energy accelerator would be world-wide and involve thousands of physicists.

Nuclear physics: ELI would be highly attractive to the nuclear physics community. At least ten experimental and theoretical groups in Europe are currently involved in laser-induced nuclear physics, and about 20 worldwide. Since this is a very young field, interest is expected to grow, particularly, when advanced applications of laser nuclear physics in medical isotope production or nuclear waste transmutation prove to technologically feasible. Here, too, the community will grow in the future with new ideas not yet identified.

Impact on society, education and training: The different applications mentioned in the project have the potential of making a great impact on society. ELI could help to clarify the aging of nuclear power plants, control the lifetime of nuclear waste, fabricate new nuclear pharmaceutical products at the patient's bedside, or develop new types of hadron therapy. At present, it is reasonable to claim that ELI will interest a very broad community of at least hundreds of persons, physicists, engineers, oncologists, and environmental scientists. There is very little doubt that with its broad scientific and engineering scope ELI will attract and train a large number of students in the field of ultra-relativistic optics.

E.II Why ELI in Europe?

The number of potential users is very large and represents hundreds of laboratories in Europe. This is evidenced by the spectacular increase of workshops, conferences and summer schools organized in high-field and, more recently, attosecond science. To name a few: Workshop on "New opportunities of ultrafast X-rays", Napa (USA), 2002 (http://www-esg.lbl.gov/esg/meetings/ultrafast/); Winter School on "Ultrafast X-rays" Hamburg (Germany), 2002 (http://www-hasylab.desy.de/conferences/Xray-Course/); Workshop on "Ultrafast science with electrons and X-rays", Montreux (Switzerland), 2003 (http://sls.web.psi.ch/view.php/science/events/uscience03); Summer School "Ultrafast X-ray science with lasers and accelerator sources", Cargèse (France), 2003 (http://loa.ensta.fr/ufx/); and Workshop on "Ultrafast X-rays 2004", San Diego (USA), 2004 (http://ultrafast2004.lbl.gov/). European users recently gathered in thematic networks within the 5th Framework Programme ("XPOSE") as well as the 6th Framework Programme ("FLASH"). NEST projects have been proposed within the FP6 "Adventure" programmes.

The relevant scientific communities have also voiced their needs during the scientific cases of the large-scale X-ray Free-Electron Lasers (XFEL) at DESY (Hamburg, Germany) (http://tesla.desy.de/new_pages/TDR_CD/PartV/fel.html) and LCLS (Stanford, USA) (http://www-ssrl.slac.stanford.edu/lcls/).

European scientists have remarkably consolidated expertise in the field. Many key concepts have been demonstrated by European scientists and many laboratories are leading the field. This leadership will continue with ELI. Furthermore, ELI will be a scientific platform that will promote aggressive technology transfer. Fields such as laser and particle accelerator engineering, nuclear pharmacology, oncology, X-ray and γ-ray imaging could be revolutionized by ELI. ELI could help European industries in these fields to maintain their leadership.

European scientists strongly support ELI, as was demonstrated by the scientific workshop of December 9-10, where more that 130 scientists came for two days from thirteen countries to discuss future scientific and technological prospects. Countries such as France, Germany, Greece, Italy, and Spain support ELI

E.III Why Now?

Given a time constant of typically 5-7 years, for designing and building a facility such as ELI, it is important to start the concept design as soon as possible so that it will be fully completed when the relativistic facilities have reached maturity. ELI will be a pan-European facility. It will be the first such facility dedicated to the ultra-relativistic regime, attosecond science with secondary high-energy radiation and particle beam capability. It will be a scientific beacon for the rest of the community world-wide (at present 30 major laser facilities).

PART F: MATURITY OF THE PROPOSAL

The scientific case for ELI was made in Paris on 9-10 December 2005 by 135 participants from 13 countries: France (host), Germany, Italy, Japan (observer), Lithuania, Netherlands, Czech Republic, Poland, Sweden, UK, Ireland, Italy, Greece, Spain. The list can be seen in section B.IX. Beyond the immediate scientific community, this scientific case also attracted the interest of the:

(1) FEL and synchrotron community
(2) medical community interested in applications to oncology, nuclear pharmacology, x-ray and PET imaging.
(3) laser industry (Quantel, Amplitude Technologies, Thales Laser, Phasix, Fastlite)
(4) electronic industry (Thales and Siemens).

F.I Facility Design

The laser concept is being designed by scientists from MPQ Garching, the University of Vilnius, and LOA, LULI and IOTA in France Diagnostics for the attosecond pulses are under study at Heraklion. Coherent addition of beamlines and large focusing optics relying on segmented mirrors is being studied by ONERA (Office National d'Etudes et de Recherches Aérospatiales). The beamline design and experimentation halls are being studied by the Laboratoire Leprince Ringuet, MPQ Garching and the Istituto Nazionale di Fisica Nucleare (INFN) Frascatti will contribute in the design of the high energy beam lines (10 - 100 GeV beams).

F.II Financial Support

CNRS strongly supports the proposal, as evidenced by inserting some fraction of ELI's construction cost in its 2007 budget.
The Ecole Polytechnique (Palaiseau, France) is offering 5000 m^2 of land for the ELI project.
The Ecole Polytechnique will offer additional space for the beam lines and experimentation halls.
The Ecole Nationale de Techniques Avancées will match the Ecole Polytechnique contribution.
Scientists from Germany, Greece, Italy, and Spain are seeking commitments from their respective governments.

PART G: BUDGETARY INFORMATION PREPARATION, CONSTRUCTION AND OPERATION COSTS

G.I Financial Estimation for ELI Project

G.I.1 Laser equipment

Phase 1 : 50-PW single-beam line design and construction (700 J in 10 -15 fs) at 1 shot/mn. Front-end part delivering ultra-short pulses is running at 100 Hz

Phase 2 : Second beam line #2 + new grating concept studies + coherent phase-locking of the 2 beam lines (100 PW on target – 10^{25} W/cm²). Front-end part up to PW level is running at 1 kHz.

Phase 1 details :

- Front-end : MPQ Garching design and construction of a 5 fs/5 J (1 PW) source running at 100 Hz :

- Duty end : 2 amplification stages and final compression

- 1rst stage : Ampli 100 TW 0.5 J (**1/10** front end) → 50 J at 0.1 Hz
- 2nd stage : Booster amplifier 50 J → 1000 J at 1 shot/mn
- Final compressor : 50 PW

Phase 1 (in M€)

LASER EQUIPMENT		
Description	Estimated costs	Remarks
Front end 5 J/ 5 fs 100 Hz	**7**	Work in charge of **MPQ** and based on diode pumping/5 NOPCPA stages
1rst stage with pump lasers	3	Estimation based on LASERIX project (2M€ with a 130-J green pump laser) and 4-pass amplifier
2nd stage with pump lasers	20	Estimation (waiting for data from Quantel Co)
Compressor	4	Optic 2M€ (8 large gratings) Mecanic 2M€
Grating phase-locking	2	Large gratings are 2 phase-locked gratings
Control command	1	
Beam propagation	4	
Adaptive optics	2	
Homogenization and	2	

diagnostics		
Total duty end	**38**	
Total laser phase 1	**45**	

Phase 2

Front end 1000 Hz	**9**	
#2 beamline	30	
New grating concept studies	10	
Beamline phase locking	2	
Total phase 2	**51**	

Total amount for a 0.1-exawatt (100 PW) laser system 96 M€

G.I.2 Experimental set up and beam lines :

The estimated cost for experimentation areas including interaction chambers, and beamlines for users is **20 M€.**

G.I.3 Building

The estimated area is 5000 m² with a cost of 3000€/ m².
Leads for the whole building. **Building cost: 15 M€.**

G.1.4 Manpower for laser and experimental beam-lines set-up

*Average cost for 1 man/year**: 100 k€ (for laser and experimental beamline design and construction).***

Laser phase 1 : 3 years - 10 full-time people
Laser phase 2 : 2 years - 10 full-time people
Experimental beam-lines : 5 years - 5 full-time people

	# of men/year	Total cost (in M€), tax included
Laser phase 1 (3years)	**30**	**3**
Laser phase 2 (2years)	**20**	**2**
Experimental beamlines (5 years)	**25**	**2,5**
TOTAL (5 years)	**75**	**7,5 M€**

G.II Maintenance and operation (consumables)

Laser phase 1 (3 years) :
- laser maintenance 1rst year : 0,5 M€
- Laser maintenance 2nd year : 1,0 M€
- Laser maintenance 3rd year 3,0 M€
- **Total maintenance phase 1 4,5 M€**

Laser phase 2 (2 years) :
- Laser maintenance 4th year 4,0 M€
- Laser maintenance 5th year 6,0 M€
- **Total maintenance phase 2 10,0 M€**

Experimental beamlines (5 years) (0,2+ 0,4+ 0,6 + 0,8 + 1) = **3 M€**

Beyond this construction period, the total cost for operation and maintenance could be estimated at **7 M€/year** (6 M€ for the laser itself and 1 M€ for the beamlines).

G.III Operation and maintenance costs summary over the first 10-year period (in M€)

	Years 1 to 3	Years 4 and 5	Years 6 to 10 (5)	Total
Laser	4,5	10	30	44,5
Experim. beamlines	1,2	1,8	5	8
Total	**5,7**	**11,8**	**35**	**52,5**

G.IV ELI budget summary over the first 10 years (in M€)

Years→	**1**	**2**	**3**	**4**	**5**	**6**	**7**	**8**	**9**	**10**	**Total**
Equipment Laser (phase 1)	20	15	10								45
Equipment Laser (phase 2)				30	21						51
Equipment Exp. beamlines	7	5	3	3	2						20
Total equipment	**27**	**20**	**13**	**33**	**23**						**116**
Building	8	7									**15**
Manpower for laser/ beamline construction	1,5	1,5	1,5	1,5	1 ,5						**7,5**
Manpower for exploitation (from 2 to 10 men/year)			0,2	0,6	0,8	1.0	1.0	1.0	1.0	1.0	**6.6**
Operation and maintenance costs	0 ,7	1,4	3,6	4,8	7	7	7	7	7	7	**52.5**
Total/ year	**37,2**	**29,9**	**18,2**	**39,6**	**31,9**	**7,5**	**7,5**	**7,5**	**7,5**	**7,5**	**197,6**